AN INVESTIGATION OF RAINFALL CHARACTERISTICS, EROSIVITY AND SOIL EROSION ON ROUND ISLAND, MAURITIUS

by

Darren Rhett Calvert

submitted in accordance with the requirements for
the degree of

MASTER OF SCIENCE

In the subject

Geography

at the

University of South Africa

Supervisor: Professor D.W. Hedding

August 2017

Summary

Round Island is a small (208 ha) islet of volcanic origin located 22.5 km north east of mainland Mauritius and has been classified as a nature reserve since 1957. Two sites were chosen for the installation of environmental monitoring equipment. A series of Gerlach troughs were installed to capture surface sediment transported by runoff, which were used to document sediment yields and determine the particle size distribution. Overall, rainfall and erosivity on Round Island is far less, when compared to mainland Mauritius. However, erosivity from Round Island (2,314.76 $MJ.mm.ha^{-1}.h^{-1}.yr^{-1}$) is slightly above the global average of 2,190 $MJ.mm.ha^{-1}.h^{-1}.yr^{-1}$. In terms of sediment transport, the annual sediment movement rates for Round Island were established during this study (0.1248 $t.ha^{-1}.yr^{-1}$) and were found to be considerably lower than Mauritius (10 $t.ha^{-1}.yr^{-1}$), as well as other tropical island such as Kauai (0.86 $t.ha^{-1}.yr^{-1}$) and O'ahu (0.6 $t.ha^{-1}.yr^{-1}$). Thus, although the estimated rates of soil erosion are very low for humid tropical regions, these rates only reflect the contemporary environmental conditions and cognisance of the landscape history should be incorporated into assessments of soil erosion.

Key terms

Rainfall, erosivity, kinetic energy, soil erosion, gullies, Gerlach trough, sediment, particle size distribution, R-factor, $EI_{30,}$ vegetation, soil conservation.

DECLARATION

Name: Darren Rhett Calvert

Student number: 50857185

Degree: Master of Science (Geography)

An investigation of rainfall characteristics, erosivity and soil erosion on Round Island, Mauritius

I declare that the above dissertation/thesis is my own work and that all the sources that I have used or quoted have been indicated and acknowledged by means of complete references.

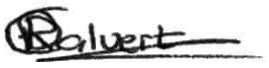

SIGNATURE

30.08.2017

DATE

Abstract

Round Island is a small (208 ha) islet of volcanic origin located 22.5 km north east of mainland Mauritius and has been classified as a nature reserve since 1957. The island was subjected to heavy overgrazing by goats (*Capra hircus*) and rabbits (*Oryctolagus cuniculus*), which detrimentally affected the ecology of the island. Since the removal of the non-indigenous grazers in 1979, intense conservation management has taken place in an effort to restore and preserve Round Island's unique ecological significance.

Round Island is a basaltic volcanic cone with steep slopes averaging between 10-30° and due to its porous and friable rock, weathering and subsequent erosion by water and wind processes are very prominent. Flooding during intense rainfall events has sculpted gullies throughout the island that intensify closer to the shoreline. Thus, the purpose of this research was to understand the drivers of soil erosion on Round Island with the aim to develop ways to better manage erosion. The characteristics of individual rainfall events with regards to kinetic energy and erosivity were determined in an effort to identify the characteristics of runoff and quantify the rate soil erosion on Round Island.

Two sites were chosen for the installation of environmental monitoring equipment, which were used to record air temperature, soil temperature, soil moisture, wind speed and direction as well as rainfall every 15 minutes on a tipping resolution of 0.2 mm. A series of Gerlach troughs were installed to capture surface sediment transported by runoff, which were used to document sediment yields and determine the particle size distribution. In 2015, mean annual rainfall for Round Island was 699 mm, which was considerably less than the previous recorded average of 866 mm. However, cognisance should be made of the fact that no tropical cyclones were recorded during the study period. Using the EI_{30} method to find the "R-factor", erosivity was calculated for the study period. The maximum erosivity produced during an individual rainfall event on Round Island was 21,516.3 $J.mm.m^{-2}.h^{-1}$, which was considerably less than the maximum erosivity calculated on Mauritius by other studies conducted.

Overall, rainfall and erosivity on Round Island is far less, when compared to mainland Mauritius. However, erosivity from Round Island (2,314.76 $MJ.mm.ha^{-1}.h^{-1}.yr^{-1}$) is slightly above the global average of 2,190 $MJ.mm.ha^{-1}.h^{-1}.yr^{-1}$. In terms of sediment transport, the annual sediment movement rates for Round Island were established during this study (0.1248

t.ha^{-1}.yr^{-1}) and were found to be considerably lower than Mauritius (10 t.ha^{-1}.yr^{-1}), as well as other tropical island such as Kauai (0.86 t.ha^{-1}.yr^{-1}) and O'ahu (0.6 t.ha^{-1}.yr^{-1}). Thus, although the estimated rates of soil erosion are very low for humid tropical regions, these rates only reflect the contemporary environmental conditions and cognisance of the landscape history should be incorporated into assessments of soil erosion. The barren landscape and very low contemporary rates of soil erosion suggest that most of the erodible soil has already been eroded.

Going forward, high resolution rainfall data recording must continue to ensure more accurate assessments and should focus on establishing the rainfall erosivity over a longer period (more than 20 years). Future research should make use of unmanned aerial vehicles (i.e. drones) in order to capture high resolution aerial photography and build digital elevation models. These can be used to model soil erosion on an island-scale as well as the hydrology of Round Island. Modelling the hydrology will allow researchers to identify key areas where soil erosion is intensified, identifying important areas for revegetation.

The island is of great biological importance and home to a number of endangered plant and wildlife species which must be protected and conserved. Therefore, conservation efforts should focus on wide-scale revegetation, especially in key areas where soil erosion is likely to be more intense. Further investigations into the potential impacts of introduced non-indigenous tortoise species and burrowing bird species as geomorphic agents should be conducted, especially with regards to sediment displacement and nutrient cycling within the ecosystem. In particular, an investigation into the spatial extent of burrowing by bird species, the volume of displaced soil by burrowing and nutrient cycling around the burrows could reveal various insights into the impacts of burrowing bird species as geomorphic agents and ecosystem engineers on Round Island; one of the few seabird breeding stations in the Western Central Indian Ocean.

Acknowledgements

There are many people and organisations to which I am very thankful. Firstly, this study was made possible through the research funds made available by the College of Agriculture and Environmental Science (CAES) at the University of South Africa. I would like to express my sincere gratitude to the Mauritian Wildlife Foundation and the Mauritian National Parks and Conservation Services for granting me permission to undertake research on Round Island, Mauritius. To Dr Vikash Tatayah for his enthusiasm in the project and for facilitating our stay and safe transfer to and from Round Island. To the rangers stationed on Round Island, for looking after us during our stay, for their valued input and most importantly, for their assistance in the collection of the sediment samples.

To my supervisor, Prof. D.W. Hedding, for introducing me to the topic and for sowing the initial seeds in my mind. He has been the most incredible mentor along this journey through which I have learnt and grown a great deal. I would like to thank him for his constant support, encouragement and guidance, his thought-provoking input, patience and continued help with the writing and feedback provided throughout this study.

To my colleagues for lightening my load at work, which allowed me more time to focus on this study. To Hellene Steenkamp for her assistance with my travel arrangements and funding applications. To Ryan Anderson for his continued support, encouragement and many conversations centered around rainfall erosivity. You were a great source of knowledge and guidance and I am lucky to have you as a friend and colleague. To Kenneth Manuel who became one of my closest friends as we both embarked on the journey to obtaining our Masters', his continued support and encouragement was unrelenting and I will be forever thankful.

To my buddies, Mike, Ayden, Shane and Ryan, I say thank you for your support and friendship throughout this study and for understanding my lack of participation in the last few years.

For me, this masters represents more than just a piece of scientific work, but rather an example of how, with consistency, success is imminent. It has taught me an immense amount along the way, provided me with many challenges, from which I have grown in stature and

learnt a great deal about myself and life in general. I am extremely thankful for this incredible journey.

To my family, extended family and all of my friends who provided a consistent source of support, love and encouragement, for which, I am very grateful.

Finally, to Claire, who came into my life right at the start of my research. She lifted me up when I was feeling down, encouraged me when I felt I couldn't do it any longer and provided the most incredible support, love and understanding a man could ever wish for. Thank you for everything you continue to do for me, without you, this would not have been possible.

Table of Contents

Summary ..... **ii**
Key terms ..... **ii**
DECLARATION ..... **iii**
Abstract ..... **iv**
Acknowledgements ..... **vi**
Table of Contents ..... **viii**
List of Figures ..... **x**
List of Tables ..... **xiii**
Chapter 1: Introduction **14**
Introduction 14
General Aims and Objectives 14
Soil Erosion 15
Erosion by Water 17
Rainsplash and sheetwash erosion 17
Rill Erosion 20
Gully Erosion 21
Rainfall Erosivity 22
Causal Factors 26
Rationale 27
Research Aims and Objectives 27
Project Outline 28
Chapter 2: Round Island: Environmental Setting **29**
Location 29
Volcanology and Geology 30
Topography 31
Climate 32
Pedology 34
Geomorphology 35
Vegetation 37
History and management of Round Island 40
Chapter 3: Methodology **45**
Data sources/Study sites 45

Data collection techniques 46
Atmospheric Monitoring 46
Sediment Transport 47
Defining an erosive event 52
Data analysis and interpretation 53
Determining rainfall event kinetic energy and erosivity 53
Determining the relationship between rainfall and sediment movement 55
Issues of reliability and validity 56
Chapter 4: Results 58
Round Island rainfall characteristics 58
Erosive characteristics of rainfall events 63
Sediment transport 73
Sediment transport and catchment area 79
Particle size analysis 89
Chapter 5: Discussion 91
Soil on Round Island 91
General rainfall attributes 92
Erosive events 93
Sediment transport rates on Round island 94
Soil conservation 96
Zoogeomorphology 98
Landscape Dynamics 101
Chapter 6: Conclusion 103
Summary and key findings 103
Scope for future research 105
References 107
Appendix 1 121

List of Figures

Figure 1.1: Diagrammatic representation of rainsplash erosion (Adapted from Summerfield, 1991). 19
Figure 2.1: Location map of Mauritius and northern islets including Round Island.....29
Figure 2.2: Contour map of Round Island. Note the transects for the cross-profiles.....30
Figure 2.3: Oblique view of Round Island looking north-west.....31
Figure 2.4: A) South-North cross-profile. B) West-East cross profile. Cross-profiles are presented in meters. 32
Figure 2.5: Map showing paths of major cyclones, including Dina (2002) and Gumede (2007), that have affected Mauritius and northern islets (Cyclone tracks adapted from U.K. Meteorological Office, 2007).....34
Figure 2.6: Satellite image of Round Island showing gully erosion and location of study sites. 37
Figure 2.7: Map of habitat types of Round Island (Adapted from Johnston, 1993).....38
Figure 2.8: The Blue Latanier (*Latania loddigeslii*) found on the south-west ridge of Round Island. Note the steep slope gradient. 39
Figure 2.9: Bare steps of tuff in the foreground with Mixed weed habitat which traps sediment, promoting vegetation growth in the background.....40
Figure 2.10: Increased vegetation cover due to soil trap, used as a conservation method to prevent sediment from moving downslope.....42
Figure 2.11: A *Casarea dussumieri* ground boa on Round Island. Individual approximately 0.6 m in length. 43
Figure 2.12: An introduced *Aldabrachelys gigantean* tortoise on Round Island. 43
Figure 2.13: A breeding pair of red-tailed tropicbirds (*Phaethon rubricauda*) on Round Island. 44
Figure 3.1: Environmental monitoring station located at the Wasteland study site. 46
Figure 3.2: Automatic rainfall tipping bucket (0.2 mm resolution) attached to environmental monitoring station. 47
Figure 3.3a: View looking east. Note the mechanical soil erosion structures and Gerlach trough in the foreground, the person for scale and the Wasteland rainfall station in the background.....48
Figure 3.3b: Gerlach trough with captured sediment. 48

Figure 3.4: Monthly sediment samples stored in bags for analysis. Wet sediment was left to dry in the sun for several hours. 49
Figure 3.5: The eight sample sites with Gerlach trough installed. 50
Figure 3.6: Map of Gerlach trough catchment areas. 51
Figure 3.7: Particle size analysis using 2 mm sieve. Note, a large amount of gravel left behind. 52
Figure 4.1: Monthly distribution of rainfall per station over study period. 58
Figure 4.2: Total rainfall and total depth of erosive rainfall (mm) over the study period. 59
Figure 4.3: Box and whisker plots displaying shape and distribution of rainfall characteristics per study site. 60
Figure 4.4: Annual erosive event totals for each station 2014-2016. 61
Figure 4.5: Average number of erosive events experienced by each station during each month for study period. 62
Figure 4.6: Mean monthly rainfall for study period. 63
Figure 4.7: Box and whisker plots displaying shape and distribution of erosive rainfall characteristics per study site. 64
Figure 4.8: Relationship between storm kinetic energy and storm depth (n=37). 68
Figure 4.9: Relationship between erosivity and storm depth (n=37). 69
Figure 4.10: Relationship between kinetic energy and storm duration (n=37). 70
Figure 4.11: Relationship between erosivity and storm duration (n=37). 71
Figure 4.12: Monthly distribution of rainfall erosivity and rainfall experienced at each station over the study period. 72
Figure 4.13: Wasteland monthly erosivity and displaced sediment weight. 76
Figure 4.14: South-West ridge monthly erosivity and sediment movement. 77
Figure 4.15: Box and whisker plot displaying shape and distribution of mean sediment displacement (g) per area (m^2). 81
Figure 4.16: Relationship between combined average displaced soil weight and average total rainfall (n=19). 83
Figure 4.17: Relationship between combined average displaced soil weight and average kinetic energy (n=19). 84
Figure 4.18: Relationship between combined average displaced soil weight and average erosivity (n=19). 85
Figure 4.19: Relationship between combined average displaced soil weight divided by catchment area and average total rainfall (n=19). 86

Figure 4.20: Relationship between combined average displaced soil weight divided by catchment area and average kinetic energy (n=19).....87
Figure 4.21: Relationship between combined average displaced soil weight divided by catchment area and average erosivity (n=19). 88
Figure 4.22: Grain size distribution diagram with site A and B indicated as points. 89
Figure 5.1: Largely barren landscape of Round Island. 96
Figure 5.2: A) Geo-technical mesh screen to slow the transport of sediment. B) Stone wall sediment trap. Hat for scale. 98
Figure 5.3: View downslope of lower “big gully” towards the coastline, which deeply dissects the landscape and represents erosion of the highest severity on Round Island with researcher circled for scale. 99
Figure 5.4: Evidence of seabird burrows into soil on Round Island. Hat for scale. 101

List of Tables

Table 3.1: Example storm and how kinetic energy is calculated. 55
Table 4.1: Total rainfall and total depth of erosive rainfall (mm), percentage of erosive rainfall and the total number of erosive events experienced by each station over the study period. 59
Table 4.2: Characteristics of erosive rainfall events measured at the Wasteland and South-West Ridge monitoring stations with the highest total from each attribute highlighted. 66
Table 4.3: Erosive event attributes at the Wasteland and South-West Ridge rainfall stations over the study period with mean and median (in brackets). 67
Table 4.4: Attributes of erosive rainfall events as measured at the Wasteland and South-West ridge. 67
Table 4.5: Attributes of each catchment area and Gerlach trough. 73
Table 4.6: Weight (g) of sediment samples collected during study period at the Wasteland with rainfall (mm) and erosivity (EI_{30}) included for reference (n = 152). 74
Table 4.7: Weight (g) of sediment samples collected during study period at the South-West ridge with rainfall (mm) and erosivity (EI_{30}) included for reference (n = 152). 78
Table 4.8: Sediment weights (g) divided by catchment area (m^2).....80
Table 4.9: Grain size distribution from each sample site. 90
Table 4.10: Wentworth textural classification in relation to particle size. 90
Table 5.1: Mean rainfall erosivity values as per Panagos *et al* (2017) for comparison to Round Island. 94

Chapter 1: Introduction

Introduction

Round Island is a small (208 ha) islet of volcanic origin located 22.5 km north east of mainland Mauritius. Before 1957, the island was subjected to heavy overgrazing by goats (*Capra hircus*) and rabbits (*Oryctolagus cuniculus*) which were introduced in the 19th Century (Cheke, 1987), detrimentally affecting the ecology of the island. Since then, the island has been classified as a nature reserve, the non-indigenous grazing animals were all removed by 1979 and weed eradication and vegetation monitoring commenced shortly thereafter (MWF, 2008). Round Island's relative isolation and close management protects it from further introductions of several pests and predators and, today, it is home to a number of endangered plant and wildlife species, with its native reptile fauna being internationally famous (Carpenter *et al*., 2003). Round Island is one of the very few islands to be rodent-free and hosts the largest native vegetation in Mauritius and, as such, is known internationally as a place of exceptional biological importance. It is home to at least 10 endemic plant species, including the largest remaining area of palm forest which once dominated the lowlands of north and west Mauritius, eight native reptile species and the only known breeding ground in the Indian Ocean for the South Trinidad Petrel (Bullock *et al*., 1982).

General Aims and Objectives

Monitoring and management on Round Island can be considered a great success story, with the rehabilitation process gaining international praise (MWF, 2008). However, many parts of the island remain barren and, despite the effort of those involved in conservation practices, erosion remains a significant hindrance to habitat restoration. In order to select appropriate conservation measures, the identification and classification of erosive rainfall events is the first step to understanding the drivers of soil erosion. The island is a basaltic volcanic cone with steep slopes averaging between 10-30°. Due to its porous and friable rock, weathering and subsequent erosion by water and wind processes are very prominent. Flooding during intense rainfall events has sculpted gullies throughout the island that intensify closer to the shoreline. The purpose of this research is thus to understand the drivers of soil erosion on Round Island with the aim to develop ways to better manage erosion. This will include determining the erosive characteristics of individual rainfall events, identifying the characteristics of runoff and quantifying the rate of soil erosion.

Soil Erosion

The form of a landscape is dependent on the nature, frequency and magnitude of geomorphic forces acting upon it, as well as the strength and resistance to deformation found in the surface materials of which it is made (Lal, 1990; Toy *et al*., 2002; Morgan, 2005). Rock and soil are the two fundamental types of material which make up a landscape. Rock being a hard, consolidated material comprised of individual particles or crystals. Soil, on the other hand, is an unconsolidated mineral and organic material which typically forms a continuous mass, often characterised by horizons or layers, lacking any joints or fissures, which is considerably weakened when saturated with water (Lal, 1990; Toy *et al*., 2002; Morgan, 2005; Waugh, 2014).

Soil can be found in most regions and landscapes and plays a crucial role in supporting the natural ecosystems on earth (Singer & Warkentin, 1996). Soil provides a medium for plant growth by supplying useful nutrients, acting as a reservoir for water and influences water quality, soil also aids in recycling dead plants and animals while providing a habitat for several important organisms (Chapman, 2005). The erosion of soil is, therefore, a significant problem experienced by many countries (Lal, 2001) and developing countries are usually the worst affected by soil erosion (Morgan *et al*., 1998). Accelerated erosion of soil often leads to socio-economic, economic and environmental problems.

Soil erosion is related to a wider concept termed soil degradation, as much as 15% of the earth's ice-free land surface has been historically affected by some form of land degradation, 56% of which can be attributed to water erosion in the form of rainfall, rivers and oceans (GLASOD, 1990). According to Schwab *et al*. (1996), soil erosion by water is one of the most important natural resource management problems to date. Research by Haynes (1997) has shown that soil degradation leads to a decline in soil fertility, loss of organic matter, the breakdown of soil structure, and changes to the physical and chemical composition of soil.

Soil erosion is a three-phase process consisting of the detachment of individual soil particles from the soil mass, the transportation by erosive forces and finally, the deposition of soil particles once carrying capacity (energy) is lost. Erosion processes and the factors influencing them vary depending on the scale at which they are studied. An example of what may be considered an "extreme" rainfall event within a small watershed may only be

classified as a normal event had the scale been larger. Soil erosion is also distinguished between “natural” and “accelerated”, with the latter being linked to the influence of human impact on the environment (Morgan, 2005). Natural erosion is caused by, for example, fire, excessive drought and floods. According to Karátson *et al.,* (1999); Németh & Cronin, (2007) the erosion of volcanic cones is a natural process that begins during and immediately after (Dóniz-Paez *et al.,* 2011) eruption. According to Bean *et al.* (2017), the bedrock incised gullies found on Round Island act as transport channels for sediment, which is eventually lost to sea, and has been deemed a natural cycle, where conservation efforts will remain ineffective. Accelerated erosion is a result of a number of factors that reduces the productive capacity of soils, they include; intense cultivation and overgrazing of vulnerable land, deforestation, pollution, as well as poor soil and water management. This has led to soil conservation becoming the focus of many studies today (Zachar, 1982). Although most erosion phenomena are natural processes that cannot be prevented, they can be reduced to an appropriate level by adopting the relevant soil conservation measures (Lal, 2001).

Erosion can be defined as the natural detachment and transport of particles by erosive agents such as water in the form of rainfall, rivers and oceans, the movement of wind, and ice. These are referred to as fluvial erosion, aeolian erosion and glacial erosion respectively (Morgan, 2005). Fluvial erosion is considered to be a major form of erosion and takes place by rainsplash, overland flow or sheetwash, rill flow and gully development (Chapman, 2005). Aeolian erosion is the process of wind forced movement of particles (Zachar, 1982), which occurs when the topsoil is displaced and transported causing surface lowering (Beckendahl *et al*., 1988). Aeolian erosion generally takes place in open landscapes that have very little wind resistance to prevailing wind such as the South-East Trade Winds and can be exacerbated by the absence of vegetation.

A major contributor to the absence of vegetation in the landscape is overgrazing. When animals are introduced to an area, grazing pressures which were previously not present can result in erosion. According to Evans (1998), up to 40% of Iceland has been affected by erosion as a result of overgrazing by sheep. Similarly, the island of Macquarie has experienced irreversible soil erosion due to the presence of rabbits (Costin & Moore, 1960) however, since their eradication, it is hoped that a positive effect on the landscape and ecosystem will take place (Bergstrom *et al*., 2009). Animal grazing tends to expand areas of

bare soil, which then becomes vulnerable to the elements, facilitating in the rapid runoff of rainfall. The acceleration of erosion is dependent on the intensity and frequency an area is grazed, as well as the area's size and physical environment (Evans, 1998). Trampling also has severe effects on the rate of erosion by removing vegetation cover and creating depressions in the soil surface. Areas that are exposed to high intensity trampling often form tracks which channel rainfall runoff. This effect has been seen particularly in paths formed by cattle, which have led to the formation of gullies (Mulholland & Fullen, 1991).

Erosion by Water

During a rainfall event, water reaches the soil by throughfall, stemflow or leaf drainage, where it infiltrates and contributes to soil moisture storage. It can also move further down within soil as subsurface flow, and when infiltrating deeper, contributes to ground water. Excess surface water that can no longer be accommodated by the soil moves downslope as surface runoff. Soil infiltration rates exert a major control over the generation of surface runoff to which several properties of the soil influence its infiltration rate, they are; compactness, texture, tendency to crusting, presence of rock fragments, moisture and other characteristics (Lal, 1990; Toy *et al*., 2002; Morgan, 2005).

The energy required for erosion to take place has two forms; potential and kinetic. The majority of kinetic energy gets dissipated by friction with the surface over which the erosive agent moves. Approximately three to four percent of the energy found in running water and 0.2 percent from falling raindrops contribute to erosion. Running water travelling down rills is considered as the most significant erosive agent followed by raindrops and overland flow (Morgan, 2005). A number of erosion processes will be discussed below, they include; rainsplash, sheetwash, rill erosion and gully erosion.

Rainsplash and sheetwash erosion

Raindrop erosion is the detachment of soil and transport resulting from the impact of water droplets on the soil particles (Schwab *et al*., 2002; Morgan, 2005; Bryan, 2000; Addison, 1987). The erosivity of rainfall is often expressed in terms of its kinetic energy. Rainsplash is driven by rainfall kinetic energy, which is a function of dropsize and velocity, however, less than 0.3 percent of that energy is used in transport (Brandt & Thornes, 1987). Expended energy compacts the soil surface, which forms a splash crater (Figure 1.1). The effect is best seen in the development of a surface seal, where fine particles are washed into

pores, which forms an impermeable layer up to 10 mm thick. This layer reduces infiltration capacity, promoting greater runoff. According to Hoogmoed & Stroosnijder (1984), reductions in infiltration capacity of up to 50 percent can occur during a single storm. This effect is particularly evident in loamy sands, where, despite their considerable hydraulic conductivity, can generate considerable overland flow volumes, even during low-intensity rainfall events (Poesen, 1993).

A theoretical model developed by Poesen (1993) shows that slope has a significant positive effect on soil detachment. However, the use of equations is unclear as many factors influence rainfall erosivity and soil erodibility, the two elements most related to detachment rate. With regards to soil erodibility, particle size ranges between 0.04-0.25 mm seem to be most susceptible to detachment (Poesen, 1993). Erodibility is also dependent on the wetness of the soil surface, when dry, soil is detached by a compression of air ahead of a wetting front, in addition to the direct impact of raindrops. When the soil is wet, it is most likely to be detached under saturation conditions since its shear strength is at a minimum (Al-Durrah & Bradford, 1982).

Raindrop impact can be regarded as a principle detachment mechanism, prior to the removal of loosened particles by other processes such as overland flow and rill flow. Considering detachment is mostly influenced by the depth of surface water, raindrop impact is most likely effective during short, intense rainfall events, which generate little surface runoff

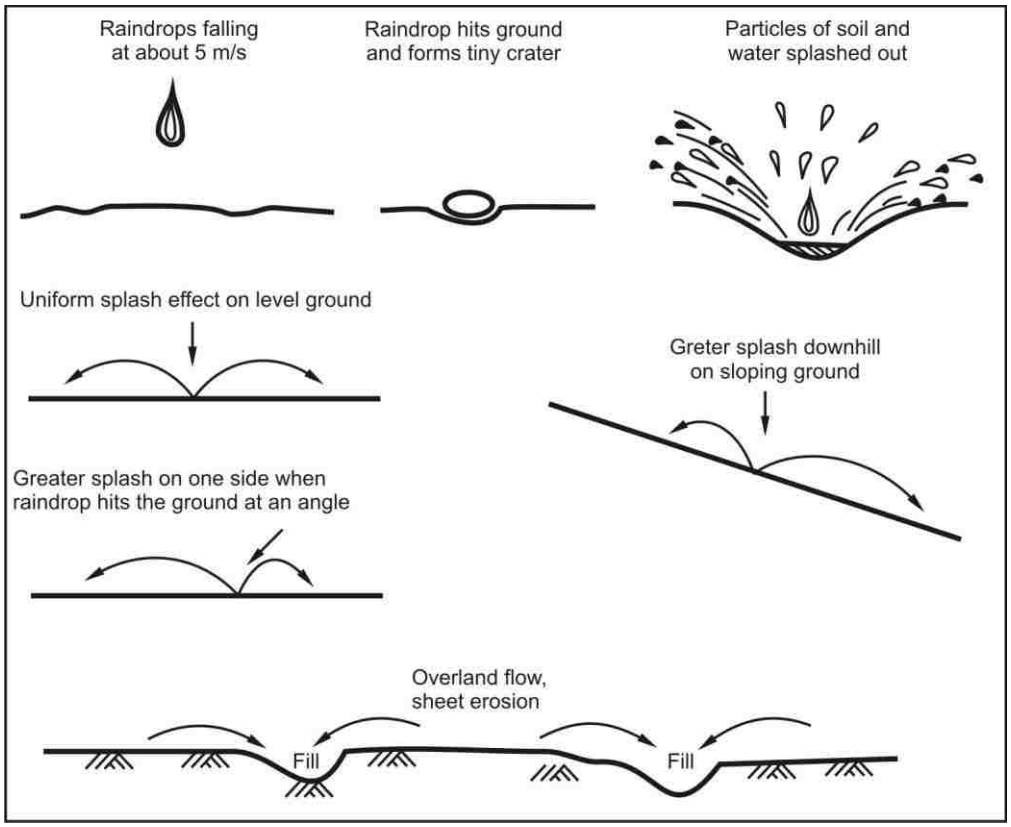

Figure 1.1: Diagrammatic representation of rainsplash erosion (Adapted from Summerfield, 1991).

or during the initial stages of bigger storms, and on drainage divides where flow is typically shallow. Once water accumulates in sufficient quantities and exceeds infiltration capacity it starts to flow downhill as overland flow.

Two types of overland flow occur, *Horton overland flow* takes place when rainfall intensity exceeds the infiltration capacity, with the subsequent discharge increasing linearly downslope (Horton, 1945). This generally occurs on surfaces which have been frozen or where large areas of bare rock are exposed. Horton's (1945) infiltration theory for runoff predicts that this type of flow occurs shortly after or during a heavy rainfall event, implying that a uniformity of rainfall and infiltration conditions exist, which is expected only in small basins. Infiltration capacity is thought to decrease asymptotically during a rainfall event as a result of surface compaction by rain impact, inwashing of fine particles into pores, and the swelling of clay particles, so that the condition (rainfall intensity > infiltration capacity) is met after a small delay (Knighton, 2014).

Saturation overland flow is dependent on the moisture content of soil before, during and after a rainfall event. As long as rainfall continues, no matter the intensity, deeper and less permeable soil layers become saturated, deflecting throughflow closer to the surface. The rising water table prevents any further infiltration, saturating the soil at the surface (Bergsma *et al*., 1996). Overland flow can be erosive without forming channels and generally occurs in sheets or small rills over land surfaces. The initiation of channel incision is dependent on the erodibility and hydraulic properties of the hillslope material. Factors contributing to channel incision include; soil texture, porosity, permeability, water content, infiltration capacity, vegetation cover and shear strength. The constant presence of overland flow is the main cause for channel incision, which eventually leads to the formation of rills and gullies (Bull & Kirkby, 1997).

Rill Erosion

The concentration of overland flow creates shallow channels known as rills (Morgan, 2005). Detachment and transportation potential increases substantially when flow is concentrated into rills. These microchannels typically have dimensions of 50-300 mm in width and can be up to 300 mm in depth. The development of rills takes place in four stages which involves a change in flow state; from unconcentrated overland flow, via overland flow with concentrated flow paths, to microchannels without headcuts and microchannels with headcuts when rills become more established (Merritt, 1984). Persistent rilling requires slopes steeper than 2-3 degrees and extend upslope through headcut erosion, becoming deeper and wider downslope due to channel erosion (De Ploey, 1989; Selby, 1994).

Soils with a mean particle size between 0.012-0.063 mm have the highest erodibility, which is finer than that associated with minimum resistance to raindrop detachment (0.04-0.25 mm). Interestingly, mean particle size represents only one aspect of the soil texture effect as bigger rock fragments embedded in topsoil increase sediment yield by concentrating erosive forces. Once these rock fragments are exposed to the surface, they play a protective role, decreasing erodibility (Poesen, 1993). Usually rills are temporary erosion features, however, permanent rills can be commonplace, particularly where they develop into emerging drainage lines or bedrock material (Beckedahl *et al*., 1988). Rilling generally contributes between 50 and 90 percent of total sediment removal (Knighton, 2014).

Gully Erosion

Gullies are considered permanent water courses but differ from river channels by having steep sides, low width, deep ratios and a stepped profile. According to Poesen (1993), gullies can be distinguished from rills by a critical cross-sectional area of 929 cm^2. Other criteria include a minimum width of 0.3 m and depth of 0.6 m (Brice, 1966). Further, research by Imeson & Kwaad (1980) and Menéndez-Duarte *et al*. (2007) suggest a minimum depth of 0.5 m and 1.0 m respectively. Due to their rapid formation, gullies are usually regarded as an indicator for accelerated erosion and landscape instability. Gullies have been associated with a slope gradient greater than 15 degrees, however, attempts to define the critical conditions for the entrenchment which characterises gully development have not been particularly successful. Three main processes have been identified in the formation of gullies, they are; surface flow, piping and mass movement.

Under suitable conditions, gullies can develop from master rills, however, their initiation is more commonly related to the presence of a localised incision point or various points where vegetation cover is lacking. Runoff is concentrated at these points, forming a headcut, which retreats upslope, leaving a downvalley trench. Many classifications for gully erosion exist based on various criteria (Poesen *et al*., 2002). The criteria include plan form, position in landscape, the shape of gully cross-section and the soil material in which the gully formed (Imeson & Kwaad, 1980; Ireland *et al*., 1939; De Ploey, 1974; Brice, 1966; Poesen *et al*., 1996). According to Ireland *et al*., (1939) there are six forms of gullies; linear, bulbous, dendritic, trellis, parallel and compound. A further distinction is made between V-shaped and U-shaped gullies, with the V-shaped gullies forming due to surface runoff and U-shaped gullies due to surface or sub-surface runoff (Imeson & Kwaad, 1980).

Many studies have recorded gully initiation by subsurface pipe erosion and subsequent roof collapse, this is particularly present in semi-arid areas (Beckedahl *et al*., 1988). This mechanism occurs when surface soils develop cracks through which storm water rapidly infiltrates. Once water breaks through the soil surface, headward retreat along the pipe takes place and can be very rapid (Knighton, 2014). Piping has been found to contribute towards the third process of gully formation, namely mass movement in which landslides leave deep, steep-sided scars, which are then exploited by further surface runoff during subsequent rainfall events. Although many of these processes apply to gully formation in soil, the same

processes can be applied to bedrock-incised gullies (Wohl, 1993; Bean *et al*., 2017). Gully erosion can lead to severe environmental issues, with huge quantities of soil being lost, making land unfit for many forms of agricultural activity (Knighton, 2014). Although Bean *et al*. (2017) indicate that gullies on Round Island incise into the bedrock instead of soil (due to a lack thereof), gully erosion typically occurs in deep soils on flat slopes with a large contributing area where water converges (see Le Roux & Sumner, 2012).

Rainfall Erosivity

According to Wischmeier & Smith (1958), in order for significant amounts of soil erosion to occur, rainfall intensities should be larger than 25 $mm.h^{-1}$. Similarly, Stocking & Elwell (1976) indicate that a maximum 5-minute intensity exceeding 25 $mm.h^{-1}$ and a total rainfall above 12.5 mm within a 30-minute period can be considered an erosive event. This definition was also adopted by Nel & Sumner (2007) to identify erosive events in the Drakensburg, South Africa. A need for high resolution rainfall data was identified in order to accurately quantify erosivity on Mauritius. The Mauritius Meteorological Services provided new high resolution 6 minute rainfall data, which allowed for many studies on storm kinetic energy, erosivity and soil erosion risk (e.g. Le Roux *et al.*, 2005; Nigel & Rughooputh, 2010; Nel *et al*., 2012; 2013; 2016; Sumner *et al.*, 2016). Work done on mainland Mauritius by Nel *et al.* (2012) investigated rainfall depth, duration, intensity, kinetic energy, and erosivity of 385 erosive rainfall events at five locations over a five year period. Nel *et al*. (2012) found that there is a marked difference in erosive storm events between the coastal lowlands and the elevated interior. The study also noted that, although erosivity measured during summer exceeds that which is recorded in winter, the data indicates that a large percentage of winter rainfall events on Mauritius are erosive and that rainfall from non-tropical cyclones can pose a substantial erosion risk.

Nel *et al.* (2016) explored the intra-event rainfall characteristics of 120 rainfall events on mainland Mauritius to provide the first detailed intra-storm data for a tropical island environment. A notable spatial variation was found across 6 rainfall stations, with an increase in rainfall depth, duration, kinetic energy, and erosivity of extreme rainfall events with altitude. Events taking place in the central plateau showed high variability of peak intensity over time as well as a higher percentage of events in which the greatest intensity occurred in the later part of a storm. The study suggests that even though intra-event rainfall

characteristics are complex, they have implications for soil erosion risk in tropical island environments and should be incorporated into soil modelling.

A recent study done by Panagos *et al.* (2017), which aimed to quantify global patterns of rainfall erosivity by analysing results collected from 3,625 stations covering 63 countries, also made use of the above criteria. According to Yang *et al.* (2003), Nearing (2001) and Wei (2007), climate and land use are the two main causes for water erosion, with rainfall being the key factor to consider. Quantifying soil loss has been a subject of extensive study over the last few decades (Capolongo *et al.*, 2008; Nyssen *et al.*, 2005; and Zhang *et al.*, 2010). There have been several models used to quantify soil loss, some of which include the Water Erosion Model (WEPP) (Flanagan & Nearing, 1995) and the Soil Loss Estimation Model for Southern Africa (SLEMSA) (Elwell, 1976).

Possibly the most extensively used models are the Universal Soil Loss Equation (USLE) and its subsequent version, the Revised Universal Soil Loss Equation (RUSLE). Developed by Wischmeier & Smith (1978) and Renard *et al.* (1994, 1997) respectively; these equations were designed to quantify soil loss, and to gain a better understanding of soil erosion at a hillslope scale. Considering various soil types and vegetation, the annual rainfall erosion losses (A) can be calculated from the Universal Soil-Loss Equation. USLE computes soil losses from the product of six major factors: A=R•K•L•S•C•P. Where (A) is the soil loss per unit area from sheet and rill erosion, normally specified in tons per acre, (R) is the rainfall erosivity factor, (K) is the soil erodibility factor, (L) is the field length factor, (S) is the field slope factor, (C) is the cropping management factor, and (P) is the conservation practice factor. For this study, we will mainly focus on the 'R-factor' or rainfall erosivity factor, which represents the runoff and erosion that results from rainfall. The RUSLE model has been widely applied and tested in a number of studies, and it can be considered an advantage to understand the validity and limitations of the model (Renard *et al.*, 1997). However, one main disadvantage of the model, is that it was developed for the Midwest of the USA, and therefore, significant alterations to the algorithms are required before it can be applied to other areas (Shamshad *et al.*, 2008).

Rainfall erosivity (RE) has been described in several ways but it can be summed up as "a measure of erosive force of rainfall to cause soil erosion" (Zhang *et al.*, 2010:102) or the ability of rainfall to detach soil particles (Mihara, 1951; Free, 1960). It is the sum of the

erosivity index (EI) values for all rainfall events recorded in one year (Wang *et al.*, 2002). Rainfall erosivity considers the kinetic energy (the product of mass and fall velocity squared) of a rainfall event and takes into consideration the peak intensity and duration (Salles *et al.*, 2002). The 30 minute erosivity index (EI_{30}) is commonly used when calculating RE, which is calculated by multiplying the total kinetic energy (E) with the maximum 30-minute rainfall intensity of a specific rainfall event (I_{30}) (Yin *et al.*, 2007). Obtaining the amount of kinetic energy for a rainfall event is of significance as this is the energy responsible for the dislodging and transportation of soil particles. Other processes such as soil splash can also be attributed to the kinetic energy found in raindrops (van Dijk *et al.*, 2002). According to Panagos *et al* (2017), rainfall erosivity is one of the most important input parameters for describing erosive processes and although it remains the most serious cause of soil degradation globally, global patterns of rainfall erosivity are poorly quantified.

Raindrop size and kinetic energy are important factors to consider when calculating $EI_{30.}$ Drop size is directly related to terminal velocity, the larger the drop size, the greater the terminal velocity. Larger raindrops have more kinetic energy, and therefore have a higher potential to dislodge soil particles. The kinetic energy of a raindrop as it hits the ground is expressed as $E_K=½mv^2$. During stable conditions a raindrop falling to earth will achieve a constant terminal velocity and will eventually reach a state of equilibrium, where gravitational forces are equal to frictional forces (van Dijk *et al*., 2002). According to Gunn & Kinzer (1949) and Hinkle *et al*. (1987), the relationship between drop size and terminal velocity is not a linear one, as larger drops tend to be more flattened by drag forces during their fall. Laws & Parsons (1943) and Joss & Waldvogel (1967) found that as a consequence of air drag, the upper limit to the size of raindrops is between 6-8 mm, above which they become unstable and break apart. According to Salako *et al*. (1995), raindrops with a diameter of larger than 3 mm are to be considered erosive. There are a number of other factors which influence the energy of a raindrop before it reaches earth's surface, some of which include: side winds, altitude, canopy and ground cover (van Dijk *et al*., 2002).

A study done by Angulo-Martinez & Begueria (2009) concluded that the largest proportion of soil erosion occurs during intense rainfall events. This was also confirmed later by Nel *et al.* (2012), who found that that extreme rainfall events generate the bulk of the erosivity and that soil erosion risk occurs from a storm-scale to a synoptic-scale. The influence that rainfall erosivity has in contributing to soil loss depends largely on the climate

and weather of an area as well as the environmental conditions such as topography and slope. When calculating an area's soil erosion risk, estimating rainfall erosivity is vital as it is considered one of the significant contributing factors. According to Wang *et al*. (2002), when all other factors are kept constant, the R-factor is directly proportional to the potential annual soil loss. Similarly, van Dijk *et al*. (2002) found that soil that is dislodged following a rainfall event is directly related to the intensity of the rainfall received. This fact is highly dependent on the product of the total storm energy and the maximum 30-minute rainfall intensity.

Another important factor to consider when calculating erosivity and soil loss, is the temporal scale and the use of time increments. The erosivity index depends on a high temporal scale of at least 15 minute intervals for results to be accurate. Angulo-Martinez & Begueria (2009) confirm this by suggesting that at least 15 minutes of continuous rainfall data be used to accurately assess the R-factor. Further stating that for accurate calculations to be made, it is preferable to have a series of short high resolution data as well as long series at a day resolution. Nel *et al.* (2013) assessed the value of using high-resolution data versus long-term totals in erosivity calculations, and found that the use of high resolution data at 6 minute intervals resulted in estimates of around 10 percent more erosivity than 30 minute intervals and 33 percent more rainfall erosivity than 60 minute data. The 30-minute interval is considered the most commonly used and accepted interval for calculating the erosivity index, however, there has also been usable results from the use of an hourly scale (Bhattarai & Dutta, 2007; Yin *et al*., 2007). Vrieling *et al*. (2010) examined whether erosivity can be accurately mapped using 3-hourly TRMM (Tropical Rainfall Measuring Mission) Multi-Satellite Precipitation Analysis (TMPA) data and found that it does not provide sufficient detail to represent high-intensity erosive events.

Research has also been conducted using small time intervals. However, Panagos *et al* (2017) stress the need for high temporal resolution rainfall data for long time periods but found that many regions of the world have limited observational data of sufficient temporal resolution. Mongwa (2011) and Anderson (2012) made use of 6 minute intervals to conduct research on mainland Mauritius. Yin *et al.* (2007) investigated the use of 5 to 60-minute breakpoint rainfall data and found that greater temporal resolutions provided more accurate results for estimating rainfall erosivity. According to Stocking & Elwell (1976) there is an explainable difference in the best erosion predictor and suggest that the time interval used depends on the conditions of vegetation cover. It was found that EI_5 gave the best assessment

of the erosive potential of rainfall in areas where vegetation was at a maximum. Where vegetation was poorer and bare, the use of EI_{15} and $EI_{30,}$ respectively, were considered more applicable.

Causal Factors

Erosion is determined, firstly, by the nature of processes operating, and secondly, by the response of an area to the environmental conditions taking place such as climate, geology, topography, soil properties and vegetation cover (Beckedahl *et al*., 1988). In terms of topography, soil erosion is proportional to slope gradient and the associated length, referred to as slope-length (Morgan, 2005). Terrains with higher slope-length have higher rates of erosion due to the higher runoff energy and volume associated with the slope-length. Conversely, flat terrains, that are characterised by lower slope-length, have comparatively lower erosion potential (Pimental & Kuonang, 1998). Mararakanye & Sumner (2017) suggest that gully erosion propensity increases rapidly for hillslopes steeper than 4.5°. Vegetation cover plays a significant part in the protection and prevention of soil erosion as raindrop and wind energy is dissipated by vegetation. Organic matter produced by plant cover assists in binding soil particles, which builds aggregate stability, effectively acting as a buffer between the atmosphere and the soil (Pimentel & Kuonang, 1998; Lal 1990; Toy *et al*., 2002; Morgan, 2005). Morgan (2005) suggests that the potential for soil erosion is much higher at the start of the rainy season when rainfall intensity is high and vegetation cover is too sparse to hold the soil in place.

On Round Island, visual observations indicate that vegetation cover is currently sparse and slope gradients are typically steeper than 4.5°, which Mararakanye & Sumner (2017) indicate plays a significant influence on gully erosion. Moreover, Bean *et al*. (2017) indicate that the erodibility of the soil is relatively high which may also facilitate soil erosion processes. These endogenic causal factors combine to influence the rate of soil erosion in an area. Exogenic causal factors, such as rainfall erosivity and rainfall totals, associated with surface runoff, also play a role in determining the rate of soil erosion and form the focus of the study.

Rationale

Prior studies investigating the 'R-factor' have taken place across the globe and in a variety of environments. Each study focused on varying aspects of rainfall erosivity. Work done by Nyssen *et al.* (2005) took place in a highland environment, Capolongo *et al.* (2008) covered Mediterranean regions and Zhang *et al.* (2010) did a study based on inland continental areas. Research done by Le Roux (2005), Nigel & Rughooputh (2010), Mongwa (2011), Anderson (2012) and Nel *et al*. (2016) have covered the isolated tropical island environment of Mauritius. Although the rate of soil erosion on Round Island increased significantly following the introduction of the various herbivores (Tatayah, 2010), many of the gullies on the island extend below sea level, suggesting that this process is a natural one, and occurred before the introduction of the goats and rabbits (Cheke, 2004). As the island is now home to the last remnant of palm savannah, which was previously lost to mainland Mauritius, it is of utmost importance that soil erosion on Round Island be limited. It may be a challenge to completely halt the gully growth but with the correct measures in place, the rate of expansion can be slowed.

Knowledge of the relationship between rainfall intensity and kinetic energy is important for the prediction of erosion hazards (van Dijk, 2002). Prior studies of soil erosion have been conducted on mainland Mauritius by Le Roux (2005), Nigel & Rughooputh (2010) and Anderson (2012), as well as one study investigating the erosion phenomena found on Round Island by Bean (2014). Currently, however, there is very little information on the geomorphology of the island and more specifically the rate of soil erosion resulting from intense rainfall events. Round Island is regarded as pristine, with little to no influence from humans but, due to limited vegetation cover, it is at risk of further soil erosion. Therefore, conducting a study here would provide baseline information against which geomorphological processes on mainland Mauritius can be compared. Moreover, the study will greatly assist in identifying key areas for conservation and management efforts, while becoming the first assessment of its kind to be conducted on a small volcanic tropical island.

Research Aims and Objectives

The aim of the project is to investigate the role that erosive rainfall events have on soil erosion on Round Island. The study will establish the amount of soil erosion that takes place following rainfall events in an attempt to quantify soil erosion on Round Island. To achieve this, the following objectives have been set out:

- Establish the differences in rainfall characteristics between two environmental monitoring stations on Round Island
- Determine the kinetic energy and erosive characteristics of individual rainfall events on Round Island
- Determine the relationship between rainfall and sediment movement on Round Island
- Establish monthly sediment movement rates to determine the contemporary rate of soil erosion for Round Island
- Establish sediment characteristics through particle size analysis

Project Outline

The project has six chapters, the first presents an introduction to the project with a brief overview of soil erosion and rainfall erosivity as well as the context and aims of the project. The second chapter covers a description of the study area and gives further background to the island by introducing information about its topography, geology, pedology, climate, geomorphology, vegetation and history. Chapter three outlines the methodology used in the project. Chapter four presents the results produced from the investigation after which chapter five gives a detailed discussion of the results. Chapter six concludes with a summary and the conclusions of the project along with recommendations for further research on Round Island.

Chapter 2: Round Island: Environmental Setting

This chapter provides a background to the location, volcanology and geology, topography, climate, pedology, geomorphology, vegetation, and lastly, the chapter gives a brief background into the history and management of Round Island.

Location

Round Island is an islet located in the Indian Ocean situated 22.5 km northeast of Mauritius between 19°54'03" S and 57°47'03" E (Figure 2.1). The island has an area of 208 ha (2.08 km^2) (Figure 2.2) with a maximum altitude of 280 m a.m.s.l. (MWF, 2008). It falls within the Mascarene Islands along with Mauritius, Reunion (170 km WSW of Mauritius) and Rodrigues (650 km ENE of Mauritius).

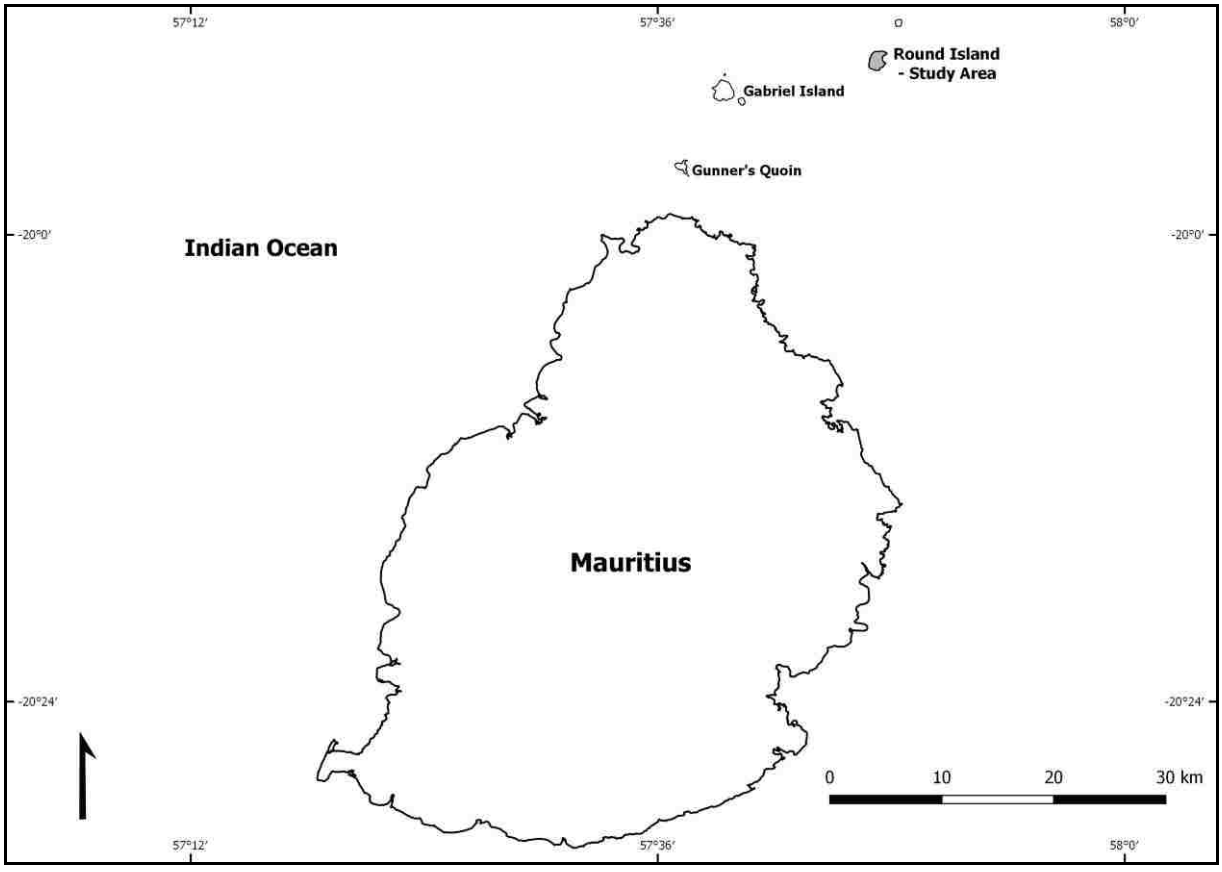

Figure 2.1: Location map of Mauritius and northern islets including Round Island.

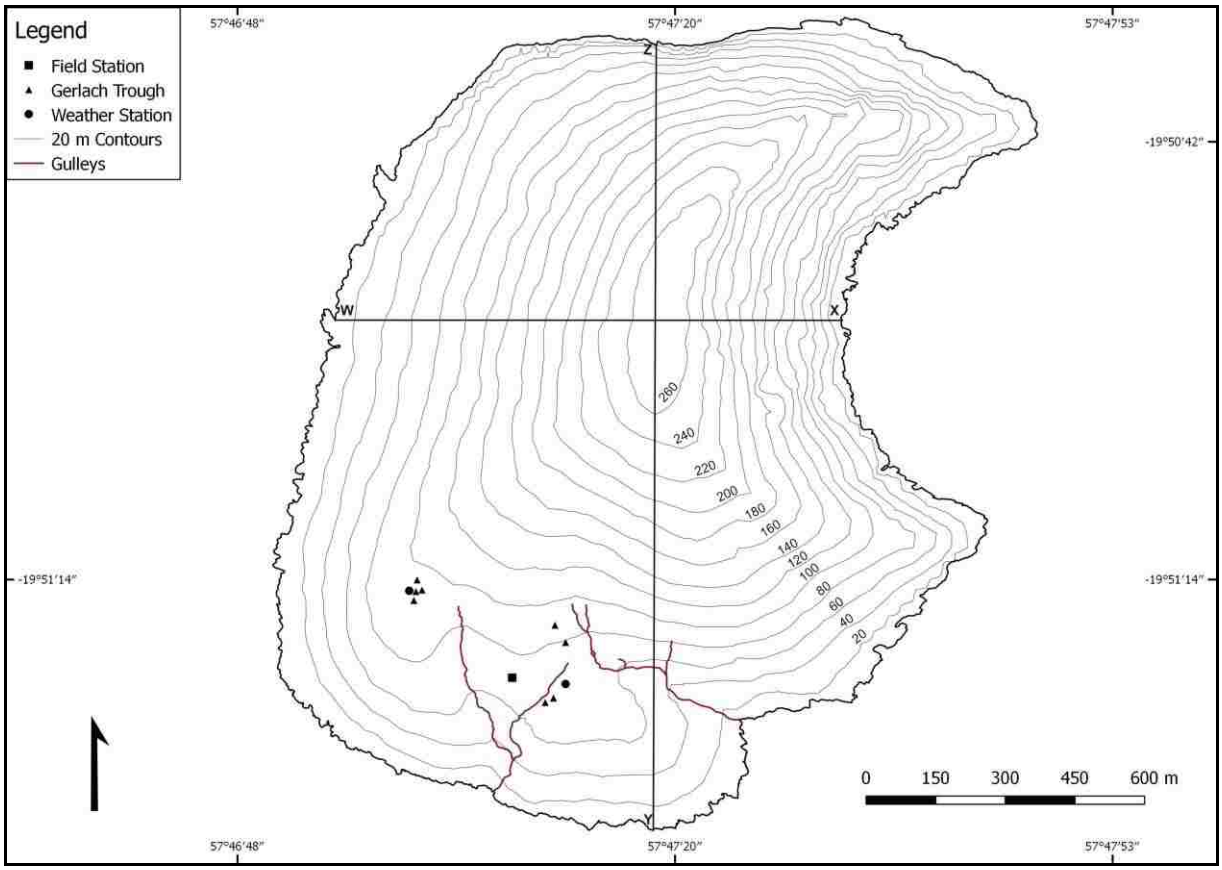

Figure 2.2: Contour map of Round Island. Note the transects for the cross-profiles.

Volcanology and Geology

Mauritius and its surrounding islands form part of the Mascarene Island group, all of which are the summits of volcanic cones that rose from the ocean floor. The area is believed to have had a complex volcanic evolution (Paul *et al*., 2007), which occurred in three phases (McDougall & Chamalaun, 1969). Baxter (1972) noted three distinct periods of volcanic activity, which are the Older series (7.8 – 5.5 Ma), Intermediate series (3.5 – 1.9 Ma), and the Younger series (0.7 – 0.003 Ma). The Older series was further divided into two stages, namely the Early and Late-Shield building stages (Baxter, 1975). Mauritius is the second youngest island in the Reunion mantle plume track which stretches northward from Mauritius to the Mascarene Plateau, the Chagos-Laccadive Ridge, and the Deccan traps of western India (Morgan, 1981; Duncan & Richards, 1991).

Round Island's volcanic core has been dated to around 25 000 to 100 000 years old, which is significantly younger than mainland Mauritius and is attributed to the Recent Series of lava flows (Saddul, 2002). The island was defined by Wohletz & Heiken (1992: 384) as a tuff cone which is a "volcano composed of indurated ash with slopes between 20-30°". The

underlying geological material is composed of consecutive beds of tuff, which has been formed from deposits of volcanic ash with coarse ejecta, mostly scoriaceous. Large boulders of solid basalt can be found throughout the island, with some calceourous boulders at the summit and quartz along fissures in the rock. Fossils incorporated within the tuff can be found within the calcarinite, which was possibly lifted up and included at the time of formation of the island (Johnston, 1993).

Topography

Round Island is crescent-shaped (Figure 2.3) with steep convex slopes throughout the island ranging from 10-30°. The southern point of the island to the summit, has an average slope of 19° (Figure 2.4 a). The western point to the summit and the summit to the eastern point have an average slope of 25° and 37°, respectively (Figure 2.4 b). The summit to the northern point has an average slope of 20°, with narrow ledges and vertical sea-cliffs of 50-100 m in height (Johnston, 1993). The sea cliffs of the island bear the full brunt of wave action since there is no exposed coral reef surrounding the island to reduce the impact of the waves (Saddul, 2002). The slopes are dissected by gullies running east southeast that intensify closer to the shoreline. There are two flat areas known as the “helipads” in the southern part of the island as well as a crater on the north-eastern part of the island.

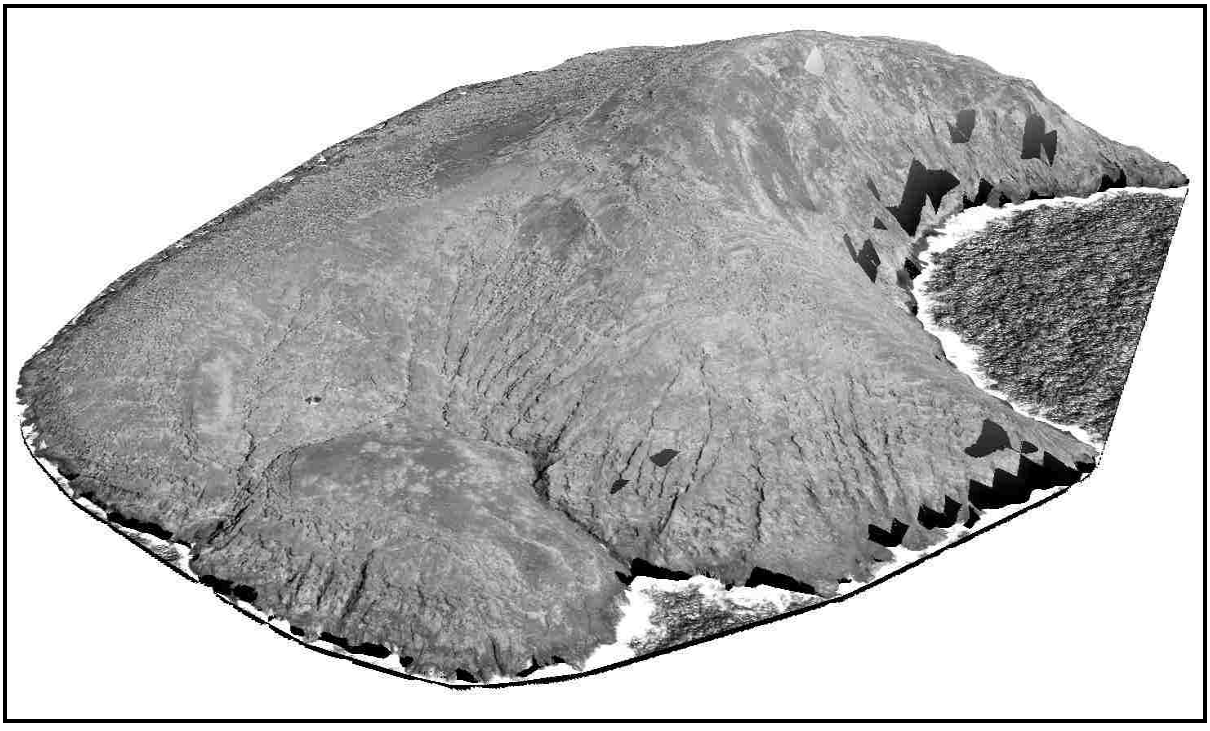

Figure 2.3: Oblique view of Round Island looking north-west.

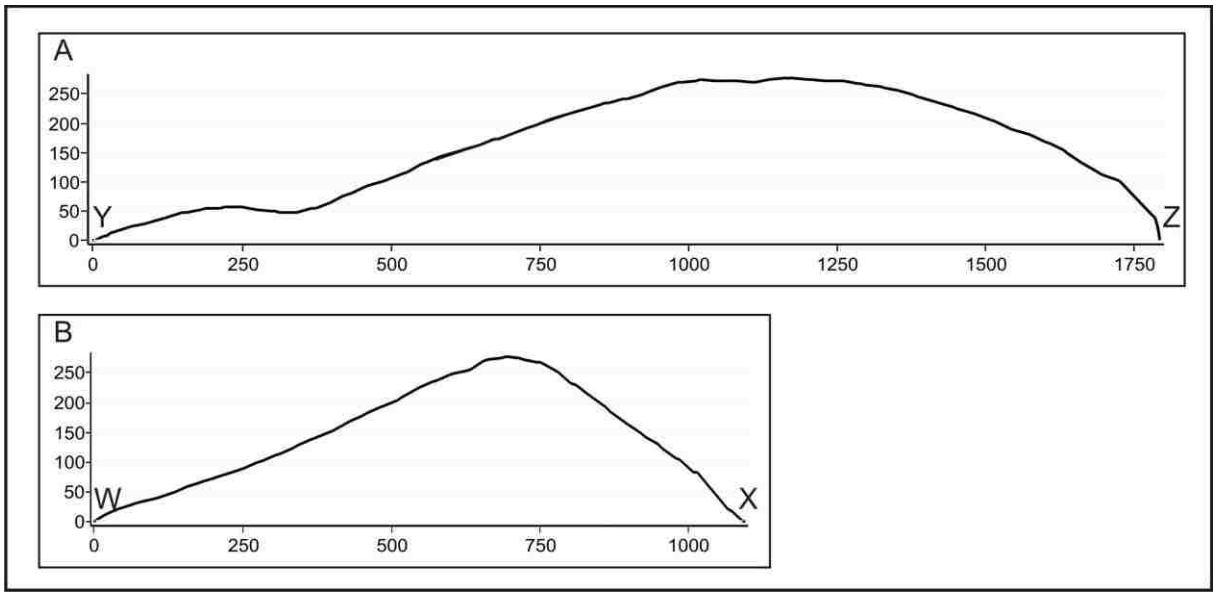

Figure 2.4: A) South-North cross-profile. B) West-East cross profile. Cross-profiles are presented in meters.

Climate

Round Island has a tropical maritime climate with a mean annual precipitation of 866 mm (MWF, 2011). Although, based on weather data collected in 2015 and 2016, mean annual rainfall is slightly lower, having been recorded as 760 mm. Located in the tropics, precipitation usually takes the form of rainfall. Weather monitoring on Round Island commenced in 2003, which recorded a mean annual air temperature of 24.7°C (MWF, 2011). The dry period takes place between the months of August and November where droughts are frequent. The rainy season is concentrated between December and April when cyclone passage and depressions associated with the movement of the Inter-Tropical Convergence Zone dominate (Dennet, 1978). Cyclones bring winds of up to 250 km/hr and are frequently accompanied by torrential rainfall. South-East Trade Winds and frontal systems dominate between the months of May and July (Padya, 1984), which has often led to monthly rainfall averaging as much as 80 mm. Nel *et al.* (2012) also found that a large amount of winter rainfall occurs on Mauritius, which was deemed to be erosive in nature and can pose a substantial erosion risk. The south-eastern side of the island is cooler and wetter than the western side of the island, which is hotter and drier as a result of the South-East Trade Winds.

A study conducted by Nigel & Rughooputh (2010) found that many summer thunderstorms on mainland Mauritius are classified as erosive rainfall events and, given the close proximity, this could also be the case on Round Island. Although, up until this study, no

detailed rainfall erosivity data are available. Morgan (2005) suggests that erosion follows a similar pattern as rainfall and peaks following a dry winter season. This is the most vulnerable time for erosion as the soils are drier and vegetation has not grown enough to protect the soil. On mainland Mauritius, the greatest rainfall erosivity period is in December as it is the month with the lowest vegetation cover; and it is, therefore, expected that the same conditions occur on Round Island (Nigel & Rughooputh, 2010).

According to Anderson (2012), moisture from circulating weather systems such as the occasional cyclone and depression results in significant orographic rainfall as a result of raised topography of Mauritius. Long-term mean annual rainfall has been reported as high as 4000 mm in the elevated central region of Mauritius, approximately 1200 mm in the eastern part of the island and as little as 600 mm on the western coast (Rughooputh, 1997; WRU, 2007). The assumption can be made that Round Island would not experience this amount of rainfall per annum since the island only has a total elevation of 280 m. This is significantly less than the highest point on mainland Mauritius, Riviere Noire-Savanne range in the Southern Uplands, which has a maximum altitude of 828 m a.m.s.l. (Anderson, 2012). It should be noted that the rainfall totals, and quite possibly erosivity on Round Island, may compare well to the relatively dry West coast of Mauritius.

On average, 10 atmospheric depressions, of which three develop into cyclones, occur each year between November and April (Padya, 1984; Cheeroo-Nayamuth *et al*., 2000). In February 2007, a particularly intense tropical cyclone , Cyclone Gumede passed 230 km off the north-west coast of Mauritius with wind speeds reaching up to 158 km/h and a total of 3929 mm rainfall over 72 hours, were recorded at the Royal Alfred Observatory in Pamplemousses, Mauritius (MMS, 2010). In January 2002, Cyclone Dina directly affected Mauritius with 488 mm of rainfall recorded at Vacoas and the highest recorded wind gust of 228 km/h. In January 1980, Tropical Cyclone Hyacinthe, resulted in over 1000 mm of rainfall recorded for Mauritius, unfortunately no rainfall data was recorded during these storms for Round Island. More recently, the 2008-2009, 2011-2012 and 2014-2015 cyclone seasons were very significant in the South West Indian Ocean, with a large number of cyclones affecting the rainfall of Mauritius (Figure 2.5). According to Le Roux, (2005) the average rainfall recorded from tropical cyclones is 245 mm.

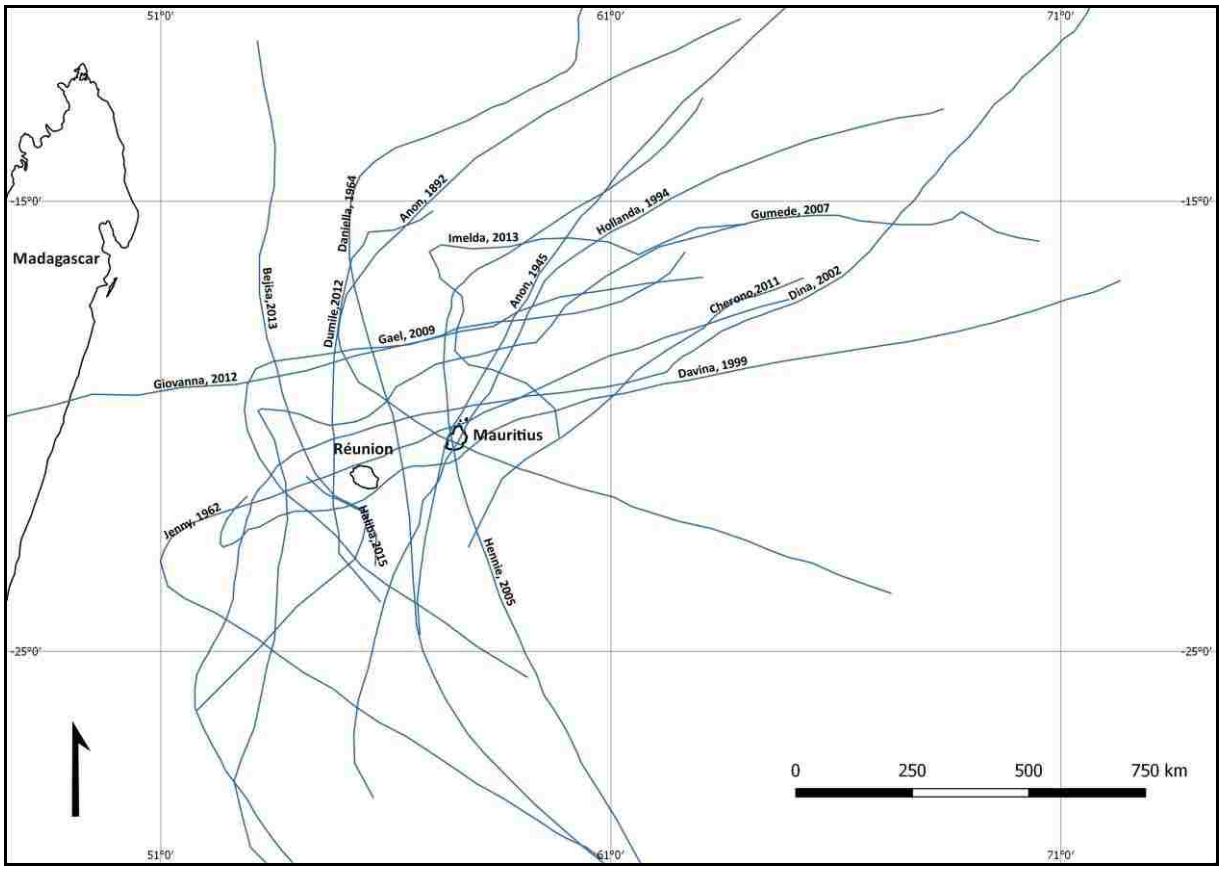

Figure 2.5: Map showing paths of major cyclones, including Dina (2002) and Gumede (2007), that have affected Mauritius and northern islets (Cyclone tracks adapted from U.K. Meteorological Office, 2007).

Pedology

The distribution of soils on Round Island is limited due to the prior introduction of herbivores (Johnston, 1993). According to Merton *et al*. (1989), the original distribution of soils was most likely continuous but slope steepness suggests that certain areas on the island are likely to have remained barren. Two types of soils were identified during a soil survey by Johnston (1993), using the FAO International Soil Classification System. Lithic leptosols found on the western facing slopes where the A-horizon has developed poorly on bedrock that can be found less than 10 cm below the surface. Dystric leptosoils with Dystric regosol components can be found in the southern spur areas where depths reach up to 50 cm. Soils in this area are poorly developed with an orchic A-horizon, where below, homogenised, stable old soil material can be found above welded tuff. Compared to the mature ferralatic (Latosols) and Latosolic soils found on mainland Mauritius (Proag, 1995), soils on Round Island show very little resemblance and therefore are not suitable for comparisons (Johnston, 1993).

According to Johnston (1993), it is not possible to determine the original nature of soils on Round Island. Johnston (1993) indicates that the majority of soils found on the island are sandy loams with a relatively uniform texture, little structure and poor profile development. This can be attributed to previous soil loss and recent regeneration and may be considered as a secondary parent material overlying the original welded tuff parent material (Johnston, 1993). Round Island being a geologically young volcanic cone, stoney and relatively infertile soils are to be expected (Dóniz-Paez *et al*., 2011). The nesting seabirds on Round Island have contributed to fertility through guano, which has affected plant species distribution and rehabilitation (Johnston, 1993). Soils are acidic, with low nitrogen levels and exceptionally high phosphorous content. The percentage of organic matter is variable and averages 5.4% (Johnston, 1993). Soils formed in volcanic ejecta have many distinctive morphological, physical and chemical properties, which are rarely found in soils from other parent material. These properties can be attributed to the formation of noncrystalline materials, such as allophane and imogolite, and the accumulation of organic carbon, which are considered the two main pedogenic processes occurring in volcanic soils (Ugolini & Dahlgren, 2002). The high phosphorous retention, high degree of variable charge, low bulk density and a pH level between five and six of soils found on Round Island are all common properties of soils developed from volcanic ash in humid tropical environments.

Geomorphology

Weathering and erosion occurs throughout the island with wind and water acting as the major agents, sculpting the overlapping ash beds into several cavernous overhangs, steps and pedestals. Large, deep gullies can be found across the island, with many of them extending below sea level, a sign that these gullies were possibly formed during the late Quaternary glacial low-stand, when the sea level was much lower than it is today (Figure 2.3). This is an indication that the formation of these landforms occurred long before human influence on the island (Cheke, 2004). Steep cliffs around the island are an indication of erosion of the coastline by wave action. The porous nature of the rocks, steep slopes and gullies makes it difficult for water to accumulate except in small ephemeral pools (MWF, 2008). During the rainy season, when flash flooding occurs, water is quickly channelled via the gullies and into the sea, which hinders plant regeneration, and at the same time, increases the risk of erosion (Johnston, 1993).

The rills and gullies present on Round Island are bedrock incised, which are contrary to the norm where formation usually takes place in the soil layer and terminates at the bedrock level (Bean *et al.*, 2017) This can be attributed to the properties of the scoriaceous basalt. Bean *et al.* (2017) used Schmidt Hammer values to quantify rock hardness characteristics for Round Island and found that values were very low throughout, with mean R-values as low as 13.5, which is inherent in the properties of volcanic tuff. Other studies confirm that tuff rock produces low rebound values, Kihç & Teymen (2008) found that tuff rock produced mean rebound values between 17 and 26. Compared to other volcanic rock types such as granite (mean R-values of 53.48, Lifton *et al*., 2009), basalt (mean R-values ranging from 42.2 to 62.3, Dickson *et al*., 2004 and quartzite, which was found to have mean R-values of 63 (Kihç & Teymen, 2008).

The geology of Round Island is predominantly volcanic tuff. Thus, bedrock erosion rates are expected to be relatively high (see Bean *et al*., 2017). When measuring rock strength, it is important to consider factors such as the degree of weathering and the presence of joints and fractures. Different rocks vary considerably in what is known as intact strength, which is a rock's strength excluding the effects of fractures and joints (Summerfield, 1991). The majority of rocks found on Round Island can be classified as "very weak" according to the intact strength classification tables.

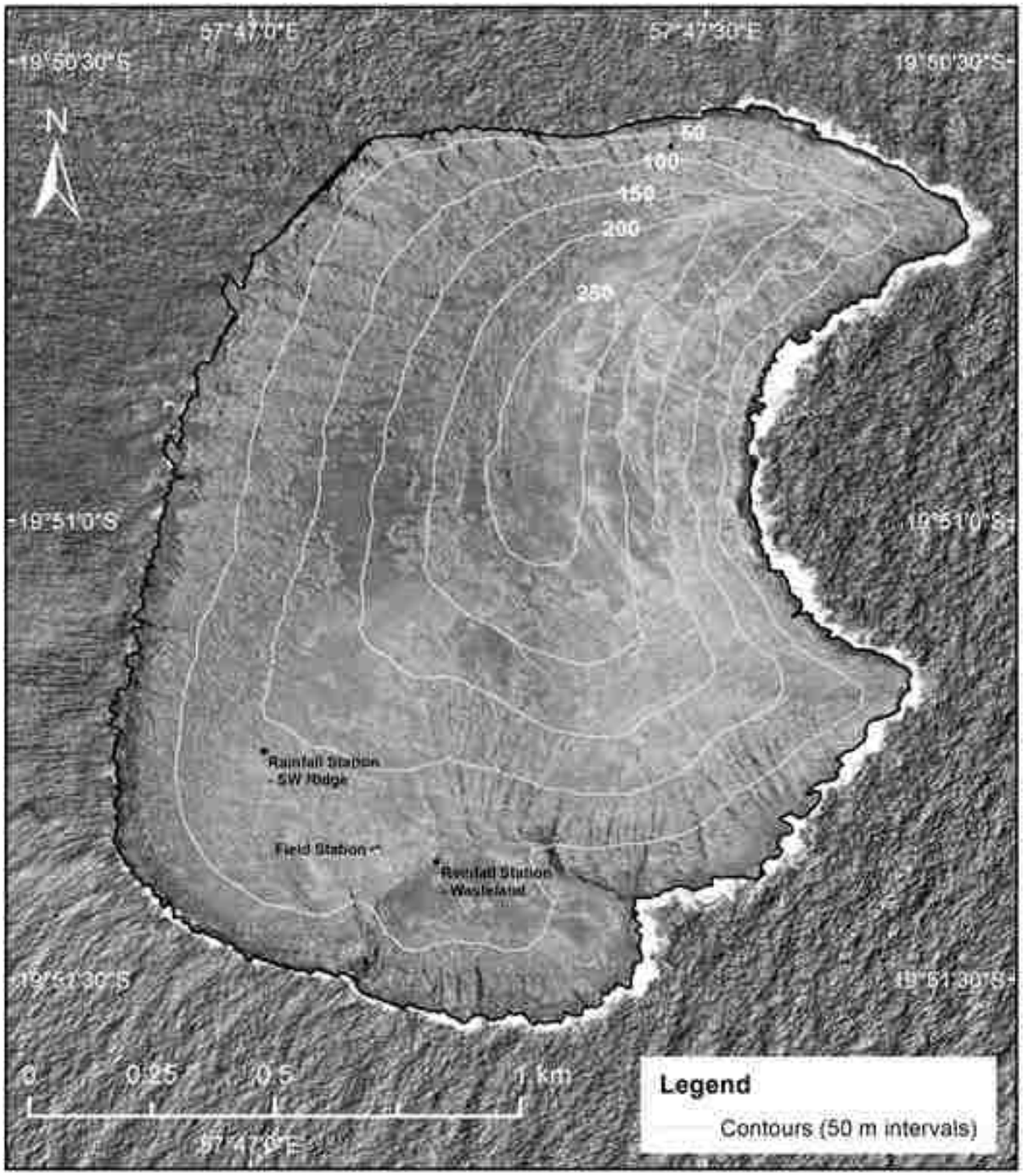

Figure 2.6: Satellite image of Round Island showing gully erosion and location of study sites.

Vegetation

According to Merton *et al.* (1989), vegetation on Round Island has significant conservational value. Unfortunately, the hardwood forest was lost (Bullock, 1977) and only two hardwood species Gagnebina pterocarpa and one individual of Fernelia buxifolia managed to survive on Round Island (Tatayah, 2010). Since 2000, a number of other hardwood species have successfully been re-introduced (Tatayah, 2010). The island is home to the last remnant of palm savannah, which was completely lost to mainland Mauritius. It is

home to the largest area of native vegetation in Mauritius and is the only relatively large island free of major woody species in the Mascarene group. A detailed analysis on the vegetation types on Round Island revealed seven distinct habitat types, described according to vegetation and substrate, they include; the open and closed palm savannah, mixed weed, herb-rich, rock slab, the "helipads" and the summit communities (Johnston, 1993) (Figure 2.7). Each vegetation type contains critically endangered species but perhaps the most valued is the closed and open palm forest (MWF, 2008). The one remaining individual of the hurricane palm (*Dictyosperma album var conjugatum)* found on Round Island is the last known wild individual of the taxon, which has fortunately been saved from extinction.

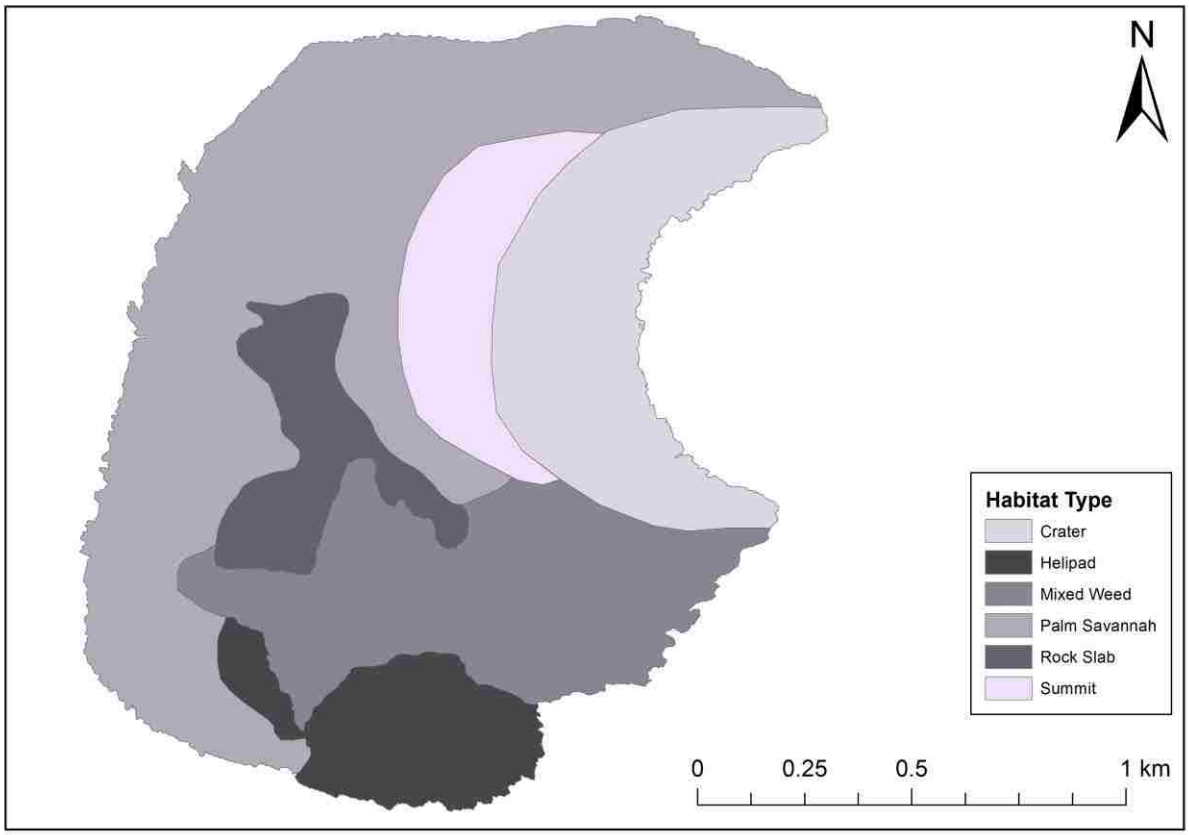

Figure 2.7: Map of habitat types of Round Island (Adapted from Johnston, 1993).

The Round Island Bottle Palm, (*Hyophorbe lagenicaulis)* is grown as an ornamental plant in Mauritius and all over the tropics. The place of origin of these individuals is unknown and the last wild population is restricted to Round Island. By 1988, the Bottle Palm population consisted of only 8 adult and 6 juvenile trees, which were lucky enough to survive the rabbit activity. Round Island supports at least ten threatened native plant species, including six which are endemic to Mauritius. The Blue Latanier (*Latania loddigeslii)* is the most abundant palm to be found on the western and northern slopes of Round Island (Figure

2.8) and is the largest population of its kind in Mauritius. A comprehensive list of plant species was compiled by the Edinburgh University expedition in 1975, which recorded 43 species (Bullock & North, 1975; 1984). Later, Wendy Strahm recorded 55 species in 1986 and Dulloo made a list of up to 60 species in 1993 (Bell *et al.*, 1994). Today, the number of recorded species has increased to 114 as documented by (Johansson, 2003). Vegetation communities on Round Island have managed to retain most of their original elements, although they have been severely modified by the introduction of mammals (herbivores) in the 1800's.

Figure 2.8: The Blue Latanier (*Latania loddigeslii*) found on the south-west ridge of Round Island. Note the steep slope gradient.

The introduction of goats and rabbits to Round Island between 1840 and 1865 (Bullock, 1977) greatly degraded the soil and vegetation. This lead to major reductions, and in some cases, extinction of some vegetation communities as well as leaving large areas of bare ground exposed due to the removal of vegetation (North & Bullock, 1986) (Figure 2.9). Once the removal of mammals was completed in 1986, a steady regeneration of vegetation has taken place and vegetation monitoring remains ongoing. In particular, the *Latania* species has shown a significant increase on the south-west slope. Ile Aux Aigrettes, off the south-west coast of Mauritius has acted as a nursery for propagation of critically endangered species, which at a later stage were reintroduced to Round Island as part of the management plan, with many reintroductions being successful (Khadun *et al.*, 2008).

Figure 2.9: Bare steps of tuff in the foreground with Mixed weed habitat which traps sediment, promoting vegetation growth in the background.

History and management of Round Island

Before humans colonised Mauritius in the 17th century, at least 15 land reptile species were present. Four species are now extinct and six are confined to the small islets off the north coast of Mauritius (Vinson & Vinson, 1968). According to Tatayah (2010), the first published biological report of the island is provided by J.A., Lloyd (Surveyor General and Civil Engineer), who spent one week on Round Island in December 1844 with several others (Lloyd, 1846). The primary goal of the landing party was to search for exploitable sources of guano on Round Island and Serpent Island. Lloyd (1846) notes that no significant deposits were found since the topography of the island coupled with the rainfall tend to wash most of the guano into the sea. This is an interesting early observation from a soil erosion perspective. Although Round Island was declared a nature reserve in 1957 under the Forests and Reserves Act No. 41 of 1983, a scientific expedition visited Round Island in 1975 and found that the introduction of goats and rabbits had destroyed most of the vegetation, threatened the survival of endemic reptiles and caused widespread soil erosion (Johnston, 1993).

Today, four of these species exist on Round Island making it the largest remnant of an ecosystem which contains some of the world's rarest palms and reptiles. Perhaps the most significant event in Round Island's recent history has been the extermination of goats and rabbits. Goats (*Capra hircus*) were first introduced to the island in 1844 (Cheke & Bour, 2014), by 1976 marksmen had shot all but two individuals and in 1979 the last goat was eradicated (Bullock & North, 1984). The rabbit (*Oryctolagus cuniculus)* population on Round Island was estimated at 2900 by 1982, which led to a markedly reduced amount of seedling lantan palms and a severely reduced ability for the palm savannah regeneration (Bullock *et al*., 1982). In 1986, the rabbits were eradicated from Round Island, making it the largest area within the Mascarene group that is free of introduced mammals. Along with the eradication of both goats and rabbits by 1986, vegetation monitoring, conservation and weed removal are currently on-going. The first management plan for Round Island was published in 1988 (Merton *et al.*, 1989), with a second version in 2009 (MWF, 2008).

From 1990 through to 1998, many management visits to Round Island took place with the aim of eradicating alien invasive plant species. In 1993, the Raleigh International Round Island expedition took place, which focused on surveying the small islands surrounding mainland Mauritius, this gave practical effect to the aims set forth by the management plan set out by Merton *et al.* (1989). Also during this period, Johnston (1993) carried out an extensive soil survey and experimental erosion control measures were put in place (Daszak, 1994). In terms of soil erosion, the management plan aims to gain a greater understanding of erosion processes on the island and implement soil conservation measures where possible. Previous methods of soil conservation have been implemented with success, soil traps have proven to be effective, although only at a local scale (Figure 2.10) The regeneration of *Latania loddigessii* and *Ipomea pes-caprae* have also shown positive results by reducing soil erosion within the gullies (Johnston, 1993).

Figure 2.10: Increased vegetation cover due to soil trap, used as a conservation method to prevent sediment from moving downslope.

Round Island is home to various rare species, such as the Round Island ground boa (*Casarea dussumieri*) (Figure 2.11). Unfortunately, the Round Island burrowing boa (*Bolyeria multocarinata*) is now considered extinct; having last been sighted in 1975. Soil erosion and a general decline in habitat quality have been blamed for the extinction of this boa. Two species of tortoise (*Aldabrachelys gigantea* & *Astrochelys radiata)* were introduced in 2007 as a restoration tool to replace a previously extinct species (Figure 2.12). The tortoise species act as ecosystem engineers, dispersing seed all over the island, and were introduced with the primary objective of influencing plant communities in a beneficial way (see Griffiths *et al*., 2010; Griffiths *et al*., 2012; Griffiths *et al*., 2013). Specifically, the tortoises eat and disperse large seeds from the endemic *Latania loddigesii* palm. Although it has been shown by Griffiths et al. (2010) and Griffiths et al. (2013) that the introduction of non-indigenous species, in this instance tortoises can have various beneficial ecological impacts, it is important to also consider that tortoises consume large amounts of vegetation and can leave

soils bare and susceptible to erosion (Griffiths *et al.*, 2010), leaving a question on the geomorphological impacts that the tortoises are having on Round Island.

Figure 2.11: A *Casarea dussumieri* ground boa on Round Island. Individual approximately 0.6 m in length.

Figure 2.12: An introduced *Aldabrachelys gigantean* tortoise on Round Island.

Round Island is also an important breeding site for various species of seabirds (Figure 2.13). Nesting occurs on the surface under small overhangs as well as in burrows. According to Tatayah (2010) the island has areas of soil accumulation which typically exhibit thick ground vegetation cover where Wedge-tailed Shearwaters *Puffinus pacificus* dig their nest burrows, but much of the deep soil described by Lloyd (1846) has since been lost. Burrowing seabirds have various geomorphological and ecological impacts on Round Island but these impacts have not yet been studied in detail.

Figure 2.13: A breeding pair of red-tailed tropicbirds (*Phaethon rubricauda*) on Round Island.

This chapter has provided relevant background information for this research. This includes information about the location, geological development of Round Island, the topography, climate with particular reference to rainfall and tropical cyclones. Pedology and geomorphology have also been discussed to provide context. Lastly, the vegetation and history of management was discussed. The next chapter will go on to discuss the methodology that was used in the study.

Chapter 3: Methodology

This chapter deals with the methods and materials used in the study. The research design is described followed by data sources and equipment used, the data and analysis that were undertaken. As stipulated in chapter 1, the objectives were set forth as follows:

- Establish the difference in rainfall characteristics between two environmental monitoring stations
- Determine the kinetic energy and erosive characteristics of individual rainfall events
- Determine the relationship between rainfall and sediment movement
- Establish monthly sediment movement rates
- Establish sediment characteristics through particle size analysis

Data sources/Study sites

To investigate the characteristics of individual rainfall events on Round Island, high resolution automatic rainfall data from November 2014 to October 2016 (700 record days) was obtained from the rainfall stations on Round Island. Two sites were selected for the installation of automatic rainfall stations, one is located on the "Wasteland" (69 m a.m.s.l) and the other is situated on the South West Ridge (95 m a.m.s.l) (Figure. 3.1). The environmental monitoring stations installed on the island have rainfall gauges that log total rainfall every 15 minutes on a tipping resolution of 0.2 mm rainfall. The stations also record air, rock and soil temperature, soil moisture, wind speed and direction, as well as solar radiation.

Figure 3.1: Environmental monitoring station located at the Wasteland study site.

Data collection techniques

Atmospheric Monitoring

Pace Scientific™ rainfall buckets (Figure. 3.2) and data loggers were installed to monitor rainfall patterns as well as gauge the intensity of individual rainfall events. To conduct this study, rainfall data is recorded at a high temporal resolution to accurately calculate rainfall erosivity (Yin, 2007). Therefore, rainfall is measured in increments of 0.2 mm. Rainfall buckets were secured to bedrock surfaces with concrete nails and are a sufficient distance from any other obstructions that may influence readings by potentially adding splash from other surfaces. The weather data was downloaded annually when researchers visited Round Island. Data was then imported into an Excel spreadsheet for analysis, providing an overall view on the climate and environmental conditions of the island.

Figure 3.2: Automatic rainfall tipping bucket (0.2 mm resolution) attached to environmental monitoring station.

Sediment Transport

A series of Gerlach troughs (Figure. 3.3a and b) were installed to capture surface sediment transported by runoff, which was used to document sediment yields and determine the particle size distribution. Soil samples were collected monthly from January 2015 to September 2016 and stored in plastic bags (Figure. 3.4).

Figure 3.3a: View looking east. Note the mechanical soil erosion structures and Gerlach trough in the foreground, the person for scale and the Wasteland rainfall station in the background.

Figure 3.3b: Gerlach trough with captured sediment.

Figure 3.4: Monthly sediment samples stored in bags for analysis. Wet sediment was left to dry in the sun for several hours.

Eight Gerlach troughs (Figure. 3.5) were installed across the island. A total of 168 soil samples were collected during the study period. Soil particle size analysis was carried out on a total of 40 samples. These samples were chosen from the months with the highest sediment yields, which were January and February 2015 and January, February, March of 2016. Particle size analysis was conducted for each of the eight Gerlach trough sites for each month stated above. The results of the soil analysis were used to compare erosion processes on Round Island in relation to rainfall characteristics. Each sample site's coordinates were recorded with a Garmin G62 Global Positioning System (GPS). The catchment area above each Gerlach trough was mapped (Figure 3.6). The mapped area will be used to determine the weight of sediment transported in relation to the area of the catchment. Gerlach troughs (A5 and A6) were located in the same catchment with A5 located at the exit of the catchment. Other parameters recorded in the field were the proximal vegetation cover, elevation, aspect and slope gradient.

Figure 3.5: The eight sample sites with Gerlach trough installed.

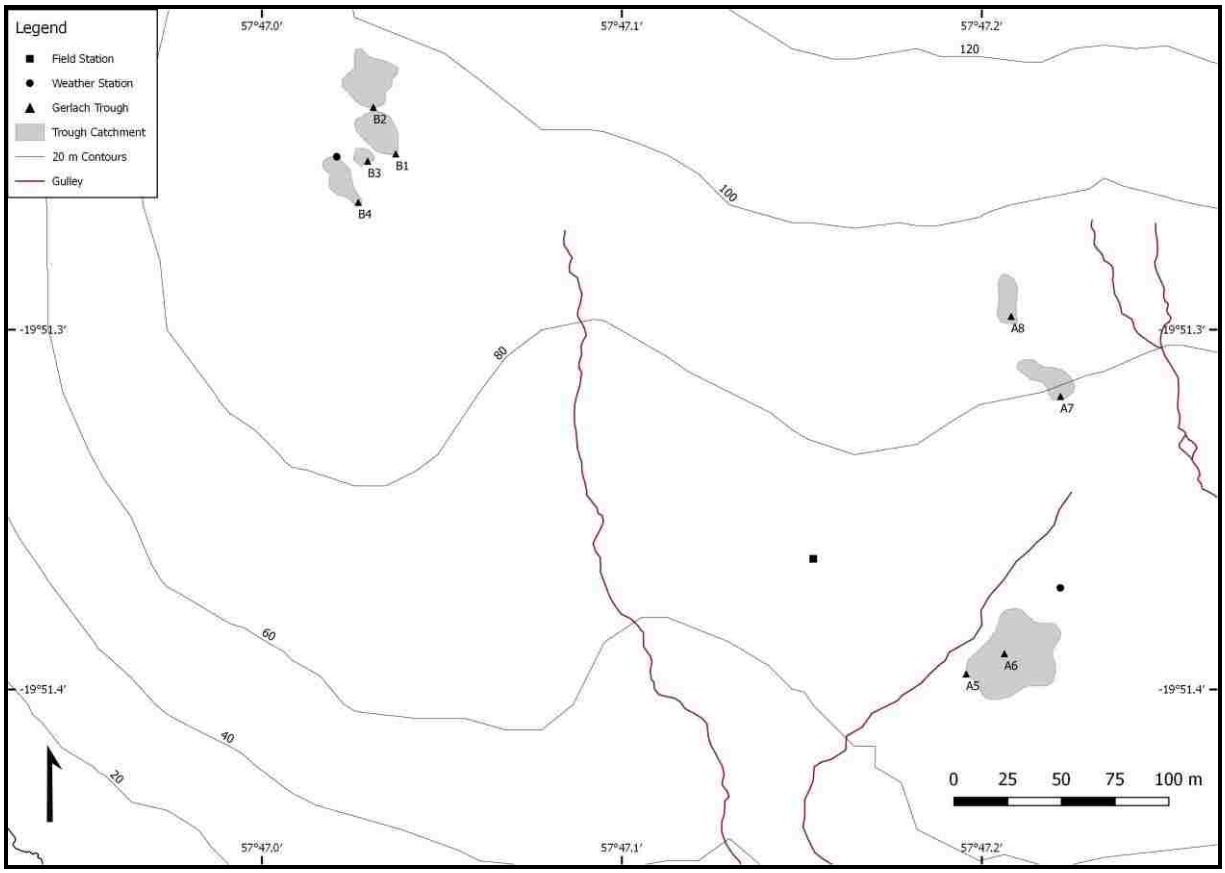

Figure 3.6: Map of Gerlach trough catchment areas.

Particle size analysis was conducted to determine sediment characteristics (Figure 3.7). Manual sieving was done for 3 minutes per soil sample using a Haver & Boecker sieve set with different size classes (i.e. <0.045 - 2 mm) on the Wentworth scale. The percentage of sample weight remaining on each sieve was weighed to conduct a particle size analysis. Data was input into a Gradistat Excel spreadsheet, which described the shape of particle size distribution of the samples (i.e. mean, skewness and sorting).

Figure 3.7: Particle size analysis using 2 mm sieve. Note, a large amount of gravel left behind.

Defining an erosive event

The rainfall data was extracted from the raw dataset and used to calculate the rainfall erosivity index. An erosive event was initially defined as when rainfall intensities are larger than 25 $mm.h^{-1}$ in order to move significant amount of soil (Wischmeier & Smith, 1958). Similarly, Stocking & Elwell, (1976) concluded that "a maximum 5-minute intensity exceeding 25 $mm.h^{-1}$ and a total rainfall above 12.5 mm can be considered an erosive event". Thus, for a rainfall event to be considered erosive in nature, a peak 5-minute intensity of at least 25 $mm.h^{-1}$ must be achieved, a two-hour rain-free interval should be observed between erosive events as well as a total rainfall exceeding 12.5 mm within 30 minutes. Since rainfall data was collected every 15 minutes, entries were multiplied by 4 to obtain the maximum intensity per hour. Entries found with a 15-minute intensity of more than 6.25 mm were extracted from the raw data and used to calculate kinetic energy and the Erosivity Index (e.g. EI_{15} and EI_{30}) (Wischmeier & Smith, 1978; Diodato, 2005; Angulo-Martínez & Beguería, 2009). The definitions above have been used in numerous studies to identify erosive events on Mauritius including Mongwa (2011); Anderson (2012); Nel *et al.* (2013) and Nel *et al.* (2016).

Data analysis and interpretation

As mentioned in the above section, data processing was carried out by analysing the data once it was imported into an Excel Spreadsheet. Focus was given to identifying individual rainfall events, recording the depth of rainfall (mm), duration of rainfall events, and the maximum 15-minute intensity ($mm.h^{-1}$). Events that met the criteria stipulated above were extracted from the data and used to determine the kinetic energy and erosivity. The following section explains how the kinetic energy of a rainfall event is determined as well as how the erosivity index (EI_{30}) is calculated using the total storm kinetic energy.

Determining rainfall event kinetic energy and erosivity

When determining the erosivity index, the R-factor is calculated as follows (Renard *et al.*, 1997):

$$R = \frac{1}{N}\sum_{j=1}^{n}\sum_{k=1}^{m}(E)_k\,(I_{30})_{30j} \qquad (1)$$

where E is the total erosive event kinetic energy ($MJ.h^{-1}$), I_{30} is the maximum 30-minute rainfall intensity ($mm.h^{-1}$), j is an index of the number of years used to produce the average, k is an index of the number of erosive events per annum, N is the number of years used to obtain the average n, and m is the number of erosive events in each year (Wischmeier & Smith, 1978).

To calculate the erosivity index, we need to know the product of the total erosive event kinetic energy (E) ($MJ.h^{-1}.mm^{-1}$) and the maximum amount of rainfall (I_{30}) in a 30-minute period which is expressed in millimetres per hour ($mm.h^{-1}$). Santosa *et al.* (2010) describes the formula as:

$$E = \sum_{j=1}^{m} e_r \Delta V_r \qquad (2)$$

where e_r is the rainfall energy per unit depth of rainfall per unit area ($MJ.ha^{-1}.mm^{-1}$) and ΔV_r is the depth of rainfall (mm) (Brown & Foster, 1987; Santosa *et al.*, 2010). Although rainfall intensity can be measured directly, measurements of kinetic energy and raindrop sizes are

mostly unavailable. Since an erosive event with higher intensity is generally associated with an increase in drop size and terminal velocity, a number of formulae have been created that have attempted to calculate the rainfall intensity-kinetic energy relationship (R-E_K). Wischmeier & Smith (1958) proposed the relationship as a logarithmic function in the form:

$$E_K = 11.87 + 8.73Log_{10}R \quad (3)$$

where intensity (R) is in mm^{-1}. During a study in Zimbabwe, Elwell and Stocking (1973) show that kinetic energy from rainfall in subtropical climates can be predicted by the equation:

$$E_K = (29.82 - 127.51/I) \text{ in } J.m^{-2}.mm^{-1} \quad (4)$$

where the intensity I is in mm^{-1}. This equation has been adopted for use in the SLEMSA (Soil Loss Estimation Model for Southern Africa) as well as in a study by Nel & Sumner (2007) which looked at the intensity, energy and erosivity in the Drakensburg, South Africa. Van Dijk *et al.* (2002) critically appraised the literature related to the R-E_K relationship, and based on the average parameter values derived from the available data, found that the general equation to predict storm kinetic energy content from rainfall intensity data is:

$$E_K = 28.3\ [1\text{-}0.52 \exp (\text{-}0.042R)] \quad (5)$$

where R = rainfall intensity in mm h^{-1}.

Any of the equations above can be used to estimate the kinetic energy contents on Round Island, however, to remain consistent with global studies, the equation by Van Dijk *et al.* (2002) (5) will be used in this study. The formula proposed by Van Dijk et al., (2002) makes use of the 15-minute kinetic energy content derived from rainfall intensity. To determine the total kinetic energy during each rainfall event ($J.m^{-2}$), each of the 15-minute kinetic energy values for an event need to be summed. A uniform drop size is assumed for analysis purposes. Energy generated during each erosive rainfall event is calculated through the 15-minute kinetic energy content (I_{15}), which is then multiplied by the quantity of rain (mm) received for that specific 15-minute interval. These values will then be added together to give the total kinetic energy for the rainfall event ($J.m^{-2}$) (Nel & Sumner, 2007; Nel *et al.*,

2013). An example of how the kinetic energy is calculated using formula (5) can be seen below (Table 3.1):

$$E_K=28.3\ [1-0.52\ \exp\ (-0.042x11.2)]\ x\ 2.8$$

$$E_K=53.4972$$

Table 3.1: Example storm and how kinetic energy is calculated.

Time	Rainfall	I_{15}	Kinetic Energy ($J.m^{-2}$)
11:15	2.8	11.2	53.49720571
11:30	9.2	36.8	231.4976256
11:45	3.6	14.4	72.94450093
12:00	0.8	3.2	12.34774381
12:15	7.6	30.4	183.8841964
12:30	0.6	2.4	8.99703646
12:45	0.4	1.6	5.816167843
13:00	0.0	0	0
13:15	0.0	0	0
13:30	1.0	4	15.85977297
13:45	0.0	0	0
14:00	1.2	4.8	19.5249844
	Total Event K_E		**604.4**

Wischmeier & Smith (1978) concluded that erosivity can be determined by the product of the total kinetic energy (K_E) of the storm multiplied by the storm maximum 30-minute intensity (I_{30}). This equation has been used to calculate erosivity on Mauritius (Le Roux, 2005) as well as globally as part of the Revised Universal Soil Loss Equation (RUSLE), reflecting the combined potential of raindrop impact and turbulence created by overland flow. To remain consistent with other erosivity studies in Mauritius (Le Roux, 2005; Le Roux *et al.*, 2005; Nigel & Rughooputh, 2012; Anderson, 2012; Mongwa, 2011; Nel *et al.*, 2012, 2013; 2016), the rainfall erosivity potential was determined by the product (EI_{30}) of each erosive event ($J.mm.m^{-2}.h^{-1}$).

Determining the relationship between rainfall and sediment movement

Globally, there are conflicting studies with regards to the effect of individual rainfall events on soil erosion, with either very intense rainfall events producing much of the soil loss or the cumulative influence of more frequent, low intensity storms (Hudson, 1971; Rydgren, 1996; Boardman & Favis-Mortlock, 1999; Trustrum *et al.*, 1999). Using the equations

discussed above, the kinetic energy as well as erosivity from each month during the study period were calculated. These figures were compared to the monthly sediment weights and monthly sediment weights in relation to catchment area to establish the relationship between sediment movement rates and storm erosivity. It is hypothesised that extreme events are producing the bulk of the erosivity (Nel *et al.,* 2013). To test this hypothesis, all the events meeting the parameters set above were isolated and compared to the annual rainfall kinetic energy, erosivity totals and sediment yields.

Issues of reliability and validity

Inherent limitations in the models used need to be considered: Renard *et al.* (1997) state that records of more than 20 years should be used when calculating the rainfall erosivity of a region. This allows for the consideration of cyclic changes in rainfall that are associated with the El Niño-Southern Oscillation (ENSO) phenomenon (Hoyos *et al.,* 2005). This is an important consideration, especially since rainfall totals would be significantly less if a below average number of tropical storms occur during the study period. Since rainfall data on Round Island has only been collected in recent years, this project is limited in representing long term erosivity, however, the main objective remains, to determine the nature of erosive rainfall events and their effect on sediment movement rates. Therefore, the data collected for the study are deemed sufficient for this investigation.

Other limitations include:

- The formulae do not account for erosion resulting from rainfall that is less than the set parameters (for example saturation overland flow which results from long duration rainfall with low intensities).
- Because EI_{30} is an average that is calculated, inconsistent high or low values that may have been recorded can skew the results.
- Due to the prominence of the South-East Trade Wind, horizontal rain may be considered a limitation as the amounts of rainfall captured by the buckets could be less, particularly in the winter months.

Due to the nature of the study (many of the data collection instruments are out in the field and exposed to the elements), technical issues did occur. The environmental monitoring station on the South-west Ridge malfunctioned shortly after it was reset in October 2015, this

resulted in one of the data loggers not recording. Fortunately, the data logger recording rainfall continued operating throughout the study. Severe corrosion was observed on the environmental monitoring station tripod at the South-west Ridge, while the “Wasteland” station only needed minor maintenance. For the period of the study, rainfall data collection was continuous, with no sign of missing or incomplete data. Blockages and instrument malfunction can lead to inaccuracies and the problem of not being able to compare individual rainfall events to one another, fortunately this did not occur during the study period.

In conclusion, the instrumentation used for collecting and analysing the data in this project as well as the methodology are described. A number of formulae necessary for this project have been provided and explained. The results of the data analysis are presented in the following chapter.

Chapter 4: Results

This chapter presents the results of the data analysis following the methodology that was set out for the objectives of the study.

Round Island rainfall characteristics

The rainy season on Round Island is typically concentrated between December and April (Figure 4.1). From the data collected during the study period, above normal rainfall was also recorded in June 2015 (approximately 80 mm) which could be attributed to local convection and cold frontal activity, which confirms the findings by (Padya, 1984), Hauptfleisch (2016) and Nel *et al.* (2016). Data collection commenced in November 2014 and terminates in October 2016 for this study, thus the data only captures one full calendar year, namely 2015. In 2015, total annual rainfall for the Wasteland and South-West ridge was 715.2 mm and 682 mm, respectively. Rainfall totals from the two stations were considerably less than expected (a reduction of approximately 20%) when compared to earlier literature by the (MWF, 2011), which states a mean annual rainfall of 866 mm. This may be indicative of a below normal rainfall for 2015.

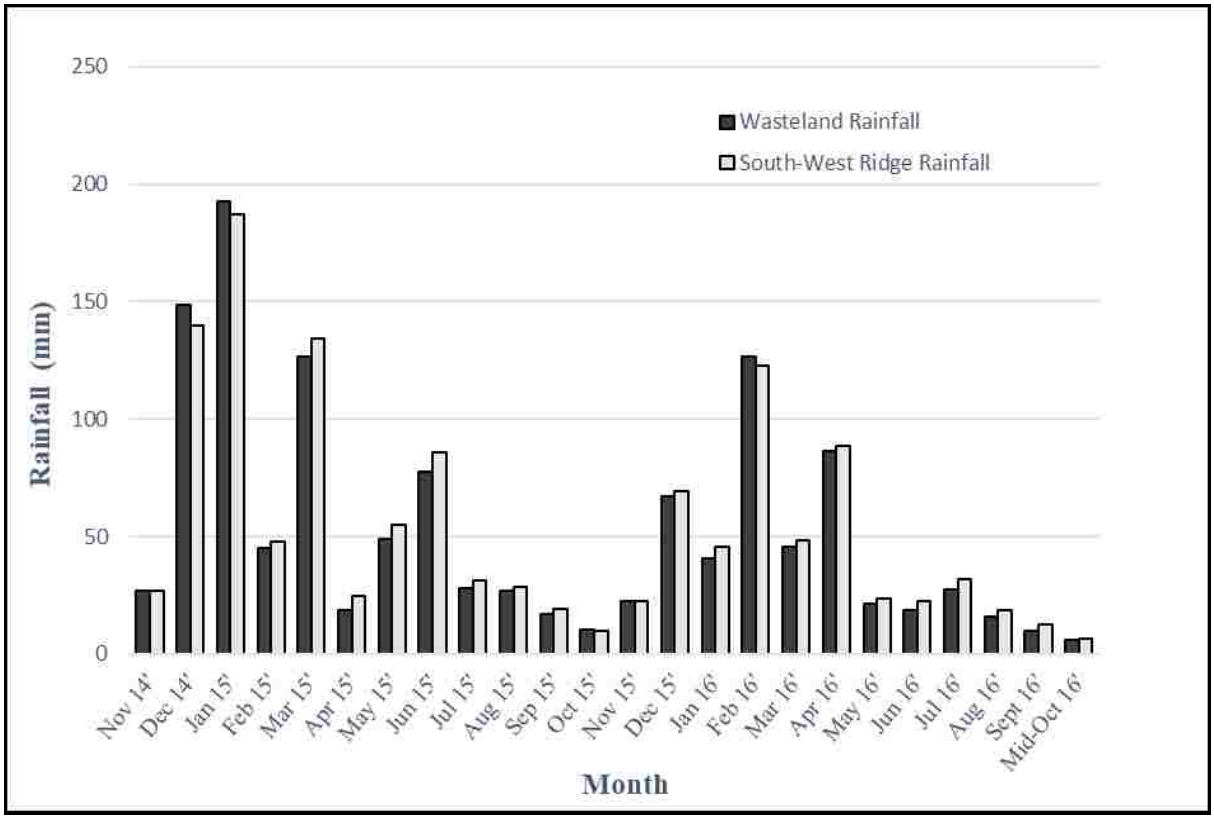

Figure 4.1: Monthly distribution of rainfall per station over study period.

The total rainfall experienced by each environmental monitoring station during the study period and the total depth of erosive rainfall recorded are indicated in Figure 4.2. When applying the definition set forth in Chapter 3, the data collected from Round Island for the period November 2014 to October 2016 indicated that a total of 22 and 15 erosive rainfall events occurred at the Wasteland and South-West ridge study sites, respectively (Table 4.1). The Wasteland station recorded a total of 1302.6 mm rainfall for the study period, of which 286.6 mm was deemed erosive (Table 4.1). The South-West ridge station recorded a total of 1254.8 mm rainfall over the study period, of which 232.2 mm was deemed erosive. The percentage of erosive rainfall experienced by the Wasteland and South-West ridge are 22% and 18.50%, respectively.

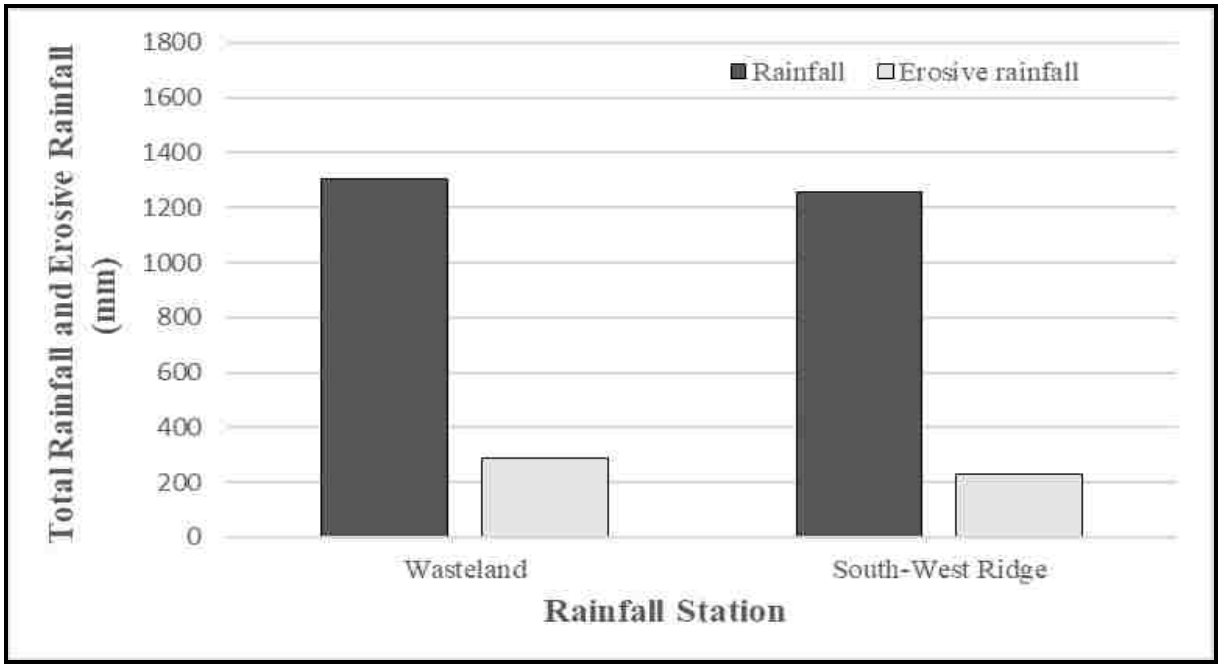

Figure 4.2: Total rainfall and total depth of erosive rainfall (mm) over the study period.

Table 4.1: Total rainfall and total depth of erosive rainfall (mm), percentage of erosive rainfall and the total number of erosive events experienced by each station over the study period.

Rainfall characteristics	Wasteland	South-West Ridge
Rainfall	1302.6	1254.8
Erosive rainfall	286.6	232.2
% Erosive rainfall	22.00%	18.50%
Number of events	22	15

For reference, the shape of the distribution of rainfall characteristics have been plotted in box and whisker plots below (Figure 4.3) and will be discussed in further detail in the section below.

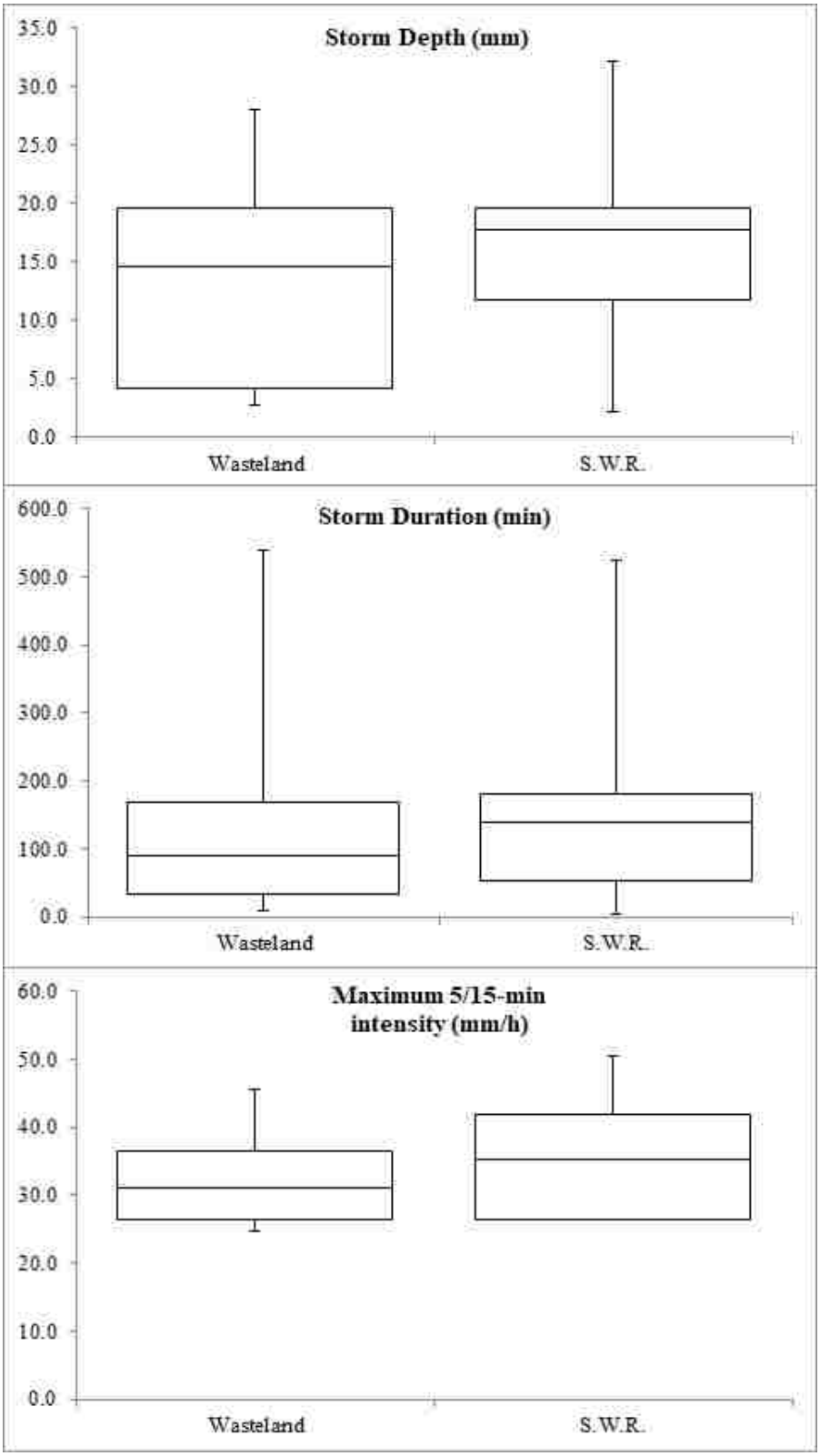

Figure 4.3: Box and whisker plots displaying shape and distribution of rainfall characteristics per study site.

The number of erosive events received annually for each station is displayed in Figure 4.4. There is a 26 m height difference and a 400 m horizontal equivalent between the two stations, however, the Wasteland station received slightly more erosive rainfall events annually. When comparing an event between the two stations, the intensity found at the South-West ridge was often lower than at the Wasteland, and, on several occasions, intensities fell below 25 $mm.h^{-1}$ as defined in the methodology. The Wasteland station experienced the higher number of erosive events recorded during one year (2016), with a total of 12 events. Overall, rainfall intensities on the eastern side of the island exceed the 25 $mm.h^{-1}$ parameter on more occasions. This could be due to the presence of the South-East Trade Winds, causing the majority of rainfall events to begin on the eastern side of the island. Since the rainfall moves in an East-West direction, by the time it reaches the South-West ridge rainfall station, it has dissipated slightly, resulting in less kinetic energy. Although the eastern side of the island recorded a higher total number of erosive events over the study period, some exceptions do occur, possibly due to the presence of nearby cyclones off the western coast of the island. On at least six occasions rainfall intensities were significantly higher at the South-West ridge rainfall station. One such event occurred in February 2016, where the South-West Ridge had rainfall intensities of 26.4 $mm.h^{-1}$ and the Wasteland received a maximum intensity of only 19.2 $mm.h^{-1}$. The South-West ridge also experienced the highest single rainfall intensity recorded during the study period (50.4 $mm.h^{-1}$), where in the same storm the Wasteland station recorded 39.2 $mm.h^{-1}$.

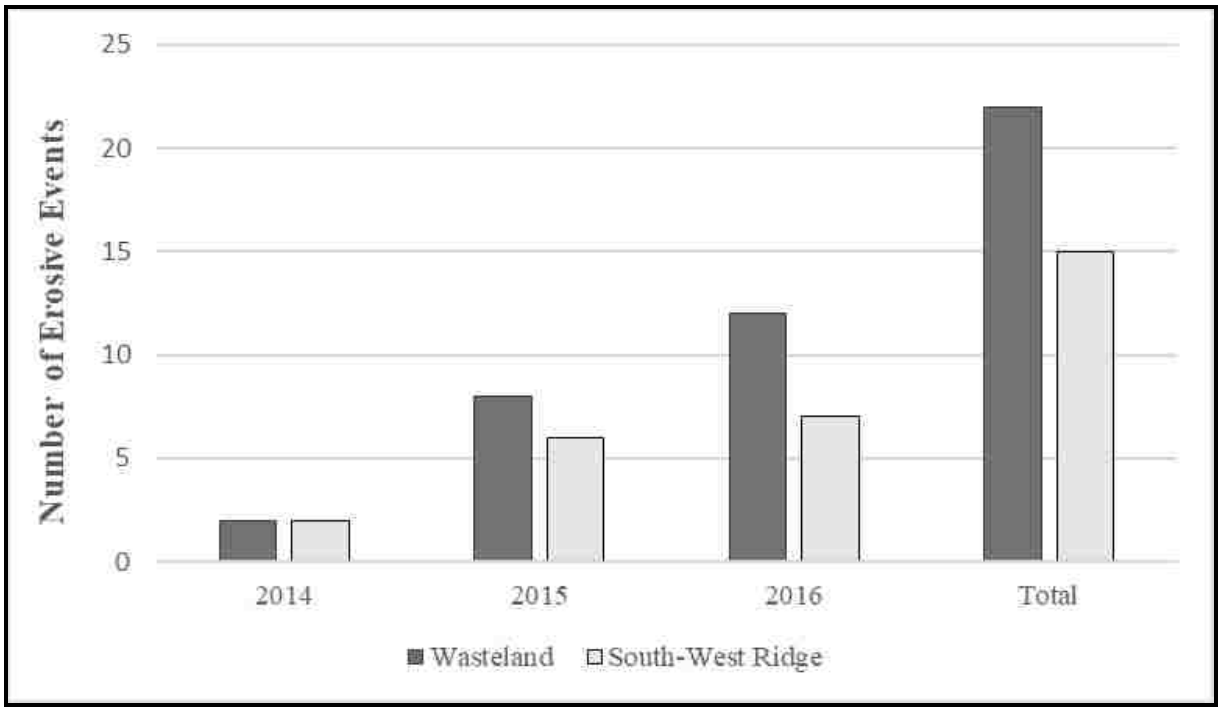

Figure 4.4: Annual erosive event totals for each station 2014-2016.

Investigation of the average number of erosive events experienced at both stations for each month during the study period (Figure 4.5) reveals that the month of March has, on average, the highest number of erosive events, even though, on average, less rainfall was received during this month (Figure 4.6). Besides a single event during the months of June and July, the dry period had no erosive events.

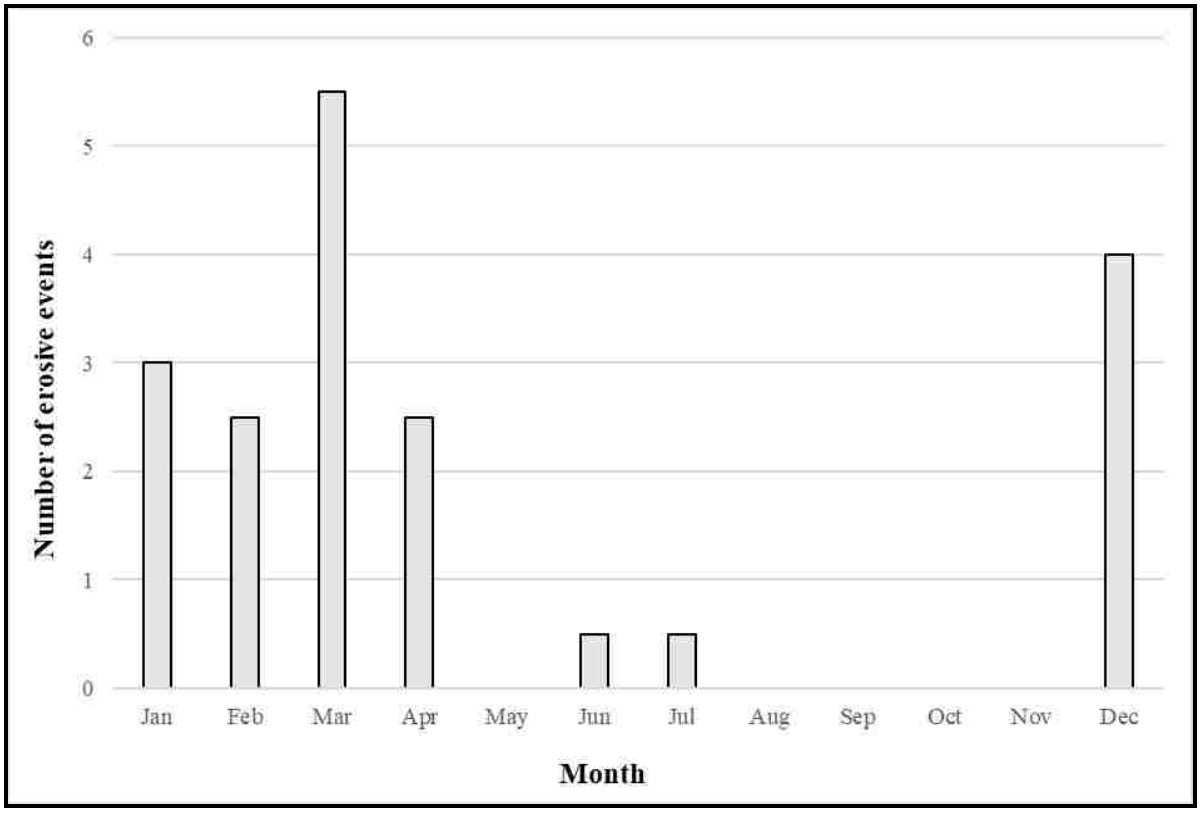

Figure 4.5: Average number of erosive events experienced by each station during each month for study period.

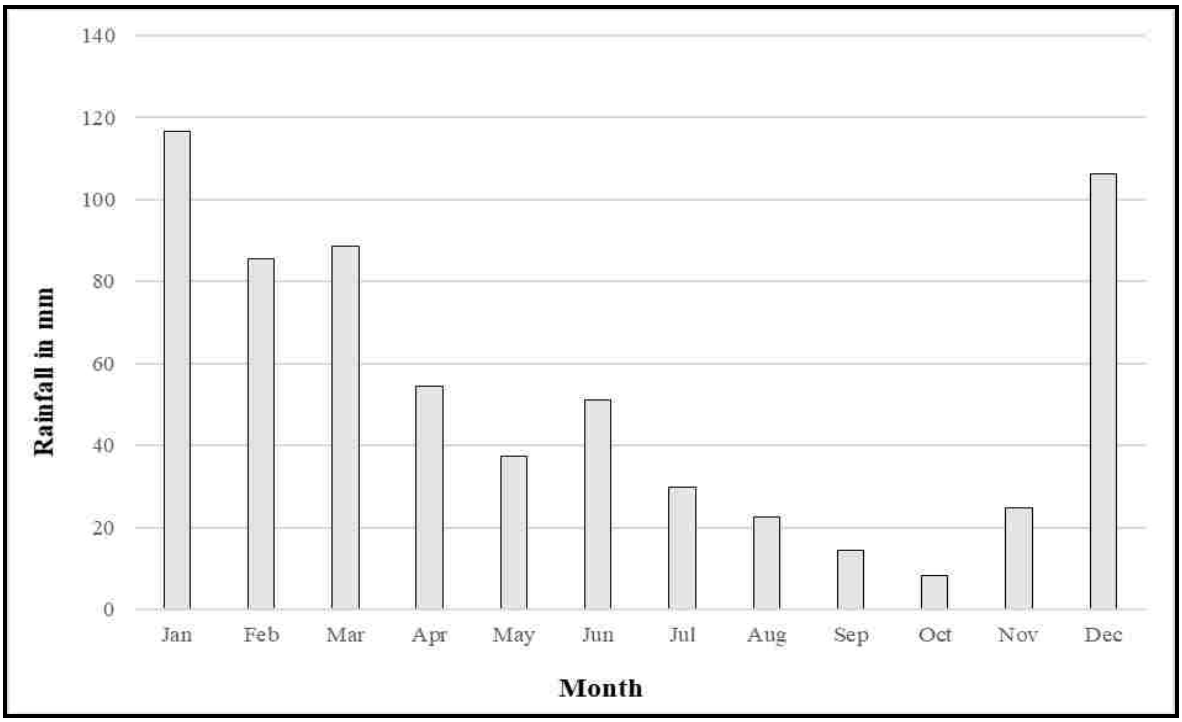

Figure 4.6: Mean monthly rainfall for study period.

Erosive characteristics of rainfall events

The characteristics of each erosive rainfall event measured at the Wasteland, with corresponding rainfall characteristics measured at the South-West ridge, are given in Table 4.2. For reference, the shape of the distribution of erosive rainfall characteristics have been plotted in box and whisker plots below (Figure 4.7) and will be discussed in further detail in the section below.

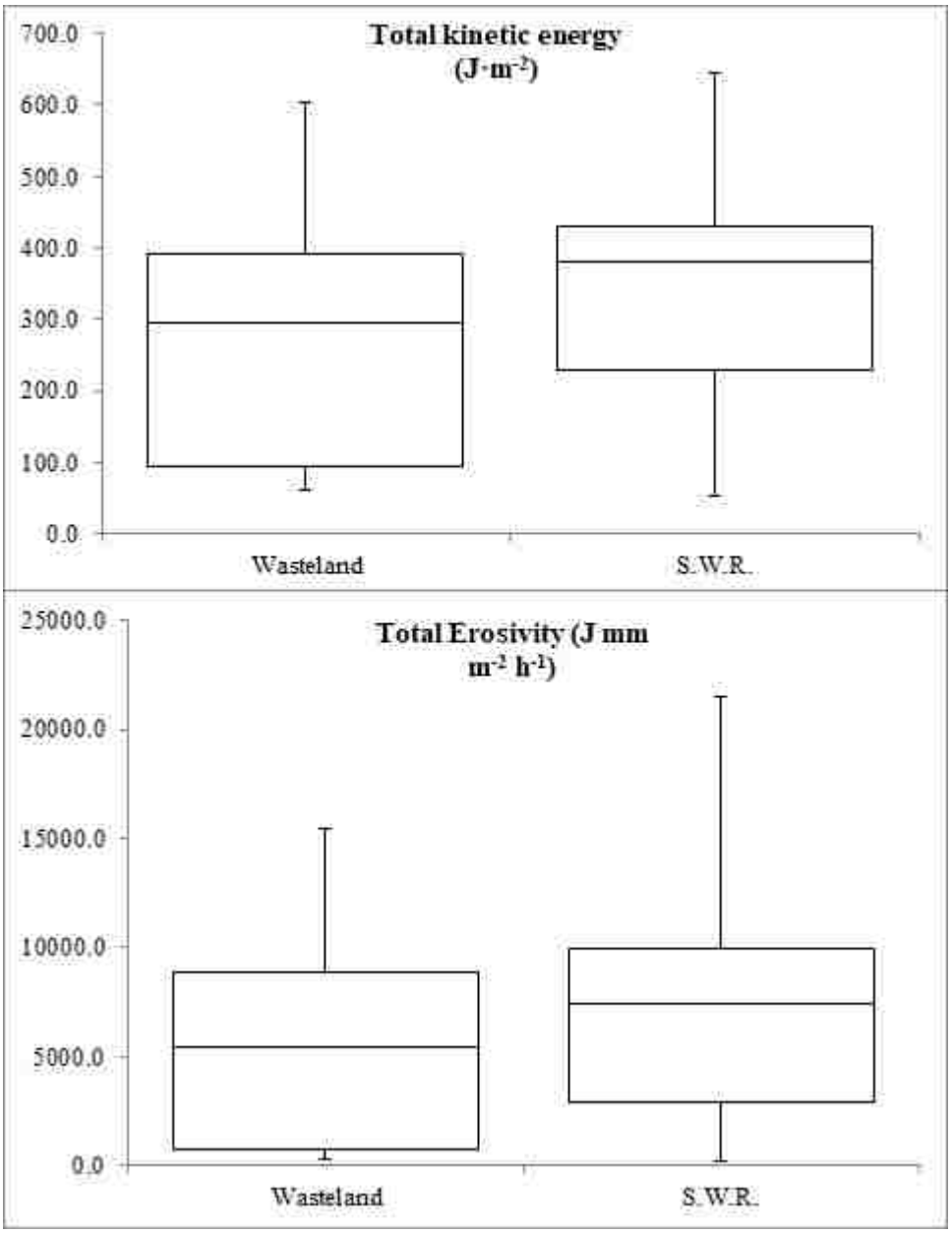

Figure 4.7: Box and whisker plots displaying shape and distribution of erosive rainfall characteristics per study site.

The maximum kinetic energy produced during any individual storm was 645.1 $J \cdot m^{-2}$, recorded at the South-West ridge. The storm with the lowest kinetic energy was also recorded at the South-West ridge (51.6 $J \cdot m^{-2}$). Mean kinetic energy for all erosive events was 263.5 $J \cdot m^{-2}$ and 331.2 $J \cdot m^{-2}$ for the Wasteland and South-West ridge, respectively (Table 4.3). Median kinetic energy for all erosive events was 296.5 $J \cdot m^{-2}$ and 380.0 $J \cdot m^{-2}$ for the Wasteland and South-West ridge, respectively (Table 4.3). Despite the two stations being located relatively close to one another, there is a considerable difference in mean kinetic energy. In terms of erosivity, the maximum erosivity produced during an individual rainfall

event was 21,516.3 J.mm.m^{-2}.h^{-1}, recorded at the South-West ridge. The rainfall event with the lowest erosivity (226.9 J.mm.m^{-2}.h^{-1}) was also recorded at the South-West ridge. Mean erosivity was recorded at 5441.6 J mm.m^{-2}.h^{-1} and 7630.9 J.mm.m^{-2}.h^{-1} for the Wasteland and South-West ridge, respectively. The South-West ridge recorded significantly higher erosivity, indicating a correlation between storm kinetic energy and erosivity. A statistically significant correlation (ρ= 0.01; r= 0.87) is evident between erosivity and storm depth, whereas a lower correlation (ρ= 0.01; r= 0.55) exists between erosivity and storm duration. For example, event number four at the South-West ridge had a storm duration of 75 minutes and a total storm erosivity of 21,516.3 J.mm.m^{-2}.h^{-1}. This is significantly higher than storm number two, which had a storm duration of 525 minutes, but a total erosivity of only 19,094.3 J.mm.m^{-2}.h^{-1}. This is an initial indication that erosive events with long duration may not necessarily produce maximum erosivity. In the case of storm number four, rainfall intensity was a significant factor in the production of erosivity.

Overall erosive rainfall event attributes for each station during the study period are given in Table 4.3. As discussed above, the Wasteland experienced the higher amount of erosive rainfall, a higher amount of erosive rainfall events and therefore received a higher overall kinetic energy and total erosivity. However, the difference in total erosivity between the two stations was only 5251 J.mm.m^{-2}.h^{-1}, which is interesting in terms of the concepts of frequency versus magnitude of climatic phenomena. The South-West ridge station saw far fewer erosive events when compared to the Wasteland station but the South-West ridge experienced more intense rainfall during the 15 events that occurred there.

Table 4.4 outlines the attributes of individual erosive rainfall events at each station. The South-West ridge station experienced the highest storm depth of 32.2 mm, while the Wasteland station reached a maximum of 28 mm. Although the Wasteland recorded the longest rainfall duration (540 minutes), the South-West ridge had the highest mean duration of 146.3 minutes. Maximum as well as mean rainfall intensity were achieved at the South-West ridge with 50.4 mm.h^{-1} and 35.5 mm.h^{-1}, respectively. This trend continued for the attributes of kinetic energy as well as erosivity. This again indicates that kinetic energy and erosivity have a relationship with rainfall depth and rainfall intensity but not rainfall duration.

Table 4.2: Characteristics of erosive rainfall events measured at the Wasteland and South-West Ridge monitoring stations with the highest total from each attribute highlighted.

Event No. & Date	Station name	Storm Depth (mm)	Storm Duration (min)	Maximum 5/15-min intensity (mm/h)	Total kinetic energy ($J \cdot m^{-2}$)	Total Erosivity ($J\ mm\ m^{-2}\ h^{-1}$) (EI_{30})
1 - 12/19/2014	Wasteland	14.6	30	36.8	352.2	10,285.4
	S.W.R	15.4	30	46.4	382.0	11,764.7
2 - 12/25/2014	Wasteland	28	540	31.2	543.1	13,468.4
	S.W.R	32.2	525	40.8	645.1	19,094.3
3 - 1/9/2015	Wasteland	15.2	90	30.4	333.3	7,998.0
	S.W.R	18.4	90	44	432.3	11,587.0
4 - 1/22/2015	Wasteland	15	60	39.2	345.7	9,126.7
	S.W.R	21.2	75	50.4	532.6	21,516.3
5 - 3/7/2015	Wasteland	20.4	165	32.8	440.6	10,749.6
	S.W.R	17.8	165	35.2	380.0	8,359.8
6 - 3/8/2015	Wasteland	24.4	360	24.8	455.5	8,198.8
	S.W.R	.	.	.	.	.
7 - 3/11/2015	Wasteland	27.2	180	36.8	604.4	15,471.9
	S.W.R	20.8	180	27.2	430.4	7,747.9
8 - 6/24/2015	Wasteland	8.6	105	25.6	182.3	2,625.2
	S.W.R	.	.	.	.	.
9 - 12/23/2015	Wasteland	26	275	33.6	514.4	10,082.1
	S.W.R	22.4	270	26.4	433.3	7,453.0
10 - 12/29/2015	Wasteland	2.8	10	26.4	62.0	347.4
	S.W.R	2.2	5	26.4	51.6	226.9
11 - 1/30/2016	Wasteland	20.4	150	31.2	403.6	6,618.9
	S.W.R	18	145	26.4	350.4	5,325.9
12 - 2/8/2016	Wasteland	5.2	45	26.4	101.8	936.7
	S.W.R	.	.	.	.	.
13 - 2/10/2016	Wasteland	14.6	215	45.6	300.1	5,881.8
	S.W.R	15.6	220	40.8	324.7	6,882.8
14 - 2/11/2016	Wasteland	4	25	26.4	82.0	656.0
	S.W.R	.	.	.	.	.
15 - 2/15/2016	Wasteland	.	.	.	.	.
	S.W.R	8.8	140	26.4	173.4	1,109.8
16 - 3/3/2016	Wasteland	2.8	30	26.4	62.0	347.4
	S.W.R	3	30	26.4	64.6	387.6
17 - 3/7/2016	Wasteland	3.8	10	40.8	93.7	712.2
	S.W.R	3.8	10	40.8	93.7	712.2
18 - 3/8/2016	Wasteland	4	90	26.4	80.5	483.2
	S.W.R	.	.	.	.	.
19 - 3/11/2016	Wasteland	10	90	31.2	201.7	3,065.4
	S.W.R	.	.	.	.	.
20 - 4/19/2016	Wasteland	4.6	60	31.2	98.7	868.4
	S.W.R	.	.	.	.	.
21 - 4/28/2016	Wasteland	14.6	150	28.8	292.9	4,921.3
	S.W.R	18	130	43.2	388.4	7,612.3
22 - 4/29/2016	Wasteland	17	170	38.4	336.1	6,318.5
	S.W.R	14.6	180	31.2	285.6	4,683.6
23 - 7/10/2016	Wasteland	3.4	15	36	81.2	551.9
	S.W.R	.	.	.	.	.
TOTAL	**Wasteland**	**286.6**	**2865**	.	**5967.8**	**119,715.3**
	S.W.R	**232.2**	**2195**	.	**4968.0**	**114,464.2**

Table 4.3: Erosive event attributes at the Wasteland and South-West Ridge rainfall stations over the study period with mean and median (in brackets).

Station name	Total rainfall (mm)	Erosive Rainfall (mm)	% Erosive rainfall	Number of Events	Total duration (min)	Mean duration (min)	Total Kinetic Energy ($J \cdot m^{-2}$)	Mean Kinetic Energy ($J \cdot m^{-2}$)	Total Erosivity ($J\ mm\ m^{-2}\ h^{-1}$)	Mean Erosivity ($J\ mm\ m^{-2}\ h^{-1}$)
Wasteland	1302.6	296	22.0	22	2865	130.2 (90)	5967.8	263.5 (296.5)	119 715	5441.6 (5401.5)
South-West Ridge	1254.8	350.8	18.5	15	2195	146.3 (140)	4968.0	331.2 (380)	114 464	7630.9 (7453)

Table 4.4: Attributes of erosive rainfall events as measured at the Wasteland and South-West ridge.

Station name	Attribute	Storm Depth	Storm Duration	Intensity ($I_{5/15}$ mm/h)	Intensity (I_{30} mm/h)	Kinetic Energy ($J \cdot m^{-2}$)	Total Erosivity ($J\ mm\ m^{-2}\ h^{-1}$)
Wasteland	Maximum	28.0	540.0	45.6	29.2	604.4	15471.9
	Mean	**13.0**	**130.2**	**32.1**	**15.9**	**263.5**	**5441.6**
	Median	14.6	90.0	31.2	16.6	296.5	5401.5
South-West ridge	Maximum	32.2	525.0	50.4	40.4	645.1	21516.3
	Mean	**15.5**	**146.3**	**35.5**	**18.8**	**331.2**	**7630.9**
	Median	17.8	140.0	35.2	18.0	380.0	7453.0

To test the relationship between erosive rainfall attributes, the Pearson Product-Moment Correlation (PPMC) was used along with linear regression to establish the correlation coefficient and the related degree of significance. For all analyses n=37. A statistically significant (ρ= 0.01) near linear correlation (r=0.99) was found between storm kinetic energy and storm depth. Considering the linear regression coefficient, using the regression formula, y=10.3+20.3x, there is an approximate increase of 213 $J \cdot m^{-2}$ of kinetic energy for every 10 mm of depth (Figure 4.8).

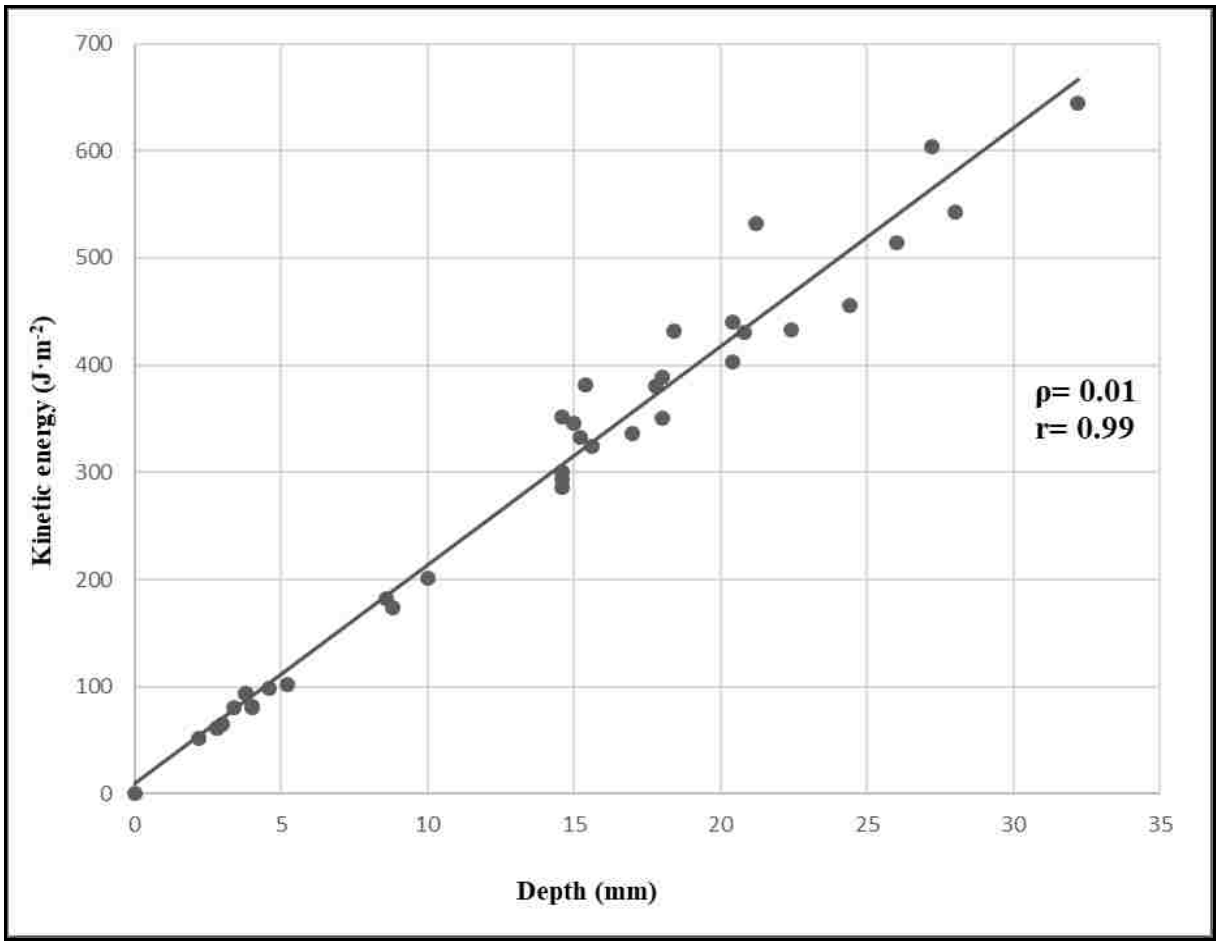

Figure 4.8: Relationship between storm kinetic energy and storm depth (n=37).

A statistically significant (ρ= 0.01) strong positive correlation (r=0.87) exists between erosivity and storm depth (Figure 4.9), although slightly weaker than the relationship between storm kinetic energy and storm depth (ρ= 0.01; r=0.99). Event number four is clearly visible as an outlier at the top of the chart (21,516.3 J.mm.m^{-2}.h^{-1}) and may have had a slight influence on the correlation. Considering the linear regression coefficient, using the regression formula, y= -1583.2+564.3x, there is an approximate increase of 4059 J.mm.m^{-2}.h^{-1} of erosivity for every 10 mm of depth (Figure 4.9).

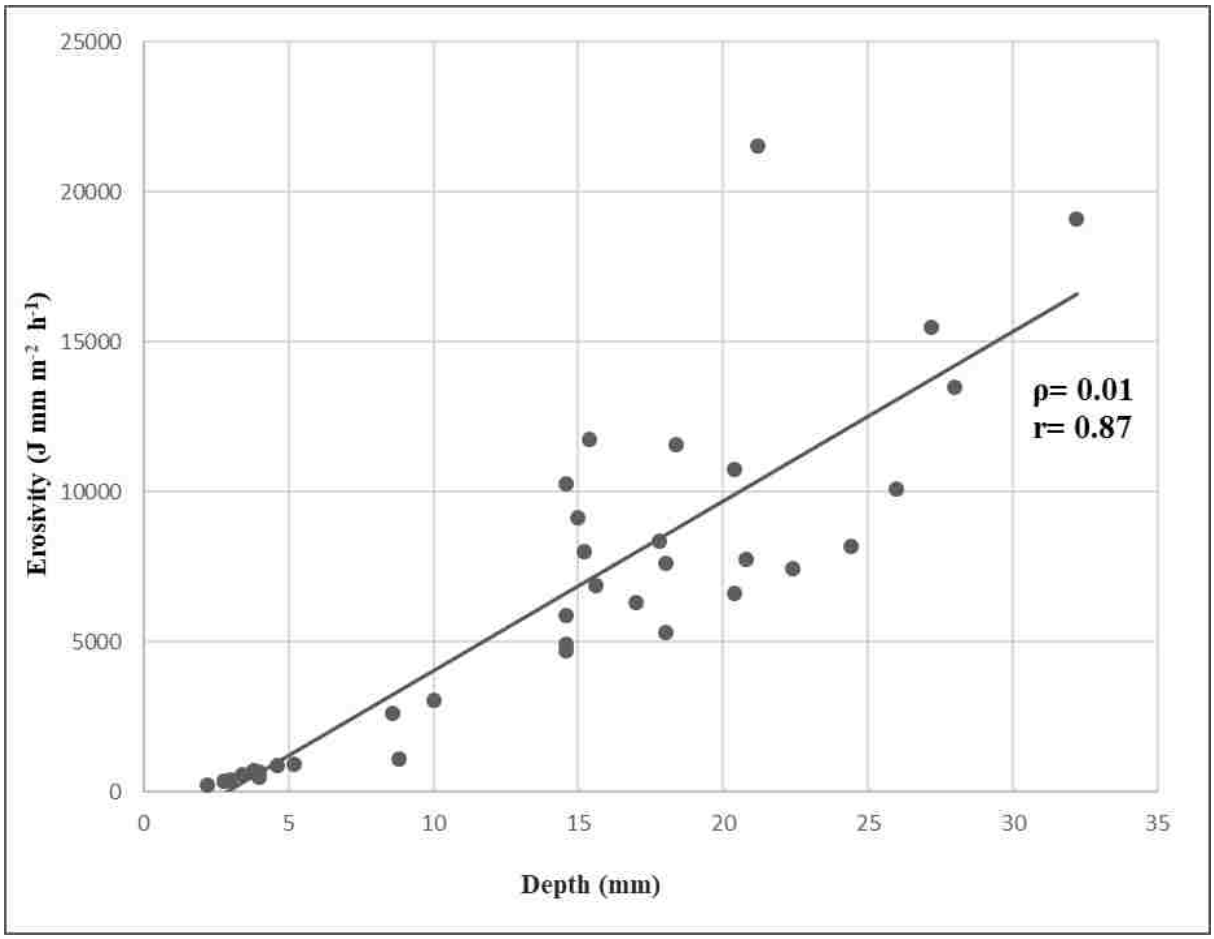

Figure 4.9: Relationship between erosivity and storm depth (n=37).

Kinetic energy and storm duration (Figure 4.10) show a significant positive correlation (ρ= 0.01; r=0.71), which confirms that an increase in storm duration does indeed increase kinetic energy, however the correlation (r=0.71) is slightly weaker than that of storm depth and kinetic energy (r=0.99).

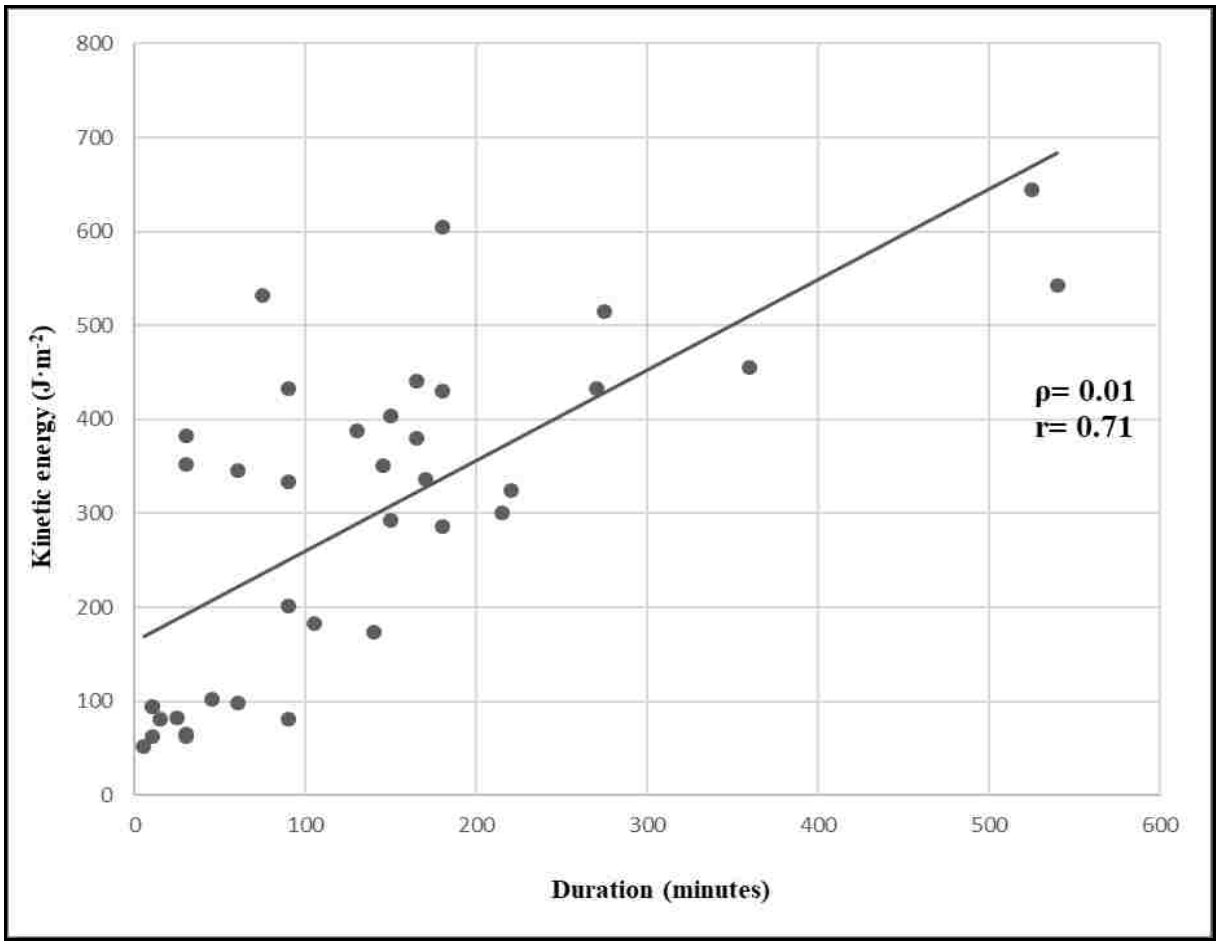

Figure 4.10: Relationship between kinetic energy and storm duration (n=37).

Erosivity and rainfall duration (Figure 4.11) show a positive correlation (ρ= 0.01; r=0.55), however, the correlation is significantly weaker than that of kinetic energy and rainfall depth (r=0.99), confirming the initial indication that erosive events with long durations may not necessarily produce maximum erosivity. Note event number four again, clearly visible at the top left of the chart (21,516.3 J.mm.m^{-2}.h^{-1}).

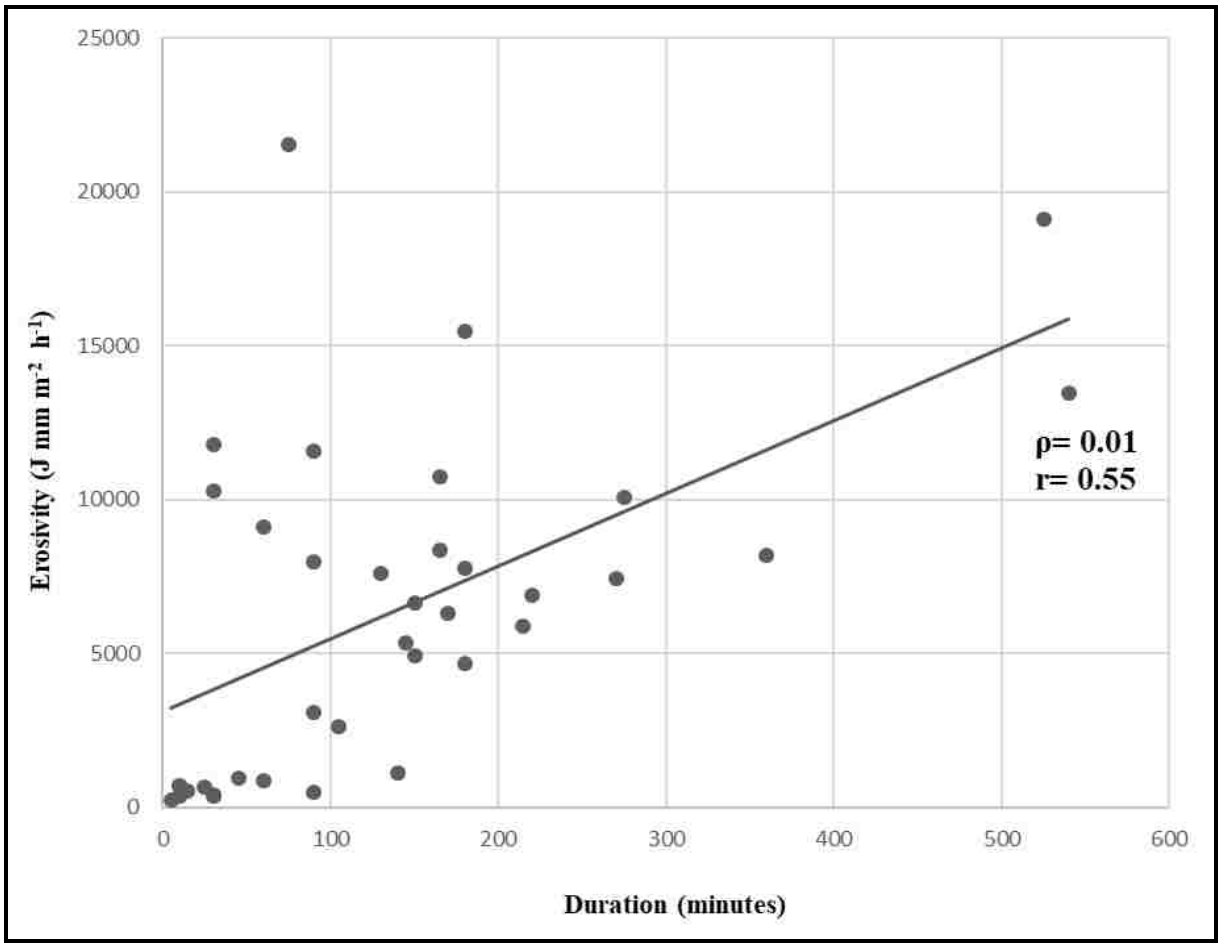

Figure 4.11: Relationship between erosivity and storm duration (n=37).

The monthly erosivity experienced at each station can be seen in Figure 4.12 below. The relationship between monthly rainfall and erosivity can be considered highly correlated, with a strong positive correlation between the Wasteland rainfall and Wasteland erosivity (ρ= 0.01; r=0.98). Similarly, a strong positive correlation is found between the South-West ridge rainfall and its corresponding erosivity ((ρ= 0.01; r=0.96).

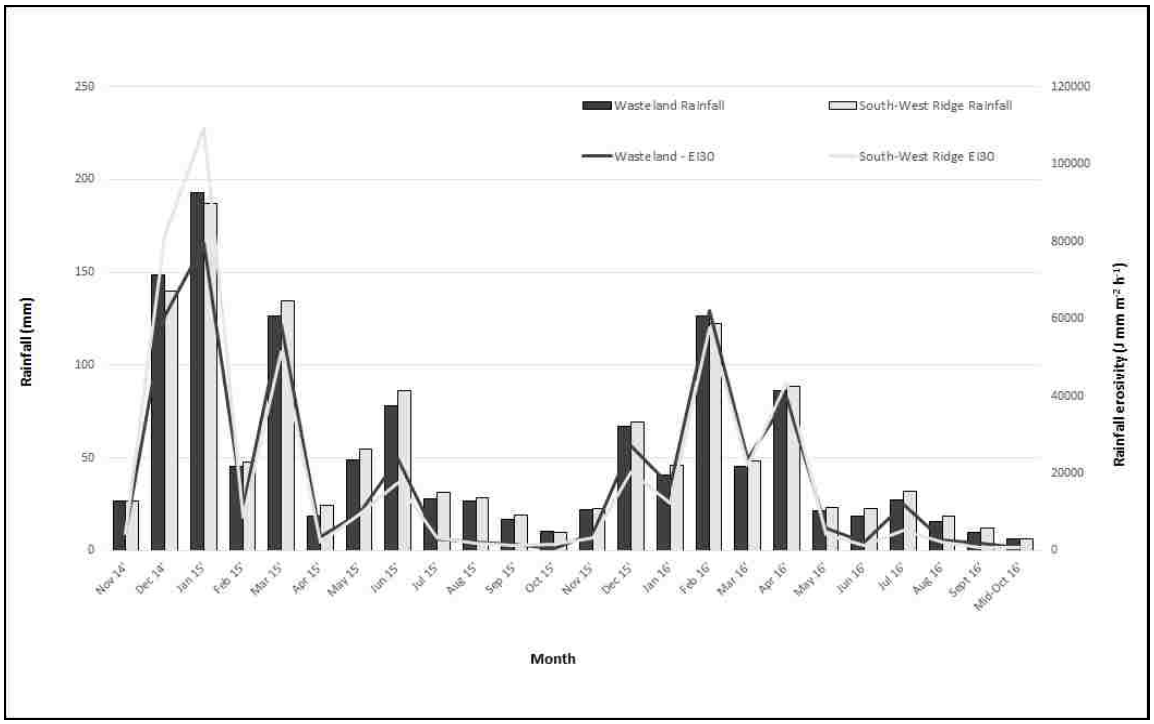

Figure 4.12: Monthly distribution of rainfall erosivity and rainfall experienced at each station over the study period.

Total erosivity (EI_{30}) for the duration of the study period was calculated at 458,889 J.mm.m^{-2}.h^{-1} and 467,015 J.mm.m^{-2}.h^{-1} for the Wasteland and South-West Ridge, respectively. This was done by adding the erosivity of each month (n=24) from each station. The totals were added together then divided by 24 to obtain the estimated monthly erosivity for Round Island (19,289.6 J.mm.m^{-2}.h^{-1}). Using this figure, the estimated annual erosivity for Round Island is calculated at 231,476 J.mm.m^{-2}.h^{-1}. When compared to results from Nel *et al.* (2012), which measured rainfall intensity and erosivity on the drier west coast of mainland Mauritius, Round Island's erosivity is slightly higher than recorded values at Albion (202,282 J.mm.m^{-2}.h^{-1}) and Beaux Songes (207,140 J.mm.m^{-2}.h^{-1}). Another important factor to note is the similarity in elevation of the stations, where Albion's elevation was 12 m a.m.s.l and Beaux Songes was 225 m a.m.s.l, quite comparable to the South-West Ridge (95 m a.m.s.l) and Wasteland (69 m a.m.s.l). As Nel *et al.* (2012) states, there is a noticeable altitudinal and temporal difference in rainfall due to the nature of topography and associated orographic effects. Since all stations compared here are of a relatively low altitude, it is expected that erosivity would be comparable between Round Island and mainland Mauritius. To be consistent with global studies (Panagos *et al.*, 2017), Round Island's erosivity was converted to MJ.mm.ha^{-1}.h^{-1}.yr^{-1}, which was estimated at 2,314.76 MJ.mm.ha^{-1}.h^{-1}.yr^{-1}. When compared to the global erosivity map compiled by Panagos *et al.* (2017), Round Island's erosivity is

comparable to the hot steppe climate (BSh), which had mean erosivity of 2,371 MJ.mm.ha^{-1}.h^{-1}.yr^{-1}.

Sediment transport

Table 4.5 outlines the catchment size (m^2) associated with each Gerlach trough, the orientation, coordinates and slope gradient. Collected sediment weights from each Gerlach trough for each month are presented in Table 4.6. 152 sediment samples were collected for the duration of the study period. Depending on the amount of rainfall recorded in the preceding month, total sediment sample weights varied between 0.014 and 1.5 kilograms. The months of January and February 2015 recorded unusually high sediment totals but it was uncertain as to when the Gerlach troughs were emptied during the December and January period. To avoid a situation of recording more than 1 month's sediment load (weighing sediment collected from December 2014-February 2015), as a single month, which would skew the results, the sediment totals were excluded from the dataset.

Table 4.5: Attributes of each catchment area and Gerlach trough.

Gerlach Trough	Size (m^2)	Coordinates	Orientation	Slope angle
A5	1300.7	19 51' 23.5" S; 57 47' 10.8" E	257˚	11˚
A6 *	1300.7	19 51' 23.2" S; 57 47' 11.4" E	250˚	9˚
A7	272.1	19 51' 18.9" S; 57 47' 12.5" E	125˚	9˚
A8	196.3	19 51' 17.8" S; 57 47' 11.5" E	161˚	10˚
B1	311.3	19 51' 14.9" S; 57 47' 01.8" E	140˚	6˚
B2	468.4	19 51' 14.7" S; 57 47' 01.3" E	141˚	5˚
B3	62.2	19 51' 15.3" S; 57 47' 01.2" E	129˚	2˚
B4	219.9	19 51' 15.9" S; 57 47' 01.2" E	171˚	5˚

*Trough A6 has been excluded from the area dataset (Figure 3.6) due to its location in the middle of the catchment.

Table 4.6: Weight (g) of sediment samples collected during study period at the Wasteland with rainfall (mm) and erosivity (EI_{30}) included for reference (n = 152).

Gerlach Trough	Mar	Apr	May	Jun	Jul	Aug	Sep	Oct	Nov	Dec	Jan	Feb	Mar	Apr	May	Jun	Jul	Aug	Sep	Total	Mean
	2015										2016										
A5 (1300.7 m^2)	670	61	35	14	32	14	32	12	17	22	20	29	18	21	31	17	17	26	37	**1,125**	**59.2**
A6 (1300.7 m^2)	1,345	35	65	29	158	28	28	22	22	29	29	482	80	27	73	22	15	20	90	**2,599**	**136.8**
A7 (272.1 m^2)	1,531	95	180	378	307	84	153	61	61	55	905	1,086	295	111	224	27	27	29	45	**5,654**	**297.6**
A8 (196.3 m^2)	918	39	127	142	131	62	62	28	43	31	280	456	172	95	268	31	27	30	58	**3,000**	**157.9**
Total (g)	**4,464**	**230**	**407**	**563**	**628**	**188**	**275**	**123**	**143**	**137**	**1,234**	**2,053**	**565**	**254**	**596**	**97**	**86**	**105**	**230**	**12,378**	**651.5**
Mean (g)	**1,116.0**	**57.5**	**101.8**	**140.8**	**157.0**	**47.0**	**68.8**	**30.8**	**35.8**	**34.3**	**308.5**	**513.3**	**141.3**	**63.5**	**149.0**	**24.3**	**21.5**	**26.3**	**57.5**	**3,094.5**	**162.9**
Rainfall (mm)	154.0	18.8	29.0	77.4	58.8	38.8	31.2	7.4	20.2	16.8	68.2	121.0	66.2	20.6	97.2	19.4	28.4	29.8	15.6	**918.8**	**48.4**
Erosivity (EI_{30})	108,089	2,078	6,765	22,922	26,138	5,196	4,267	537	6,593	3,941	43,580	100,238	50,898	8,247	69,523	7,680	17,586	7,076	3,565	**494,921**	**26,048**

The highest amount of monthly displaced sediment from the Gerlach troughs on the eastern (Wasteland) side of the island (sites A5-A8) was recorded in March 2015, where 4,464 g of sediment was collected across all sites in the area (Table 4.6). Site A7 recorded the highest amount in the month of March (1,531 g). Similarly, site A7 also recorded the highest overall sediment displacement weight during the study period with a total of 5,654 g and monthly average of 297.6 g. The site with the lowest sediment displacement weight was A5 with a total of 1,125 g over the study period and a monthly average of 59.2 g. Despite having a greater slope gradient (11˚) than site A7 (9˚), site A5 recorded less sediment displacement weights, which could be attributed to the vegetation cover in the catchment being far denser than site A7 (Figure 3.5), indicating that slope angle has less of an influence on sediment displacement than that of vegetation cover. It is also significant since the catchment within which A5 is located is almost five times the size (1,300.7 m^2) of the catchment within which A7 is located (272.1 m^2). Displaced soil weight per catchment size will be discussed in the section below. Figure 4.13 outlines the erosivity index ($EI_{30)}$ and corresponding displaced sediment weight collected at each Gerlach trough for the study period. High erosivity levels are clearly visible during the months of March 2015 (108,089 $J.mm.m^{-2}.h^{-1}$) and February 2016 (100,238 $J.mm.m^{-2}.h^{-1}$). Correlations between erosivity and sediment transport will be discussed in further detail below, however, it is evident that a strong positive correlation exists.

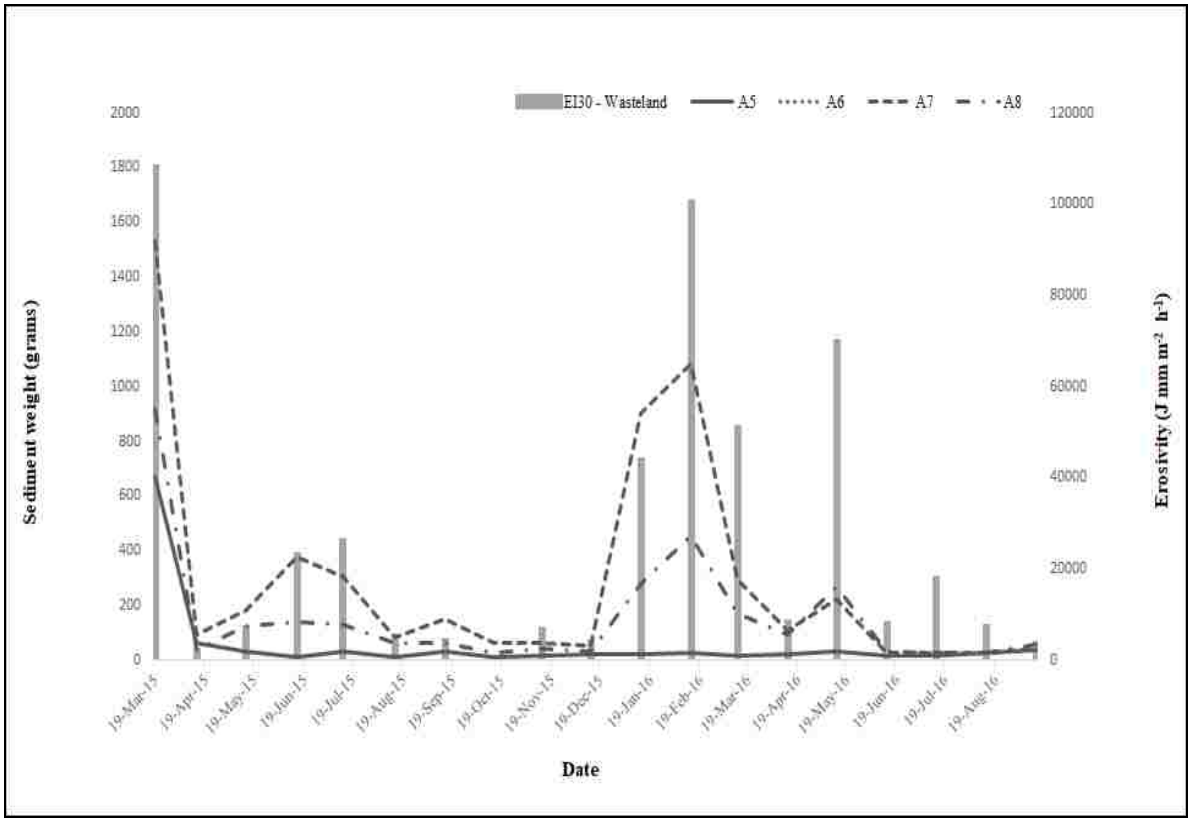

Figure 4.13: Wasteland monthly erosivity and displaced sediment weight.

The highest amount of monthly displaced sediment from the Gerlach troughs on the South-West ridge (sites B1-B4) was recorded in March 2015 (5,206 g) (Table 4.7). Site B3 recorded the highest amount of displaced sediment in the month of March (1,487 g), however, it did not follow the same trend as site A7, as it did not record the highest overall sediment displacement during the study period. The highest overall amount of displaced soil for the study period was recorded at site B1 (6,179 g) as well as the highest monthly average (325.2 g). The site with the lowest soil erosion was B2 with a total of 3,547 g over the study period and a monthly average of 186.7 g. This could be perhaps due to the presence of slightly more vegetation in the catchment area (Figure 3.5). Site B2 recorded significantly less soil erosion (3,547 g) than B1 (6,179 g), yet had a bigger catchment size, reinforcing the possible role that vegetation plays in reducing soil erosion. Figure 4.14 outlines the erosivity index (EI_{30}) and corresponding sediment weight collected at each Gerlach trough for the study period. High erosivity levels are again visible during the months of March 2015 (94,582 $J.mm.m^{-2}.h^{-1}$) and February 2016 (87,940 $J.mm.m^{-2}.h^{-1}$).

Overall, the Gerlach troughs on the South-West ridge (B1-B4) recorded a total soil loss of 18,806 g for the duration of the study period. This is significantly higher than the total

soil loss across all Gerlach troughs at the Wasteland (12,378 g). The monthly average soil loss for the duration of the study period was 3,094.5 g and 4,701.5 g for the Wasteland and South-West ridge, respectively. An interesting fact to consider is the erosivity index calculated for each area. Even though the South-West ridge recorded more soil loss, the area had a lower total erosivity over the study period (438,274 J.mm.m^{-2}.h^{-1}) when compared to total erosivity at the Wasteland (494,921 J.mm.m^{-2}.h^{-1}).

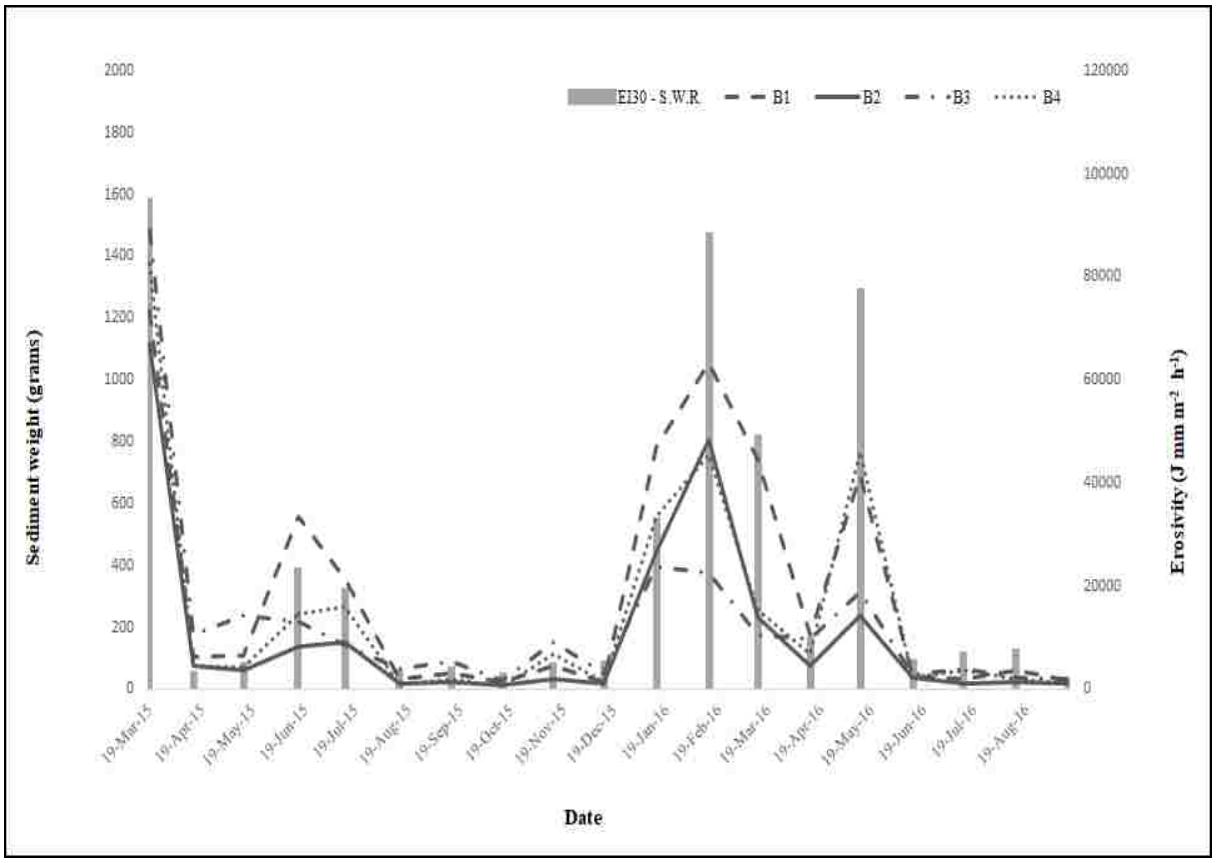

Figure 4.14: South-West ridge monthly erosivity and sediment movement.

Table 4.7: Weight (g) of sediment samples collected during study period at the South-West ridge with rainfall (mm) and erosivity (EI_{30}) included for reference (n = 152).

Gerlach Trough	Mar	Apr	May	Jun	Jul	Aug	Sep	Oct	Nov	Dec	Jan	Feb	Mar	Apr	May	Jun	Jul	Aug	Sep	Total	Mean
	2015										2016										
B1 (311.3 m^2)	1,223	105	109	560	357	31	54	25	75	24	782	1,056	746	177	691	43	34	59	28	**6,179**	**325.2**
B2 (468.4 m^2)	1,120	74	61	139	151	20	24	12	31	20	445	805	235	74	236	36	20	25	19	**3,547**	**186.7**
B3 (62.2 m^2)	1,487	175	237	217	144	66	88	30	150	52	397	376	177	161	314	47	64	39	33	**4,254**	**223.9**
B4 (219.9 m^2)	1,376	77	69	245	266	12	32	10	112	23	559	760	255	113	767	38	59	33	20	**4,826**	**254.0**
Total (g)	**5,206**	**431**	**476**	**1,161**	**918**	**129**	**198**	**77**	**368**	**119**	**2,183**	**2,997**	**1,413**	**525**	**2,008**	**164**	**177**	**156**	**100**	**18,806**	**989.8**
Mean (g)	**1301.5**	**107.8**	**119.0**	**290.3**	**229.5**	**32.3**	**49.5**	**19.3**	**92.0**	**29.8**	**545.8**	**749.3**	**353.3**	**131.3**	**502.0**	**41.0**	**44.3**	**39.0**	**25.0**	**4701.5**	**247.4**
Rainfall (mm)	144.0	16.8	23.4	71.4	52.0	34.2	28.6	8.8	19.0	17.0	65.8	119.2	64.0	20.6	95.2	17.0	21.8	26.4	12.4	**857.6**	**45.1**
Erosivity (EI_{30})	94,582	2,775	4,459	22,919	18,982	3,231	3,579	2,414	4,535	4,754	32,562	87,940	48,654	9,350	76,974	5,245	6,666	7,253	1,399	**438,274**	**23,067**

Sediment transport and catchment area

Table 4.8 below displays sediment yields calculated as the weight of the sediment collected divided by the area of the catchment. The shape and distribution of mean sediment displacement (g) per area (m^2) is displayed in Figure 4.15. This was done to normalise the data in terms of catchment area so that comparisons can be made between the catchments. As mentioned above, Gerlach trough A6, which is located within the same catchment as A5, was excluded from the area dataset due to its location in the middle of the catchment. Site A5, located on the Wasteland side of the island had the largest catchment area (1300.7 m^2), and therefore, the site recorded the lowest soil erosion (0.52 $g.m^{-2}$) in March 2015. Compared to site A7, which has a significantly smaller catchment size (272.1 m^2), and the highest soil erosion (5.63 $g.m^{-2}$), Charlton's (2009) view that larger catchments can store more sediment is confirmed, as sediment yields tend to decrease with an increase in basin size.

Table 4.8: Sediment weights (g) divided by catchment area (m^2).

Gerlach Trough	Mar (g/m^2)	Apr (g/m^2)	May (g/m^2)	Jun (g/m^2)	Jul (g/m^2)	Aug (g/m^2)	Sep (g/m^2)	Oct (g/m^2)	Nov (g/m^2)	Dec (g/m^2)	Jan (g/m^2)	Feb (g/m^2)	Mar (g/m^2)	Apr (g/m^2)	May (g/m^2)	Jun (g/m^2)	Jul (g/m^2)	Aug (g/m^2)	Sep (g/m^2)	Total (g/m^2)	Mean (g/m^2)
	2015										2016										
A5 (1300.7 m^2)	0.52	0.05	0.03	0.01	0.02	0.01	0.02	0.01	0.01	0.02	0.02	0.02	0.01	0.02	0.02	0.01	0.01	0.02	0.03	**0.86**	**0.0**
A7 (272.1 m^2)	5.63	0.35	0.66	1.39	1.13	0.31	0.56	0.22	0.22	0.20	3.33	3.99	1.08	0.41	0.82	0.10	0.10	0.11	0.17	**20.78**	**1.1**
A8 (196.3 m^2)	4.68	0.20	0.65	0.72	0.67	0.32	0.32	0.14	0.22	0.16	1.43	2.32	0.88	0.48	1.37	0.16	0.14	0.15	0.30	**15.28**	**0.8**
Total (g/m^2)	**10.82**	**0.59**	**1.34**	**2.12**	**1.82**	**0.64**	**0.90**	**0.38**	**0.46**	**0.38**	**4.77**	**6.34**	**1.97**	**0.91**	**2.21**	**0.27**	**0.25**	**0.28**	**0.49**	**36.93**	**1.94**
Mean (g/m^2)	**3.6**	**0.2**	**0.4**	**0.7**	**0.6**	**0.2**	**0.3**	**0.1**	**0.2**	**0.1**	**1.6**	**2.1**	**0.7**	**0.3**	**0.7**	**0.1**	**0.1**	**0.1**	**0.2**	**12.3**	**0.6**
Rainfall (mm)	154.0	18.8	29.0	77.4	58.8	38.8	31.2	7.4	20.2	16.8	68.2	121.0	66.2	20.6	97.2	19.4	28.4	29.8	15.6	**918.8**	**48.4**
Erosivity (EI_{30})	108,089	2,078	6,765	22,922	26,138	5,196	4,267	537	6,593	3,941	43,580	100,238	50,898	8,247	69,523	7,680	17,586	7,076	3,565	**494,921**	**26,048**

Gerlach Trough	Mar (g/m^2)	Apr (g/m^2)	May (g/m^2)	Jun (g/m^2)	Jul (g/m^2)	Aug (g/m^2)	Sep (g/m^2)	Oct (g/m^2)	Nov (g/m^2)	Dec (g/m^2)	Jan (g/m^2)	Feb (g/m^2)	Mar (g/m^2)	Apr (g/m^2)	May (g/m^2)	Jun (g/m^2)	Jul (g/m^2)	Aug (g/m^2)	Sep (g/m^2)	Total (g/m^2)	Mean (g/m^2)
	2015										2016										
B1 (311.3 m^2)	3.93	0.34	0.35	1.80	1.15	0.10	0.17	0.08	0.24	0.08	2.51	3.39	2.40	0.57	2.22	0.14	0.11	0.19	0.09	**19.85**	**1.0**
B2 (468.4 m^2)	2.39	0.16	0.13	0.30	0.32	0.04	0.05	0.03	0.07	0.04	0.95	1.72	0.50	0.16	0.50	0.08	0.04	0.05	0.04	**7.57**	**0.4**
B3 (62.2 m^2)	23.91	2.81	3.81	3.49	2.32	1.06	1.41	0.48	2.41	0.84	6.38	6.05	2.85	2.59	5.05		1.03	0.63	0.53	**67.64**	**3.8**
B4 (219.9 m^2)	6.26	0.35	0.31	1.11	1.21	0.05	0.15	0.05	0.51	0.10	2.54	3.46	1.16	0.51	3.49	0.17	0.27	0.15	0.09	**21.95**	**1.2**
Total (g/m^2)	**36.48**	**3.66**	**4.60**	**6.70**	**4.99**	**1.26**	**1.79**	**0.63**	**3.23**	**1.06**	**12.39**	**14.61**	**6.90**	**3.83**	**11.26**	**0.39**	**1.45**	**1.02**	**0.75**	**117.00**	**6.2**
Mean (g/m^2)	**9.1**	**0.9**	**1.2**	**1.7**	**1.2**	**0.3**	**0.4**	**0.2**	**0.8**	**0.3**	**3.1**	**3.7**	**1.7**	**1.0**	**2.8**	**0.1**	**0.4**	**0.3**	**0.2**	**29.3**	**1.5**
Rainfall (mm)	144.0	16.8	23.4	71.4	52.0	34.2	28.6	8.8	19.0	17.0	65.8	119.2	64.0	20.6	95.2	17.0	21.8	26.4	12.4	**857.6**	**45.1**
Erosivity (EI_{30})	94,582	2,775	4,459	22,919	18,982	3,231	3,579	2,414	4,535	4,754	32,562	87,940	48,654	9,350	76,974	5,245	6,666	7,253	1,399	**438,274**	**23,067**

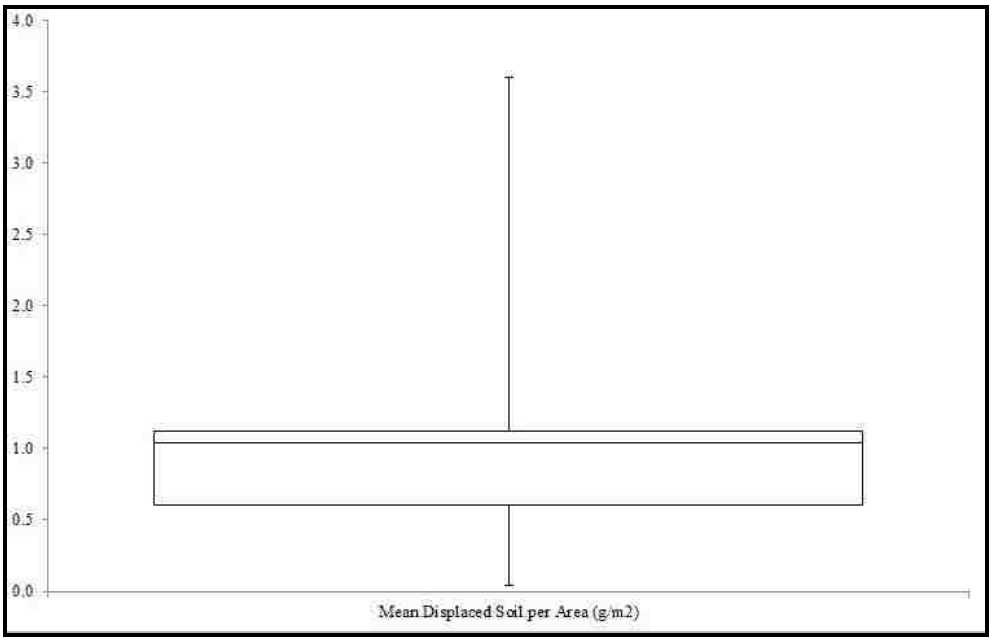

Figure 4.15: Box and whisker plot displaying shape and distribution of mean sediment displacement (g) per area (m^2).

In terms of the total amount of sediment collected over the study period divided by the area of the catchment, site A5 recorded a total of 0.86 $g.m^{-2}$, a result far lower than the rest of the sites located on the eastern side of the island, where 20.78 $g.m^{-2}$ and 15.28 $g.m^{-2}$ were recorded for A7 and A8, respectively.

A similar trend occurs on the South-West ridge, where the lowest soil erosion was recorded at site B2 (7.57 $g.m^{-2}$) for the duration of the study period. The highest soil erosion was recorded at site B3 (68.39 $g.m^{-2}$), which had the smallest catchment across all sites (62.2 m^2). Mean sediment displacement for all sites on the South-West ridge was recorded at 29.3 $g.m^{-2}$, which was more than double the mean sediment displacement per catchment area for the Wasteland sites (12.3 $g.m^{-2}$). Mean catchment size for the Wasteland and South-West ridge were calculated at 589.7 m^2 and 265.45 m^2, respectively. The monthly median of sediment displacement is 1.04 $g.m^{-2}$ which equates to 12.48 $g.m^{-2}.yr^{-1}$ or 0.1248 $t.ha^{-1}.yr^{-1}$. Using a surface area of 2.08 km^2 (2,080,000 m^2), 25,958,400 g (25,958.4 kg) or 25.96 t is displaced annually.

The results presented above confirm the notion that erosion processes and the factors influencing them vary depending on the scale at which they are studied (Morgan, 2005). What may be considered an “extreme” rainfall event within a small watershed may only be

classified as a normal event in a larger watershed. Other factors leading to the South-West ridge recording higher amounts of sediment could be attributed to the limited presence of vegetation. The Wasteland site has considerably more mixed weed habitat in the area, whereas the South-West ridge has isolated areas of mixed weed habitat and a greater amount of exposed bare ground. Vegetation helps trap sediment and plays a significant role in the protection of soil and prevention of erosion, as raindrop and wind energy is dissipated by vegetation. A third factor to consider is the significance of slope angle and the role it may play in sediment displacement. The results of this study suggest that slope angle does not play a major role in the mobilisation of sediment, although it is important to note that a maximum slope angle of 11˚ was recorded in the catchments of this study, which may not be a great enough angle to have a significant influence. As stated by Pimental & Kuonang, (1998), terrains with higher slope-length have higher rates of erosion due to higher runoff energy and volume, however, this does not appear to be a contributing factor to sediment yields on Round Island.

To test the relationship between erosive rainfall attributes and sediment transport, the Pearson Product-Moment Correlation (PPMC) was used along with linear regression to establish the correlation coefficient and the related degree of significance. For all analyses n=19. For all correlations, the values from all Gerlach trough sites excluding site A6 were averaged as well as the rainfall from both environmental monitoring stations. A strong, statistically significant ($\rho = 0.01$) positive correlation ($r=0.93$) was found between average rainfall and average displaced soil weight (Figure 4.16). Considering the linear regression coefficient, using the regression formula, $y=20.1+0.1x$, there is an approximate increase of 200 g sediment displacement per 45.5 mm of rainfall depth (Figure 4.16).

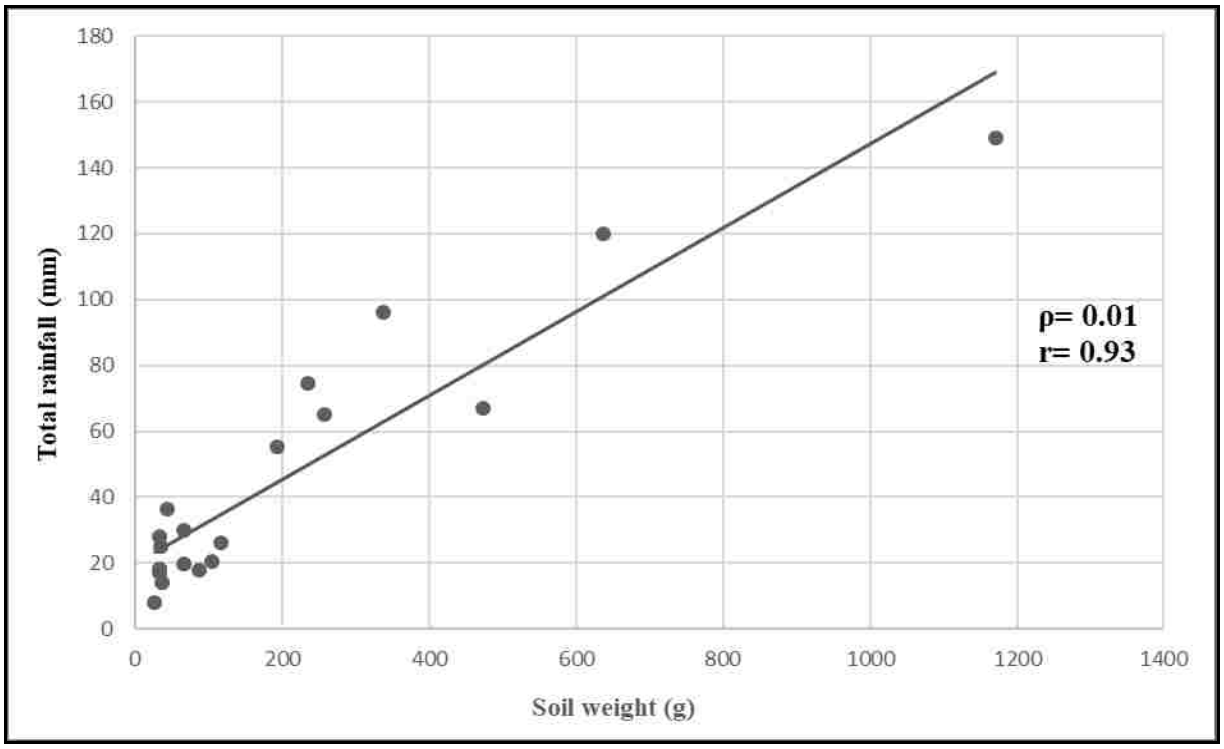

Figure 4.16: Relationship between combined average displaced soil weight and average total rainfall (n=19).

A strong, statistically significant (ρ= 0.01) positive correlation (r=0.96) was found between average kinetic energy and average displaced soil weight (Figure 4.17). Considering the linear regression coefficient, using the regression formula, y=201.9+1.9x, there is an approximate increase of 200 g sediment displacement per 586.8 $J \cdot m^{-2}$ (Figure 4.17).

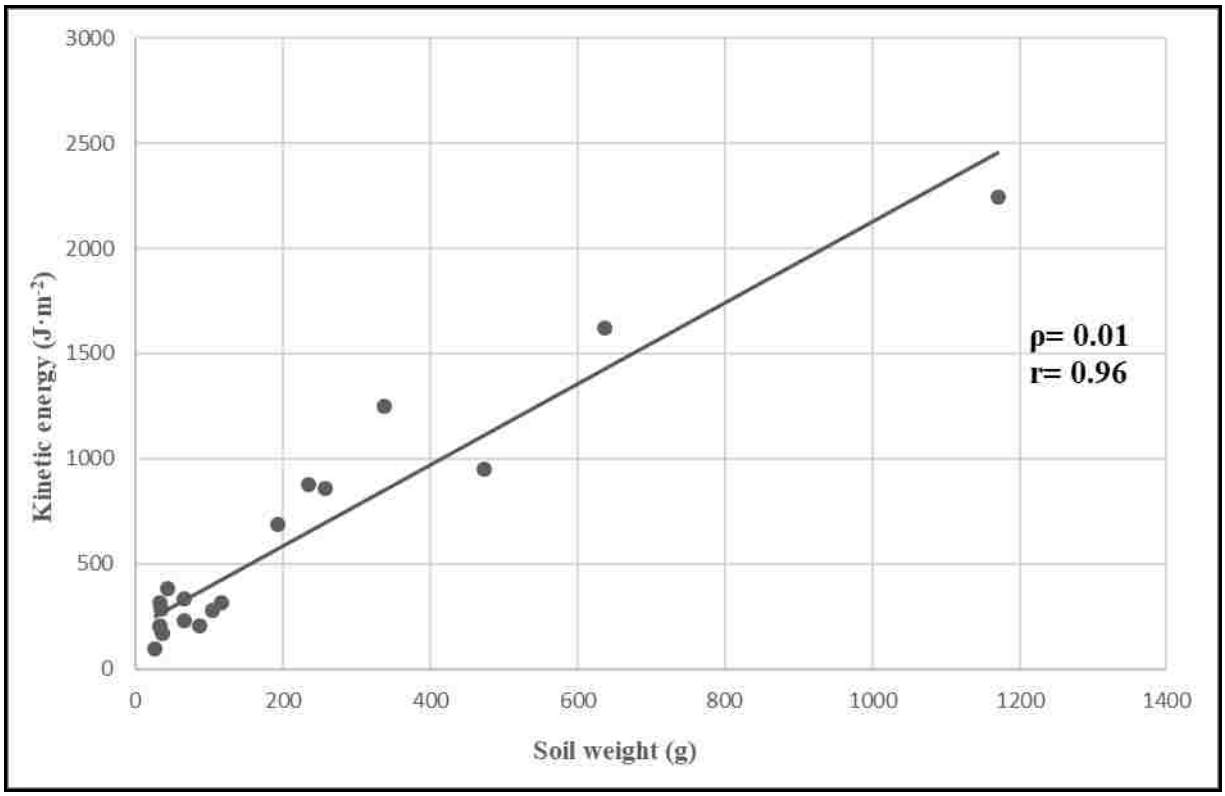

Figure 4.17: Relationship between combined average displaced soil weight and average kinetic energy (n=19).

A strong, statistically significant (ρ= 0.01) positive correlation (r=0.90) was found between average erosivity and average displaced soil weight (Figure 4.18). Considering the linear regression coefficient, using the regression formula, y=3454.4+100.7x, there is an approximate increase of 200 g sediment displacement per 23,600.4 J.mm.m^{-2}.h^{-1} (Figure 4.18).

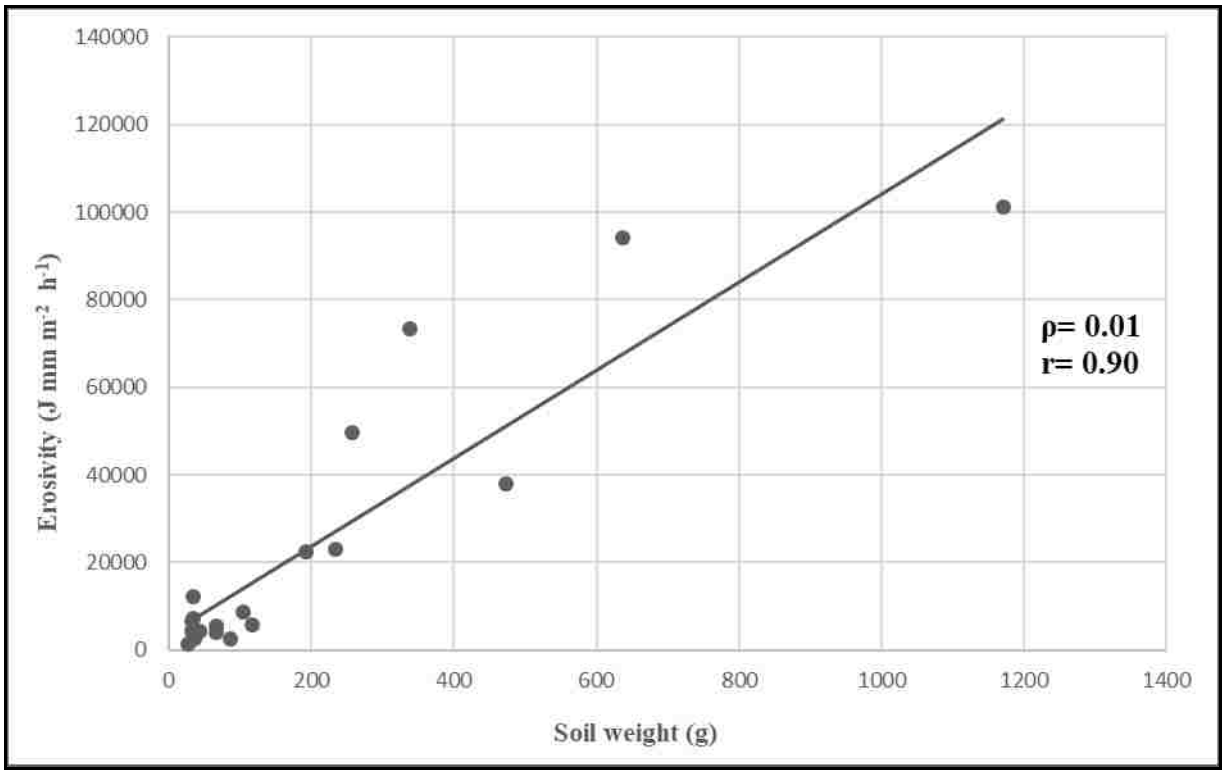

Figure 4.18: Relationship between combined average displaced soil weight and average erosivity (n=19).

A strong, statistically significant (ρ= 0.01) positive correlation (r=0.90) was found between total average rainfall and average displaced soil weight per catchment area (Figure 4.19). Considering the linear regression coefficient, using the regression formula, y=20.7+23.8x, there is an approximate increase of 1 $g.m^{-2}$ of sediment displacement per 44.4 mm of rainfall depth (Figure 4.19).

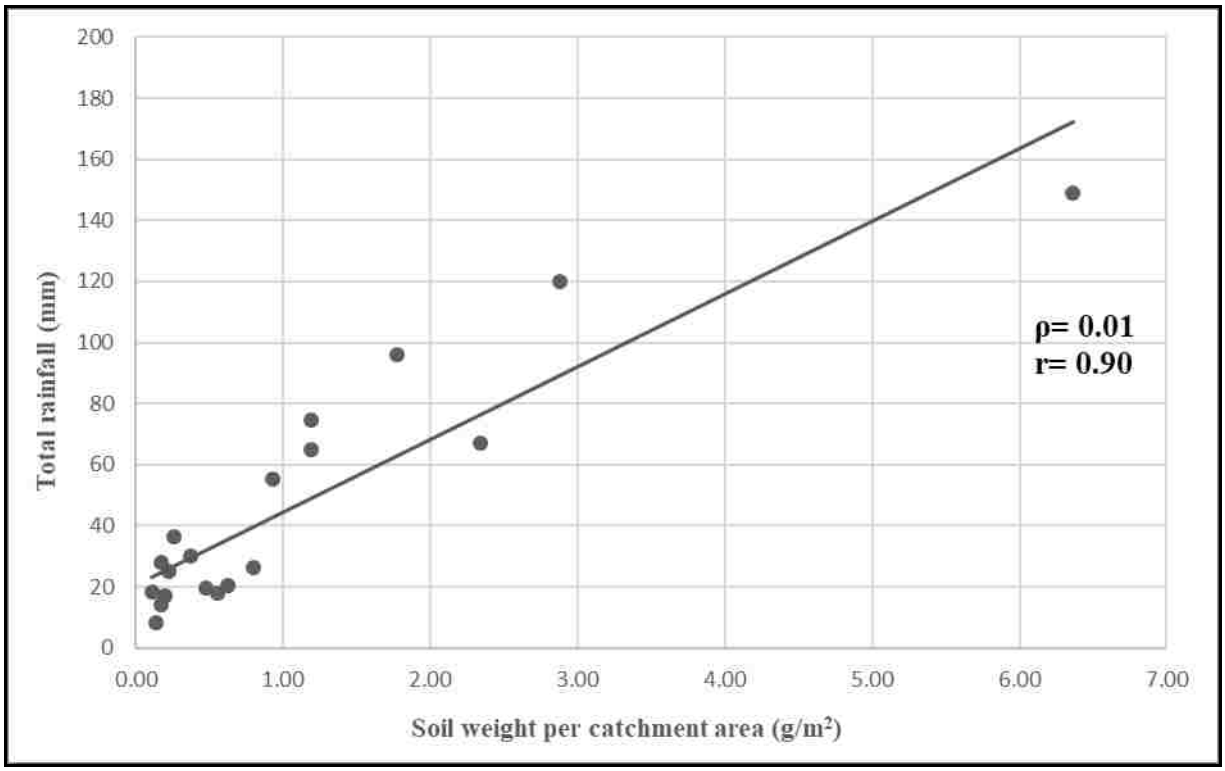

Figure 4.19: Relationship between combined average displaced soil weight divided by catchment area and average total rainfall (n=19).

A strong, statistically significant (ρ= 0.01) positive correlation (r=0.94) was found between average kinetic energy and average displaced soil weight per catchment area (Figure 4.20). Considering the linear regression coefficient, using the regression formula, y=208.3+362.6x, there is an approximate increase of 1 $g.m^{-2}$ of sediment displacement per 570.9 $J \cdot m^{-2}$ (Figure 4.20).

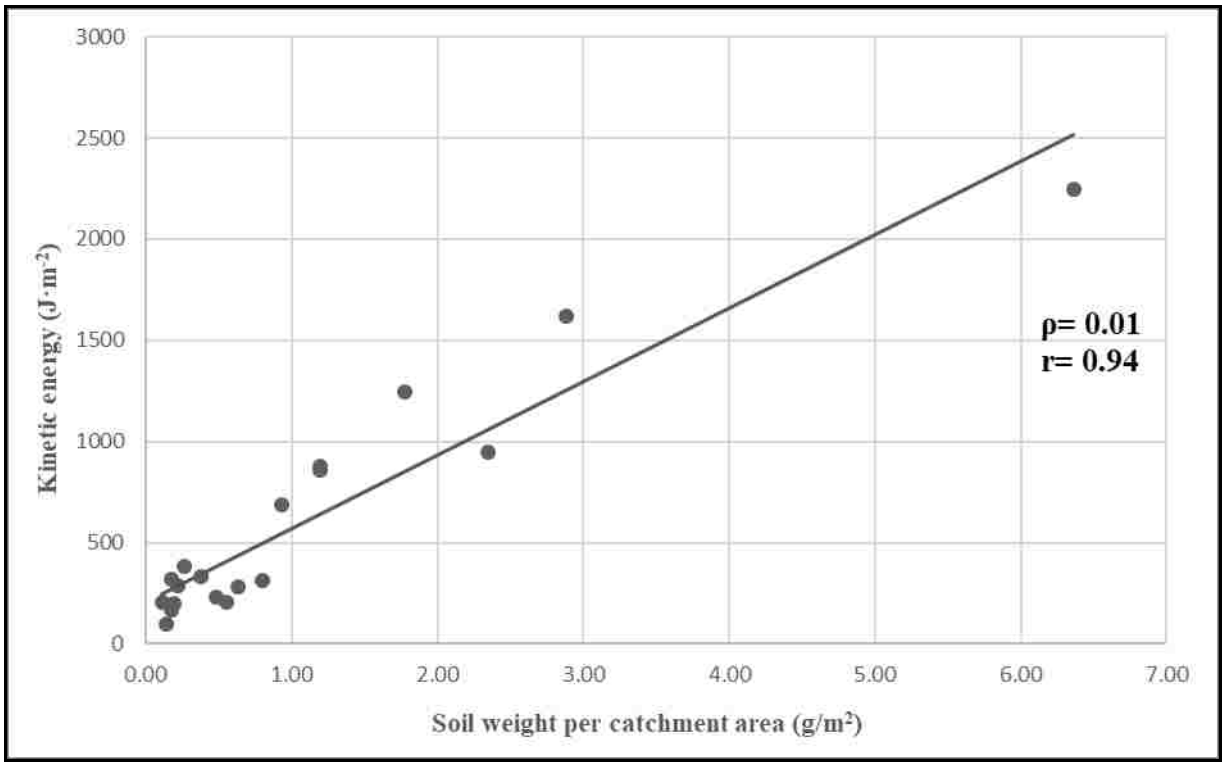

Figure 4.20: Relationship between combined average displaced soil weight divided by catchment area and average kinetic energy (n=19).

A strong, statistically significant (ρ= 0.01) positive correlation (r=0.88) was found between average erosivity and average displaced soil weight per catchment area (Figure 4.21). Considering the linear regression coefficient, using the regression formula, y=4,077.5+18,711.3x, there is an approximate increase of 1 $g.m^{-2}$ of sediment displacement per 22,788.8 $J.mm.m^{-2}.h^{-1}$ (Figure 4.21).

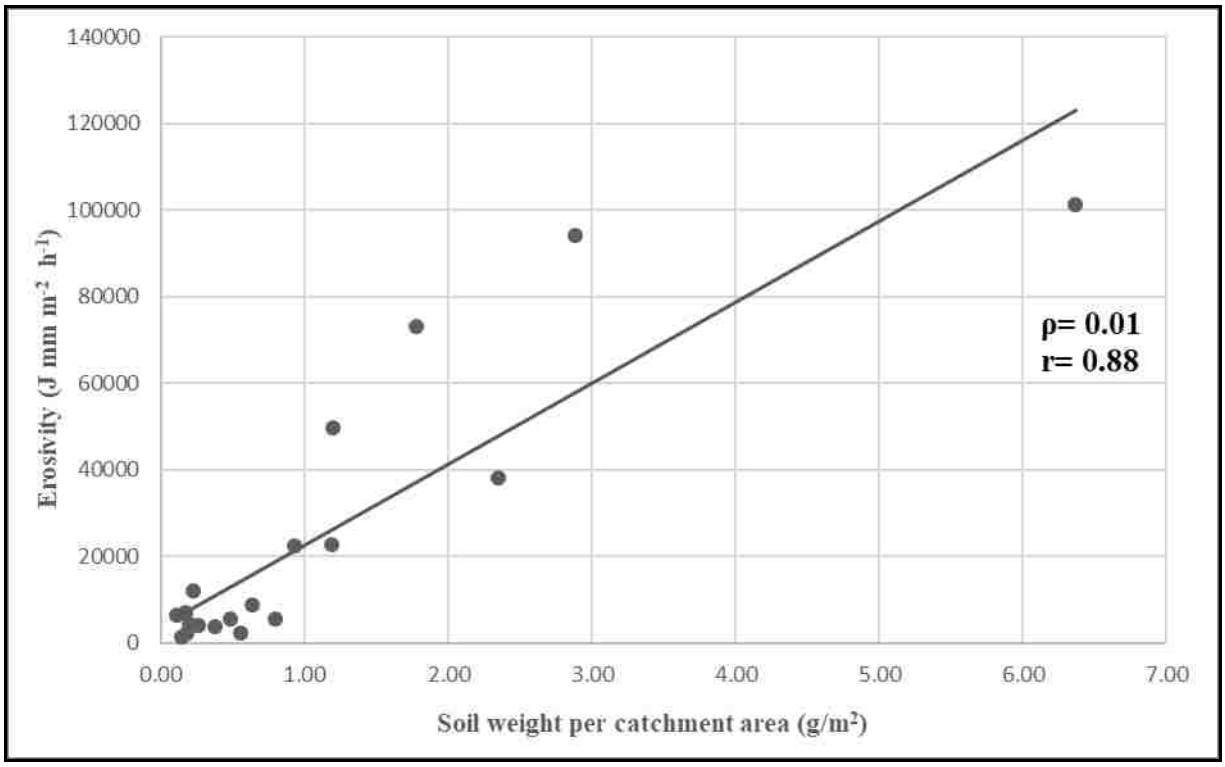

Figure 4.21: Relationship between combined average displaced soil weight divided by catchment area and average erosivity (n=19).

Particle size analysis

Sediment samples of approximately 120 grams from each Gerlach trough for the months of February and March 2015 and January, February, March 2016 were grouped together as Site A (Wasteland) and Site B (South-West ridge) for analysis in an Gradistat Excel spreadsheet (Blott & Pye, 2001), which describes the shape of particle size distribution of the samples (Table 4.9) (i.e. mean, skewness and sorting). Although both sites A and B were classed per the Wentworth grade as "sandy very fine gravel" and grouped in the textural group as "sandy gravel", there were slight differences between the two sites (Figure 4.22). For example, Site A and Site B were recorded as 36.9 percent gravel and 63.1 percent sand and 41.7 percent gravel and 58.3 percent sand, respectively (Table 4.9). Thus, Site A comprises slightly more finer particles than Site B. Table 4.9 provides a more comprehensive breakdown of grain size distribution for each site. The particle sizes recorded used in Table 4.9 are presented in Table 4.10.

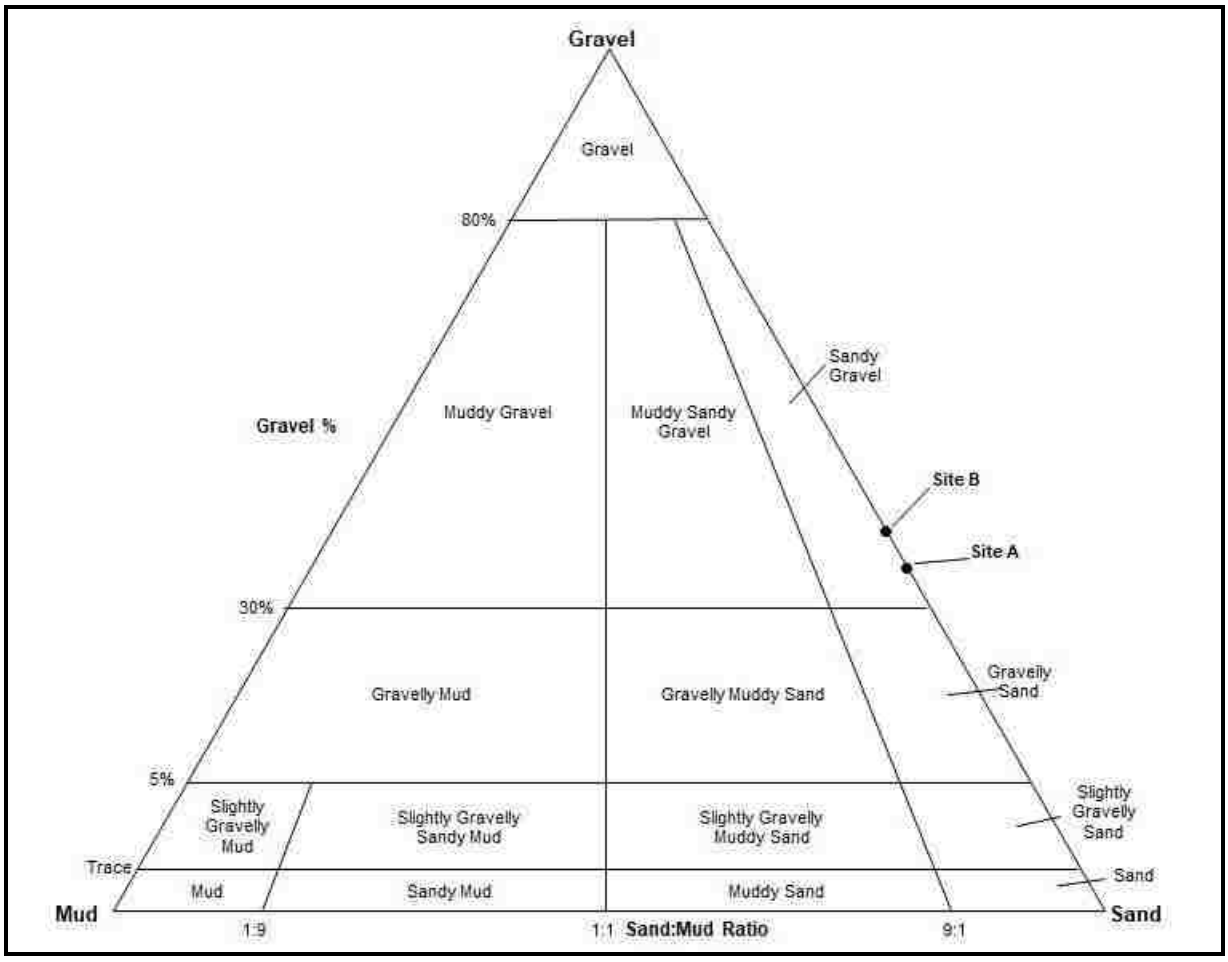

Figure 4.22: Grain size distribution diagram with site A and B indicated as points.

Table 4.9: Grain size distribution from each sample site.

Site	Gravel		Sand					Mud
	Fine gravel (%)	Very fine gravel (%)	Very course sand (%)	Course sand (%)	Medium sand (%)	Fine sand (%)	Very fine sand (%)	Very course silt (%)
Site A (Wasteland)	0.0	36.9	18.8	18.5	15.2	8.1	2.5	0.0
	36.9		**63.1**					**0.0**
Site B (S.W.R.)	0.0	41.7	19.2	19.6	9.3	7.8	2.5	0.0
	41.7		**58.3**					**0.0**

Further results of the particle size distribution analysis are presented as cumulative curves on a logarithmic scale (phi) in order to normalize the distribution (Appendix 1). Descriptive statistical analysis (mean, skewness, sorting, and kurtosis grading) of each site is also available in the appendices, however, the samples are not unimodal. The sorting, skewness and kurtosis statistics must be examined with caution. When using the geometric method of moment (µm), Site B recorded a mean particle size of 1045.9 µm, which is slightly larger than Site A (917.9 µm). Both sites are poorly sorted, with a sorting value in the range of 2.37-2.72. Both sites are negatively skewed, representing coarse sediments with -0.75 and -1.07 for Site A and Site B, respectively.

Table 4.10: Wentworth textural classification in relation to particle size.

Wentworth textural classification	**Particle Size (mm)**
Fine gravel	4
Very fine gravel	2
Very course sand	1
Course sand	0.5
Medium sand	0.25
Fine sand	0.125
Very fine sand	0.0625
Very course silt	0.031

In summary, this chapter has presented the results of the specified methodology in the previous chapter. Important findings and analysis have been highlighted and will be discussed in further detail in the following chapter. Differences in kinetic energy and erosivity between the two environmental monitoring stations were found to be relatively high. Results of the sediment displacement clearly indicate that vegetation traps sediment and plays a significant role in the protection of soil and prevention of erosion.

Chapter 5: Discussion

This chapter provides a detailed discussion based on the findings of the results presented in the Chapter 4. First, the erodibility of the soils on Round Island is discussed. Second, rainfall erosivity and its attributes are discussed for the Wasteland and South-West ridge study sites. Third, sediment displacement is discussed in the context of soil erodibility (endogenic processes) and rainfall erosivity (exogenic processes). Fourth, soil conservation and potential steps for management are discussed. Fifth, Zoogeomorphology and the effects of birds and mammals on Round Island are discussed, and lastly, the opposing factors of landscape dynamics are discussed.

Soil on Round Island

Two types of soils were identified during a soil survey by Johnston (1993), namely Lithic leptosols and Dystric leptosoils. Compared to the mature ferralatic (Latosoils) and Latosolic soils found on mainland Mauritius (Proag, 1995), soils on Round Island show very little resemblance, instead they appear to have been characterised by the island's unique environmental setting, in terms of its volcanic history, topography, climate and vegetation. Soils on Round Island are generally very thin and not continuous. According to Johnston (1993), it is not possible to determine the original nature of soils on Round Island. Johnston (1993) indicates that the majority of soils found on the island are sandy loams with a relatively uniform texture, little structure and poor profile development. This can be attributed to previous soil loss and recent regeneration and may be considered as a secondary parent material overlying the original welded tuff parent material (Johnston, 1993). Poor profile development suggests that the soils in various areas are more like sediment which has been deposited as a result of downslope movement, rather than as a consequence of physical weathering of the tuff rock. The results of the particle size analysis from sediment that was collected during the study indicate slightly different results to the Johnson (1993) study, where both sites were negatively skewed, and according to the Wentworth Grade, fall within the sediment size of gravelly sand. In addition, both sites were poorly sorted, indicating a mixture of different particle sizes, however, the samples were not unimodal. Therefore, the sorting, skewness and kurtosis statistics suggest that the trapped sediment may come from both soil and small rock fragments (parent material). Another factor to consider concerning sediment collected from the Gerlach troughs is the effect of aeolian erosion processes, where

finer particles picked up by wind energy may have been blown out of the troughs prior to collection, which would further skew the data.

Concerning soil erodibility, particle size between 0.04-0.25 mm seem to be most susceptible to detachment (Poesen, 1993). In the case of Round Island, however, soils with larger sizes, between 0.5 mm and 2.0 mm, were more commonly found to have been detached. This supports the view by Dóniz-Paez *et al*. (2011) that Round Island's relatively young volcanic cone will largely comprise gravelly sand. On average, across all study sites, more than 70% of particles were in the 0.5-2.0 mm range. From the results, the material found at the Wasteland (Site A) study site was slightly finer than particles found at the South-West ridge (Site B) study site. This may suggest that the material at the Wasteland study site has had more time to disaggregate, possibly due to the presence of more vegetation. Overall, results show that there was not much variation in soil characteristics between the different study sites. This may be due to the size of the island, which is relatively small (208 ha), resulting in little scope for environmental variations in terms of volcanic history, climate, vegetation, land use and topography.

General rainfall attributes

The rainy season on Round Island is typically concentrated between December and April, which has been confirmed in the results section of this dissertation, where December, January, February and March experienced the highest rainfall amounts. According to Proag (1995), February and March are the wettest months on mainland Mauritius. Although the months experiencing the highest rainfall amounts are well aligned, some meteorological stations on Mauritius can receive up to six times more rainfall than Round Island. Long term mean annual rainfall on Mauritius reveals that the eastern side of the island receives approximately 1200 mm of rainfall, the elevated central region receives upwards of 4000 mm, and the west coast as little as 600 mm (Rughooputh, 1997). It can be deduced that the attributes of rainfall on Mauritius are affected by the island's raised topography, which has a major influence on orographic forces. When compared to Mauritius (828 m a.m.s.l), Round Island has a maximum altitude of 280 m a.m.s.l, which evidently plays a role in the overall mean annual rainfall totals. In 2015, mean annual rainfall for Round Island was 699 mm, which was considerably less than the previous recorded average of 866 mm (see MWF, 2011). However, cognisance should be made of the fact that no tropical cyclones were recorded during the study period, and should a cyclone have occurred, average rainfall could

have increased by up to 245 mm (Le Roux, 2005). It is expected that had such a system, and the associated rainfall, passed near or over Round Island during the study period, it would have had a major impact on soil erosion and rainfall totals on the island.

Erosive events

Relatively similar rainfall erosivity totals were recorded at each station on Round Island, however, the number of erosive events experienced at each station differed slightly. The results confirm what was found in earlier literature, which states that the south-eastern side of the island is wetter and cooler, possibly due to the South-East Trade Winds and frontal systems. The same pattern, as mentioned above, can be found on Mauritius, where the eastern side of the island experiences considerably more rainfall (1200 mm) than the western side (600 mm) (Nigel & Rughooputh, 2010). The maximum erosivity produced during an individual rainfall event on Round Island was 21,516.3 $J.mm.m^{-2}.h^{-1}$. This event had a storm duration of 75 minutes and rainfall depth of 21.2 mm. This figure is far smaller than the maximum erosivity found in the study by Mongwa (2011), where a maximum erosivity of 800,000 $J.mm.m^{-2}.h^{-1}$ was recorded at Trou aux Cerfs on Mauritius. The maximum erosivity on Round Island was below the average mean erosivity across five meteorological stations on mainland Mauritius (29,043 $J.mm.m^{-2}.h^{-1}$). A study conducted by Nel *et al.* (2016) also reported significantly higher storm depth, storm duration and erosivity totals on Mauritius. The characteristics of 120 extreme rainfall events were measured and revealed a maximum storm depth of 615 mm, erosivity of 2,240,158 $J.mm.m^{-2}.h^{-1}$ (two orders of magnitude greater than Round Island) and maximum storm duration of 4,932 minutes.

Since there is a highly correlated relationship between erosivity and rainfall depth, we must also compare the maximum and mean rainfall depths recorded on both Round Island and Mauritius. On Round Island, the storm with the highest rainfall depth recorded a total depth of 32.2 mm and an average mean rainfall depth of 14.25 mm. Compared to the study done by Mongwa (2011), a maximum rainfall depth of 435.8 mm and an average mean rainfall depth of 49 mm was recorded across five rainfall stations. Rainfall depths at the elevated interior of Mauritius are markedly higher when compared to Round Island and this is heavily reflected in the erosivity totals. Similarly, storm duration on Round Island was far lower than that of storms recorded on Mauritius. The maximum storm duration and average mean duration for an erosive event was 540 minutes was 138 minutes, respectively. This is significantly lower than the maximum duration on Mauritius (4,560 minutes) and average mean duration (620

minutes). Overall, rainfall and erosivity on Round Island is far less, when compared to mainland Mauritius, which could explain why soil erosion was recorded at two orders of magnitude less than on Mauritius.

Comparing erosivity from Round Island to erosivity on a global scale is now possible following the study done by Panagos *et al* (2017), which estimated the global mean rainfall erosivity to be 2,190 MJ.mm.ha^{-1}.h^{-1}.yr^{-1}. Round Island's erosivity (2,314.76 MJ.mm.ha^{-1}.h^{-1}.yr^{-1}) is, therefore, slightly above the mean global estimate. The study by Panagos *et al* (2017) estimates the continent of South America to have the highest mean erosivity of 5,874 MJ.mm.ha^{-1}.h^{-1}.yr^{-1}, followed by Africa (3,053 MJ.mm.ha^{-1}.h^{-1}.yr^{-1}), and the middle east (1,487 MJ.mm.ha^{-1}.h^{-1}.yr^{-1}). On a country level, Mauritius and the Comoros have the highest worldwide mean annual erosivity, which was close to 20,000 MJ.mm.ha^{-1}.h^{-1}.yr^{-1}. The lowest mean erosivity values were found to be less than 115 MJ.mm.ha^{-1}.h^{-1}.yr^{-1}, estimated for Western Sahara, Libya and Egypt.

Table 5.1: Mean rainfall erosivity values as per Panagos *et al* (2017) for comparison to Round Island.

Country	Erosivity (MJ mm ha^{-1}.h^{-1}.yr^{-1})
Kuwait	220
Russia	250
Ukraine	488
Chile	1,320
Australia	1,535
China	1,600
Round Island	2,315
Argentina	2,332
South Africa	2,500
Japan	4,815
Brazil	7,500
Mauritius	20,000
Malaysia	20,000

Sediment transport rates on Round island

Nigel & Rughooputh (2012) state that soil erosion by water is one of the most important natural resources management problems in the world. Furthermore, Nigel &

Rughooputh (2012) indicate that the damage it causes on-site are soil loss, breakdown of soil structure, and a decline in organic matter content, nutrient content, fertility, and infiltration rate. The rate of soil erosion for Round Island, derived from sediment displacement in monitored catchments, is currently estimated at 12.48 $g.m^{-2}.yr^{-1}$ or 0.1248 $t.ha^{-1}.yr^{-1}$. Using this rate, the total soil loss on Round Island is estimated at 25.96 $t.yr^{-1}$. The estimated soil erosion rate is extremely low (two orders of magnitude less) when compared to modelled rates of soil erosion under natural vegetation (RUSLE = less than 10 $t.ha^{-1}.yr^{-1}$) on Mauritius (see Le Roux, 2005). Although overall sediment transport rates are low, it is important to consider that the most recent cyclone was in February 2007, and therefore, sediment transport rates are expected to be lower than had such a system, and associated rainfall, passed near or over Round Island during the study period.

In comparison to studies on other tropical islands, Calhoun & Fletcher (1999) estimated a total sediment loss of 0.86 $t.ha^{-1}.yr^{-1}$ in the densely vegetated area of Hanalei watershed on the South Pacific Island of Kauai. McMurtry *et al.* (1995) calculated a sediment yield of 0.6 $t.ha^{-1}.yr^{-1}$ in the 42.9 km^2 catchment of O'ahu Island, that drains Honolulu and has steep undeveloped mountains. Le Roux (2005) concludes that the overall higher rates of erosion on Mauritius (11 $t.ha^{-1}.yr^{-1}$) are most likely due to the extensive cultivation. Thus, the very low rate of sediment displacement calculated for Round Island is most likely due to the observation that most of the soil has already been eroded, leaving a largely barren landscape (Figure 5.1) with evidence of erosion into bedrock (Bean *et al*., 2017), as well as the fact that no tropical cyclones passed near or over the island during the study period.

Figure 5.1: Largely barren landscape of Round Island.

Soil conservation

Much work has been done on Round Island to limit soil erosion. Since Johnston's (1993) soil survey, the recovery of degraded soils and the protection of areas known to have deeper soils that favour regeneration of plant communities have been carried out successfully. The establishment of pioneer species (grasses and shrubs) have assisted in increasing vegetation cover and has played a role in protecting planted areas from shearwater burrowing. Extensive planting of the *Latania loddigessii* and *Ipomea pes-caprae* have greatly assisted in reducing soil loss in the gullies. Several ad hoc mechanical conservation methods have also been implemented through the construction of soil traps, which have proven to be successful in trapping soil (Figure 5.3) locally but have not been successful in treating the source of the problem or the gully systems. Overall, vegetation cover has increased considerably, indicating positive results from the rehabilitation programme. Le Roux (2005) notes that vegetation cover is a primary controlling factor with regards to soil erosion. Thus, going forward, the most appropriate steps would be to continue establishing vegetation regeneration but on an island-wide scale, and if possible, extensive revegetation should be carried out in key areas

where soil erosion is likely to be more intense. Steep slopes and high rainfall are also noted as contributing factors, however, rainfall and slope steepness are not manageable components and, therefore, revegetation must be prioritised. After consultation of 55 studies covering 21 countries regarding soil loss, Labrière *et al.* (2015) concluded that soil loss was maximum on bare soils and exceeded that of all other land-use types. The results of this study confirm the above, and when considering the slope gradient, catchment size, erosivity and vegetation for each of the study sites, it is vegetation that seems to be the defining factor in the rate of soil erosion on Round Island. Sites at the South-West Ridge (Figure 5.2) have significantly less vegetation present, resulting in more soil erosion.

Another point to consider is the predominantly convex slopes found throughout the island, which influence soil movement as there are no relatively flat areas for soil to settle and delay or halt their movement downslope following an intense rainfall event. However, according to Bean *et al.* (2017), sediment that is displaced from the hillslopes and upper reaches is transported downslope following rainfall events, and appears to be settling in the gullies. This may be attributed to either an excessive supply of sediment or an undersupply of water. A unique geomorphological evolution has taken place, where the gullies have gone from being a sediment source, to a sediment sink. The result is an increase in vegetation, specifically the *Latania loddigessii*, which has played a significant role in further slowing the process of erosion in the gullies as vegetation cover increases flow resistance thereby reducing runoff velocity and sediment transport (Rey, 2003). It would appear that due to the extensive nature of gullies on Round Island (Figure 5.3), erosion is a naturally accelerated process, which has been enhanced by prior disturbances, thus, the establishment of revegetation is of paramount importance.

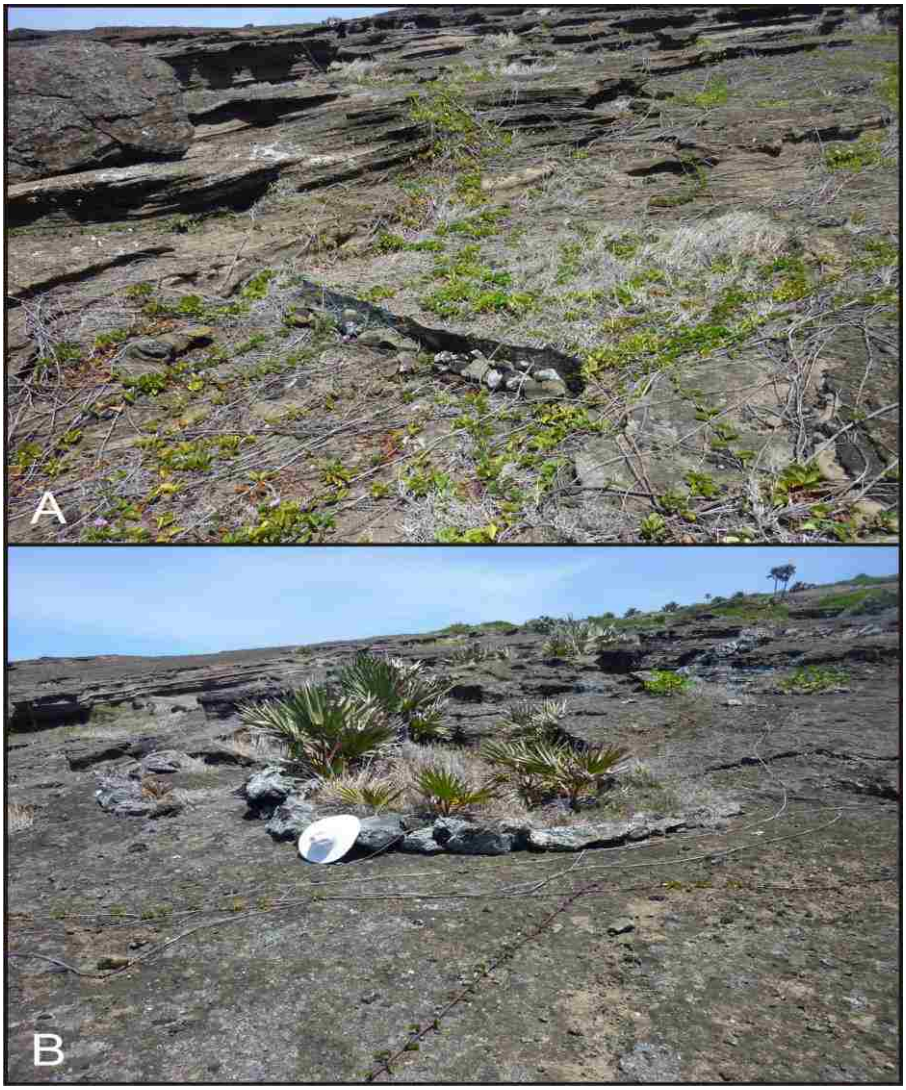

Figure 5.2: A) Geo-technical mesh screen to slow the transport of sediment. B) Stone wall sediment trap. Hat for scale.

Zoogeomorphology

The idea of animals acting as geomorphic agents have long been considered curiosities in geomorphology literature. However, on Round Island, there is a definite influence from birds and mammals. For instance, the introduction of goats and rabbits to Round Island between 1840 and 1865 has resulted in the destruction of natural vegetation, perhaps the worst loss has been the hardwood forest (Bullock, 1977). Overgrazing has also detrimentally affected the ecology of the island, and resulted in the extinction of various species such as the burrowing boa (*Bolyeria multocarinata*) and Mascarene giant tortoise (*Cylindraspis*). The extinction of the tortoises led to the disruption of many ecosystem interactions such as seed dispersal.

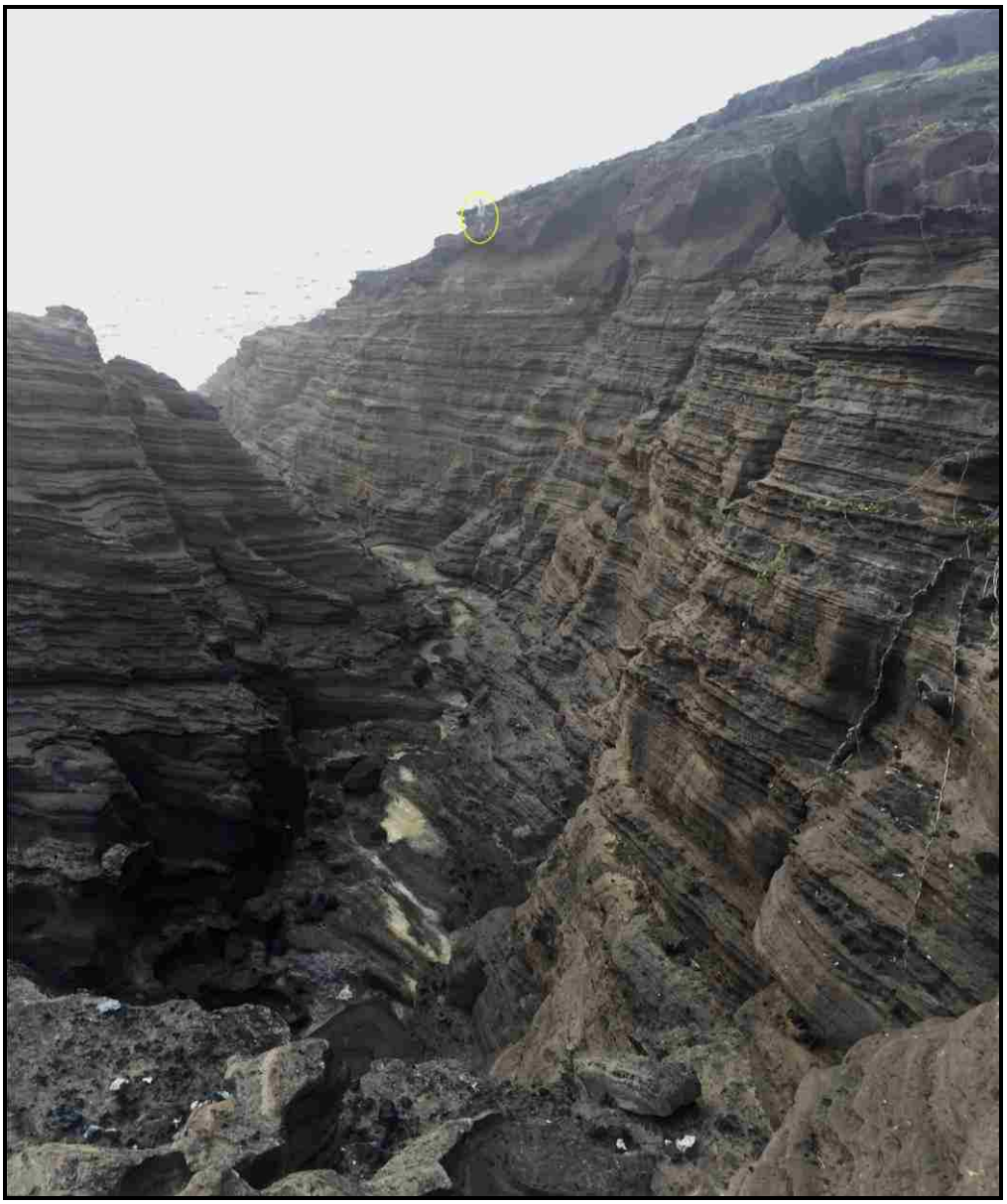

Figure 5.3: View downslope of lower “big gully” towards the coastline, which deeply dissects the landscape and represents erosion of the highest severity on Round Island with researcher circled for scale.

As part of the ecosystem restoration process, the MWF introduced Giant Aldabran (*Aldabrachelys giganta)* and Madagascan radiated (*Astrochelys radiata)* tortoises to Round Island in 2007 to replace the missing plant-herbivore interactions. The tortoises, taxonomically and functionally, perform similarly to the extinct Mascarene giant tortoises (*Cylindraspis),* and seem to have had a largely beneficial impact on the island (Griffiths *et al*., 2010). The innovative landscape restoration approach is to use the tortoises to control the non-native plants that are threatening persistence of the native species. Griffiths *et al.* (2010) conclude that the introduction of the tortoises are a more cost-effective approach to

controlling the non-native vegetation than manual weeding. Although the tortoises form wallows for resting and, by doing so, remove vegetation, exposing the underlying soil, they are mostly very shallow as reported by Bean *et al*., (2017) and seem to have a relatively small impact. No linear erosion forms were created as a result of the wallows, although the exposed soil may be susceptible to sheatwash during times of intense rainfall. Exclusion plots have previously been set up to monitor the effects of tortoises on vegetation consumption. Bean *et al*., (2017) reported that vegetation cover was greater within the plot, indicating that tortoises do have an effect on vegetation biomass, although did conclude that there appears to be no overall negative impact on soil loss. Tortoises are largely seen as ecosystem engineers, through the distribution of seeds, namely the large seeds of the endemic *Latania loddigessii* palm species, and the preferential grazing of invasive plant species, creating various ecological benefits. Observations indicate that the tortoises also tend to eat the leaves of plants and do not disturb the roots when grazing. Therefore, it is believed that at the current tortoise density, and as long as overgrazing does not occur, their reintroduction can be considered as beneficial to plant regeneration and soil conservation on Round Island.

The current influence of the Wedge-tailed Shearwater (*Puffinus pacificus),* which have created hundreds of burrows in areas of deeper soils in the Mixed Weed habitat (Figure 5.4), remains unclear. Johnston (1993) observed the presence of rill erosion below burrows. These burrowing seabirds are known to have an impact on soil properties and increase the risk of soil erosion due to a loss in vegetation, compaction of nearby soils and reduced infiltration (Bancroft *et al*., 2005). However, according to Kinlaw & Grasmueck (2012), a positive function of burrows is the turnover of soil nutrients, which can promote vegetation growth. Similarly, Butler (1995) reports that the soils surrounding a nest are considerably more acidic, which has been attributed to the collection of bird droppings, acting as a fertilizer, encouraging plant growth. Thus, more research should be conducted on the geomorphological impacts of animals on Round Island, particularly the impacts of burrowing birds on sediment displacement and nutrient cycling for vegetation.

Figure 5.4: Evidence of seabird burrows into soil on Round Island. Hat for scale.

This chapter has discussed the results and objectives set out in the previous chapters. Important findings have been highlighted with regards to the landscape dynamics, soil properties, rainfall attributes, erosivity and sediment transport. This research project concludes in the following chapter with a summary of the findings and observations.

Landscape Dynamics

Rates of primary erosion on hillslopes are determined by rainfall erosivity, runoff, and the erodibility of the surface (Al-Durrah & Bradford, 1982). Factors influencing this include geology, soil type, vegetation, slope gradient, slope length and human activity (Charlton, 2009). It is extremely difficult to quantify erodibility and erosivity in order to predict the rate of soil erosion for a particular slope or study area. Nonetheless, this study attempts to express the rate of sediment transport as a function of specific variables, namely rainfall erosivity, derived from the kinetic energy of rainfall events and soil erodibility. It is important to consider the influence of climate on erosivity and its indirect effects on soil erodibility, especially in terms of the presence of vegetation and moisture content. For example, although

the interior plateau of Mauritius experiences significantly more rainfall erosivity, the area is extremely well vegetated, which enables the landscape to withstand larger rain drops associated with high intensity rainfall, making the soils less vulnerable to direct rainfall (Nigel & Rughooputh, 2010). Rainfall erosivity is the potential of rainfall to detach soils on impact, as such, the considerations of existing vegetation cover are important. Since Round Island receives far less rainfall per annum, and has a much drier landscape than the interior of Mauritius, soil is expected to be more vulnerable to erosion at a local scale. Having said that, there are areas in Mauritius that experience comparable erosivity levels with Round Island, such as the drier West coast, and it is important to stay cognisant of this fact.

Detachability is a common term in the terminology used to describe hillslope material, and materials can be regarded as having a range of detachability. Some materials may be completely undetachable by a certain process whereas other materials may be infinitely detachable, where the rate of erosion on a slope is controlled by the transporting capacity of the process (Lal, 1990; Toy *et al*., 2002; Morgan, 2005). An example of the role of an external factor (exogenic) is the situation where the moisture content of slope materials is significantly increased during a period of intense rainfall. Soils on Round Island can be considered highly detachable. The rills and gullies present on Round Island are typically bedrock incised (Figure 5.3), which are contrary to the norm where formation usually takes place in the soil layer and terminates at the bedrock level (see Bean *et al.*, 2017). This can be attributed to the properties of the scoriaceous basalt (volcanic tuff). Bean *et al*. (2017) indicate that the underlying parent material (bedrock) has low Schmidt Hammer rebound values, making it friable and possibly more susceptible to erosion by water. However, little is known about the role of parent material properties and their influence on the resistance to gully erosion processes (Poesen *et al*., 2003).

Chapter 6: Conclusion

Summary and key findings

This project aimed to assess rainfall characteristics, erosivity and soil erosion on Round Island, Mauritius. Prior studies investigating the 'R-factor' have taken place in a variety of environments, however, none had previously been conducted on Round Island. Round Island is a small islet off the north coast of Mauritius. Prior to the mid-1970s, Round Island was subjected to heavy overgrazing by goats and rabbits, which detrimentally affected the ecology and geomorphology of the island. Currently, the island exhibits a largely barren landscape with bedrock incised gullies (Bean *et al*., 2017) that represent erosion phenomena of the highest severity which prompted this study. Now classified as a nature reserve and home to several endangered species, vegetation monitoring is ongoing and soil conservation has been implemented through the use of mechanical methods and revegetation initiatives.

The study made use of two environmental monitoring stations to determine the rainfall characteristics of Round Island. From the data collected, the Wasteland study site recorded slightly more rainfall than the South-West Ridge study site, presumably due to the presence of the South-East Trade Winds. As a result, the Wasteland station received slightly more erosive rainfall events. Although rainfall intensities on the eastern side of the island exceed the 25 $mm.h^{-1}$ parameter on more occasions, the South West Ridge station recorded the highest rainfall intensities. The month of March was noted as the month with the highest number of erosive rainfall events, even though, on average, less rainfall was received during this month.

Calculations were performed following the EI_{30} method using 15-minute interval rainfall data with the aim of identifying the erosive characteristics of individual rainfall events. Kinetic energy and erosivity recorded during the study revealed that mean values were greater at the South-West ridge station. The maximum kinetic energy produced during any individual storm was 645.1 $J \cdot m^{-2}$, recorded at the South-West ridge. Similarly, the maximum erosivity was also recorded here (21,516.3 $J.mm.m^{-2}.h^{-1}$). The findings revealed that kinetic energy and erosivity levels are far lower than those found by Mongwa (2011) for Mauritius. Statistical analysis revealed that significant positive correlations exist between certain erosive attributes on Round Island. These include positive correlations between rainfall depth and kinetic energy and erosivity. Rainfall event duration also shows a positive correlation with kinetic energy and erosivity, however, the correlations are slightly weaker than rainfall depth.

Once the erosive characteristics were measured, the attributes were considered alongside the monthly soil displacement to determine the relationship between rainfall and sediment movement. Depending on the amount of rainfall recorded in the preceding month, total sediment sample weights varied between 0.014 and 1.5 kilograms. A strong, statistically significant (ρ= 0.01) positive correlation (r=0.93) was found between average rainfall and average displaced soil weight. Considering the linear regression coefficient, there is an approximate increase of 200 g sediment displacement per 45.5 mm of rainfall depth. Significantly less rainfall was recorded on Round Island than most regions of Mauritius (see Rughooputh, 1997), which consequently lead to lower kinetic energy and erosivity levels. Erosivity was recorded at almost one order of magnitude less than Mauritius (Mongwa, 2011; Nel *et al*., 2016) and up to two orders less when considering modelled sediment transport rates (Le Roux, 2005). However, it is important to be cognisant of the fact that no tropical cyclone was recorded during the study period, which could have had a major influence on soil erosion and rainfall totals.

The annual sediment movement rates for Round Island were established during this study (0.1248 $t.ha^{-1}.yr^{-1}$) and were found to be considerably lower than Mauritius (10 $t.ha^{-1}.yr^{-1}$), as well as other tropical island such as Kauai (0.86 $t.ha^{-1}.yr^{-1}$) and O'ahu (0.6 $t.ha^{-1}.yr^{-1}$). Thus, although the estimated rates of soil erosion are very low for humid tropical regions, these rates only reflect the contemporary environmental conditions and cognisance of the landscape history should be incorporated into assessments of soil erosion. The barren landscape and very low contemporary rates of soil erosion suggest that most of the erodible soil has already been eroded. Nevertheless, findings from this study also suggests that there is a statistically significant positive relationship between rainfall and sediment transport and that catchment size as well as vegetation play major roles in the rate of sediment transport. The study confirms Charlton's (2009) view that larger catchments can store more sediment as sediment yields were markedly lower on the Wasteland side of the island. Similarly, findings from this study suggest that vegetation plays a major role in reducing soil erosion, as catchments containing denser vegetation recorded lower sediment yields. Another point to consider is the predominantly convex slopes found throughout the island, where slope gradients range between 10-30°, which influence soil movement rates. Mararakanye & Sumner (2017) suggest that gully erosion propensity increases rapidly for hillslopes steeper than 4.5° which may explain why gully erosion is so prevalent on Round Island.

The sediment characteristics were established through particle size analysis. Round Island's underlying geological material is made up of consecutive beds of tuff, which has recorded low Schmidt Hammer values (Bean *et al.*, 2017), making it highly susceptible to water erosion. Soils on Round Island between the particle sizes of 0.5-2.0 mm seem to be most susceptible to detachment, supporting the view of Dóniz-Paez *et al*. (2011) that Round Island has a relatively young volcanic cone. The particle size analysis revealed that sediment comprises of mostly gravely sand, although the samples were not unimodal and, therefore, may be considered unreliable. Findings show that there was a lack of fines found in the Gerlach troughs, possibly due to wind erosion, which would have skewed the results. The physical properties of the soil on Round Island are different in comparison to Mauritius (Johnston, 1993), which is likely due to the island's unique environmental setting, in terms of its volcanic history, topography, climate and vegetation.

Scope for future research

Going forward, high resolution rainfall data recording must continue to ensure more accurate assessments and future research, which can greatly assist the conservation effort for Round Island. Future research should focus on establishing the rainfall erosivity over a longer period (more than 20 years) could be highly beneficial as stated by Renard *et al.* (1997). Additionally, research should focus on establishing the erosive characteristics of rainfall events derived from known cyclone activity, which could be used to compare with this study and aid in establishing more accurate sediment transport rates. Future research should make use of unmanned aerial vehicles (i.e. drones) in order to capture high resolution aerial photography and build digital elevation models. These can be used to model soil erosion, on an island scale, as well as model the hydrology of Round Island. Modelling the hydrology will allow researchers to identify key areas where soil erosion is intensified, identifying important areas for revegetation.

The island is of great biological importance and home to a number of endangered plant and wildlife species which must be protected and conserved. Therefore, conservation efforts should focus on wide-scale revegetation, especially in key areas where soil erosion is likely to be more intense. Further investigations into the potential impacts of introduced non-indigenous tortoise species and burrowing bird species as geomorphic agents should be conducted, especially with regards to sediment displacement and nutrient cycling within the ecosystem. In particular, an investigation into the spatial extent of burrowing by bird species,

the volume of displaced soil by burrowing and nutrient cycling around the burrows could reveal various insights into the impacts of burrowing bird species as geomorphic agents and ecosystem engineers on Round Island; one of the few seabird breeding stations in the Western Central Indian Ocean.

References

Addison, K., 1987: Debris flow during intense rainfall in Snowdonia, North Wales: a preliminary survey, *Earth Surface Processes and Landforms*, 12, 561-566.

Al-Durrah, M.M. and Bradford, J.M., 1982: The mechanism of raindrop splash on soil surfaces, *Soil Science Society of America Journal*, 46, 1086-1090.

Anderson, R.L., 2012: Rainfall erosivity attributes on central and western Mauritius, Unpublished MSc Dissertation, University of Pretoria, Pretoria, South Africa.

Angulo-Martínez, M. and Beguería, S., 2009: Estimating rainfall erosivity from daily precipitation records: A comparison among methods using data from Ebro Basin (NE Spain), *Journal of Hydrology*, 379, 111-121.

Bancroft, W.J., Garkaklis, M.J., and Roberts, J.D., 2005: Burrow building in seabird colonies: A soil-forming process in island ecosystems, *Pedobiologica*, 49, 149-165.

Baxter, A.N., 1972: Magmatic evolution of Mauritius, western Indian Ocean, Unpublished Doctoral Thesis, University of Edinburgh, Scotland.

Baxter, A.N., 1975: Petrology of the older series lavas from Mauritius, Indian Ocean, *Geological Society of America Bulletin*, 86, 1449-1458.

Bean, T.A., 2014: Erosion phenomena on Round Island, Mauritius, Unpublished MSc Dissertation, University of Pretoria, Pretoria, South Africa.

Bean T.A., Sumner, P.D., Boojhawon, R, Tatayah, V., Khadun, A.K., Hedding, D.W., Rughooputh, S.D.D.V., and Nel, W., 2017: Bedrock incised gully erosion phenomena on Round Island, Mauritius, *Catena*, 151, 107-117.

Beckedahl, H.R., Bowyer-Bower, T.A.S., Dardis, G.F. and Hanvey, P.M., 1988: Geomorphic effects of soil erosion. In: Moon, B.P. & Dardis, G.F. (eds), *The Geomorphology of Southern Africa*, Southern Book Publishers, Johannesburg, pp. 249-276.

Bell, D.B., Dulloo, M. and Bell, M., 1994: *Mauritius Offshore Survey Reports and Management Plan.* Prepared for Government of Mauritius. Jersey Wildlife Preservation Trust & Wildlife Management International Ltd.

Bergsma, E., Charman, P., Gibbons, F., Hurni, H., Moldenhauer, W.C. and Panichapong, S., 1996: *Terminology for soil erosion and conservation*. ISSS, ITC, ISRIC.

Bergstrom, D.M., Lucieer, A., Kiefer, K., Wasley, J., Belbin, L., Pedersen, T.K. and Chown, S.L., 2009: Indirect effects of invasive species removal devastate World Heritage Island, *Journal of Applied Ecology*, 46, 73-81.

Bhattarai, R. and Dutta, D., 2007: Estimation of soil erosion and sediment yield using GIS at catchment scale, *Water Resource Management*, 21, 1635-1647.

Blott, S.J. and Pye, K., 2001: GRADISTAT: a grain size distribution and statistics package for the analysis of unconsolidated sediments, *Earth Surface Processes and Landforms*, 26, 1237-1248.

Boardman, J. and Favis-Mortlock, D., 1999: Frequency-magnitude distributions for soil erosion, runoff and rainfall-a comparative analysis, *Zeitschrift für Geomorphologie Supplement Band*, 115, 51-70.

Brandt, C.J. and Thornes, J.B., 1987: Erosional energetics. In: Gregory, K.J. (ed.), *Energetics of Physical Environment—Energetic Approaches to Physical Geography*, John Wiley and Sons, 51–87.

Brice, J.C., 1966: Erosion and deposition in the loess-mantled Great Plains, Medicine Creek drainage basin, Nebraska, *U.S. Geological Survey Professional Paper*, 352, 255-339.

Brown, L.C. and Foster, G.R., 1987: Extreme event erosivity using identical intensity distributions, *Transactions of the American Society of Agricultural Engineers*, 30, 379-386.

Bryan, R.B., 2000: Soil erodibility and process of water erosion on hillslopes, *Geomorphology*, 32, 385-415.

Bull, L.J. and Kirkby, M.J., 1997: Gully processes and modelling, *Progress in Physical Geography*, 21, 354-374.

Bullock, D.J. and North, S.G., 1975: Report of the Edinburgh University expedition to Round Island, Mauritius, July and August 1975.

Bullock, D.J., 1977: Round Island - a tale of destruction, *Oryx*, 14, 51-58.

Bullock, D.J., North, S.G., Greig, S., Osborne, B. and Snelson, D., 1982: Round Island Expedition 1982: Preliminary Report, Unpublished.

Bullock, D.J. and North, S., 1984: Round Island in 1982, *Oryx*, 18, 36-41.

Butler, D.R., 1995: *Zoogeomorphology: Animals as geomorphic agents*, Cambridge University Press, New York.

Calhoun, R.S. and Fletcher, C.H., 1999: Measured and predicted sediment yield from a subtropical, heavy rainfall, steep-sided river basin: Hanalei, Kauai, Hawaiian Islands, *Geomorphology*, 30, 213-226.

Capolongo, D., Pennetta, L., Piccarreta, M., Fallacara, G. and Boenzi, F., 2008: Spatial and temporal variations in soil erosion and deposition due to land- levelling in a semi- arid area of Basilicata (Southern Italy), *Earth Surface Processes and Landforms*, 33, 364-379.

Carpenter, A.I., Côté, I.M. and Jones, C.G., 2003: Habitat use, egg laying sites and activity patterns of an endangered Mauritian gecko (*Phelsuma guentheri*), *The Herpetological Journal*, 13, 155-157.

Chapman, P.J., 2005: Soil and the Environment. In: Holden, J. (ed.): *An Introduction to Physical Geography and the Environment*, Pearson Education Limited, Edinburgh Gate, pp. 143-174.

Charlton, R., 2009: *Fundamentals of Fluvial Geomorphology*, Routledge, New York.

Cheeroo-Nayamuth, F.C., Robertson, M.J, Wegener, M.K. and Nayamuth, A.R.H., 2000: Using a simulation model to assess potential and attainable sugar cane yield in Mauritius, *Field Crops Research*, 66, 225-243.

Cheke, A.S., 1987: An ecological history of the Mascarene Islands, with particular reference to extinctions and introductions of land vertebrates. In: Diamond, A.W. (ed.), Studies of Mascarene Island Birds, Cambridge University Press, London, pp. 5-89.

Cheke, A.S., 2004: Wind-blown sand and accumulation of soil on Round Island, Unpublished Report, Mauritian Wildlife Foundation, Mauritius.

Cheke, A.S. and Bour, R. 2014: Unequal struggle—how humans displaced the tortoise's dominant place in island ecosystems. In: Gerlach J. (ed.), Western Indian Ocean Tortoises: biodiversity, palaeontology, evolution and conservation, Siri Scientific Press, Manchester, pp. 31–120.

Costin, A.B. and Moore, D.M., 1960: The effects of rabbit grazing on the grasslands of Macquarie Island, *Journal of Ecology*, 48, 729-732.

Daszak, P., 1994: The 1993 Raleigh International Round Island Expedition, including a survey of intestinal parasites collected from animals of Round Island, Mauritius and Rodrigues and observations on Round Island Reptiles, Unpublished Report deposited in the Library of Kingston University, 1-49.

De Ploey, J., 1974: Mechanical properties of hillslopes and their relation to gullying to central and semi-arid Tunisia, *Zeitschrift für Geomorphologie Supplement Band*, 21, 177-190.

De Ploey, J., 1989: A model for headcut retreat in rills and gullies, *Catena Supplement*, 14, 81-86.

Dennet, M.D., 1978: Variations of rainfall and seasonal forecasting in Mauritius, *Mauritius*, 25, 359-370.

Dickson, M.E., Kennedy, D.M. and Woodroffe, C.D., 2004: The influence of rock resistance on coastal morphology around Lord Howe Island, southwest Pacific, *Earth Surface Processes and Landforms*, *29*, 629-643.

Diodato, N., 2005. Predicting RUSLE (Revised Universal Soil Loss Equation) monthly erosivity index from readily available rainfall data in Mediterranean area, *Environmentalist*, *26*, 63-70.

Doniz-Paez, J., Becerra-Ramirez, R., Gonzalez-Cardenas, E., Guillen-Martin, C. and Escobar-Lahoz, E., 2011: Geomorphosites and geotourism in volcanic landscape: the example of La Corona Del Lajial cinder cone (El Hierro, Canary Islands, Spain), *GeoJournal of Tourism and Geosites*, 8, 185-197.

Duncan, R.A. and Richards, M.A., 1991: Hotspots, mantle plumes, flood basalts, and true polar wander, *Review of Geophysics*, 29, 31-50.

Elwell, H.A., 1976: Natal Agricultural Research Bulletin No 7, Soil Loss Estimator for Southern Africa, Department of Agriculture Technical Services, Natal, South Africa.

Elwell, H.A. and Stocking, M.A., 1973: Rainfall parameters for soil loss estimation in a subtropical climate, *Journal of Agricultural Engineering Research*, 18, 169-177.

Evans, R., 1998: The erosional impacts of grazing animals, *Progress in Physical Geography*, *22*, 251-268.

Flanagan, D.C. and Nearing, M.A., 1995: USDA water erosion prediction project: hillslope profile and watershed model documentation. NSERL Report No. 10. USDA-ARS National Soil Erosion Research Laboratory, West Lafayette, Indiana 47907-1194.

Free, F., 1960: Erosion characteristics of rainfall, *Agricultural Engineering*, 41, 447-449.

GLASOD, 1990: *World map of the status of human-induced soil degradation,* Winand Staring Center, Wageningen.

Griffiths, C.J., Jones, C.J., Hansen, D.M., Puttoo, M., Tatayah, R.V., Müller, C.B., Harris, S., 2010: The use of extant non-indigenous tortoises as a restoration tool to replace extinct ecosystem engineers, *Restoration Ecology*, 18, 1-7.

Griffiths, C. J., Zuël, N., Tatayah, V., Jones, C.G., Griffiths, O. and Harris. S., 2012: The welfare implications of using exotic tortoises as ecological replacements, *PLoSONE*, 7, e39395.

Griffiths, C. J., Zuël, N., Jones, C.G., Ahamud, Z., and Harris. S., 2013: Assessing the potential to restore historic grazing ecosystems with tortoise ecological replacements, *Conservation Biology*, 27, 690-700.

Gunn, R. and Kinzer, G.D., 1949: Terminal velocity of water droplets in stagnant air, *Journal of Meteorology*, 6, 243.

Hauptfleisch, A., 2016: Intra-storm attributes and climatology of extreme erosive events on Mauritius, 2004 to 2008, Unpublished MSc Dissertation, University of Pretoria, Tshwane, South Africa.

Haynes, R.J., 1997: The concept of soil quality and its application to sugar cane production, *Proceedings of the South African Sugar Technologists Association*, 71, 9-14.

Hinkle, S.E., Heerman, D.F. and Blue M.C., 1987: Falling water drops at 1570 m elevation, *Transactions of the American Society of Agricultural Engineers*, 30, 94-100.

Hoogmoed, W. B. and Stroosnijder, L., 1984: Crust formation on sandy soils in the Sahel I. Rainfall and infiltration, *Soil and Tillage Research,* 4, 5-23.

Horton, R.E., 1945: Erosional development of streams and their drainage basins; hydrophysical approach to quantitative morphology, *Geological Society of America Bulletin*, 56, 275-370.

Hoyos, N., Waylena, P.R. and Jaramillo, A., 2005: Seasonal and spatial patterns of erosivity in a tropical watershed of the Colombian Andes, *Journal of Hydrology*, 314, 177-191.

Hudson, H.R., 1971: On the relationship between horizontal moisture convergence and convective cloud formation, *Journal of Applied Meteorology*, *10*, 755-762.

Imeson, A.C. and Kwaad, F.J., 1980: Gully types and gully prediction, *Geografisch Tijdschrift*, 5, 430- 441.

Ireland, H.A., Sharpe, C.F. and Eargle, D.H., 1939: Principles of gully erosion in the piedmont of South Carolina, *USDA Technical Bulletin*, 633, 1-143.

Johansson, M.C., 2003: Vegetation monitoring and change on Round Island, Mauritius. Unpublished MSc Dissertation, University of Birmingham, Birmingham, England.

Johnston, S., 1993: Round Island soil survey, Mauritian Wildlife Foundation, Mauritius.

Joss, J. and Waldvogel, A., 1967: Ein Spectrograph fűr Nieder-slagstrőpfe mit automatischer Auswertung, *Pure and Applied Geophysics*, 68, 240-246.

Karátson, D., Thouret, J. C., Moriya, I. and Lomoschitz, A., 1999: Erosion calderas: origins, processes, structural and climatic control, *Bulletin of Volcanology*, 61, 174-193.

Khadun, A., Allet, M. and Murray, K., 1996: Round Island Management Report, 6-13 December, 1995, Unpublished.

Kihç, A. and Teymen, A., 2008: Determination of mechanical properties of rocks using simple methods, *Bulletin of Engineering Geology and the Environment*, 67, 237-244.

Kinlaw, A. and Grasmueck, M., 2012: Evidence for and geomorphological consequences of a reptilian ecosystem engineer: the burrowing cascade initiated by the Gopher Tortoise, *Geomorphology*, 157-158, 108-121.

Knighton, D., 2014: *Fluvial forms and processes: a new perspective*, Routledge, New York.

Labrière, N., Locatelli, B., Laumonier, Y., Freycon, V., Bernoux, M., 2015: Soil erosion in the humid tropics: a systematic quantitative review, *Agriculture, Ecosystems, and Environment*, 203, 127-139.

Lal, R., 1990: *Soil erosion in the tropics: principles and management*, McGraw-Hill, New York, USA.

Lal, R., 2001: Soil degradation by erosion, *Land Degradation & Development*, 12, 519–539.

Laws, J.O. and Parsons, D.A., 1943: The relation of raindrop size to intensity, *Transactions of the American Geophysical Union*, 26, 452-460.

Le Roux, J.J., 2005: Soil erosion prediction under changing land use on Mauritius**,** Unpublished MSc Dissertation, University of Pretoria, Pretoria, South Africa.

Le Roux, J.J., Sumner, P.D. and Rughooputh, S.D.D.V., 2005: Erosion modelling and soil loss prediction under changing land use for a catchment on Mauritius, *South African Geographical Journal*, 87, 129-140.

Le Roux, J.J. and Sumner, P.D., 2012: Factors controlling gully development: comparing continuous and discontinuous gullies, *Land Degradation & Development*, 23, 440-449.

Lifton, Z.M., Thackray, G.D., Van Kirk, R. and Glenn, N.F., 2009: Influence of rock strength on the valley morphometry of Big Creek, central Idaho, USA, *Geomorphology*, 111, 173-181.

Lloyd, J.A., 1846: (Letter read to the society on 02/10/1845 on the subject of Round Island and Serpent Island), *Procés-verbaux de la Société d'Histoire Naturelle de l'Ile Maurice, 6 Octobre 1842-28 Aoŭt 1845*, 154-162.

Mararakanye, N. and Sumner, P.D., 2017: Gully erosion: A comparison of contributing factors in two catchments in South Africa, *Geomorphology*, 288, 99-110.

Mauritius Meteorological Service, 2010: Climate of Mauritius, Mauritius Meteorological Service Website, Mauritius. (http://metservice.intnet.mu/?page_id=644)

Mauritian Wildlife Foundation, 2008: Round Island management plan 2008-2012, Mauritian Wildlife Foundation, Mauritius.

Mauritian Wildlife Foundation, 2011: Climate monitoring data for Round Island, Unpublished Report, Mauritian Wildlife Foundation, Mauritius.

McDougall, I. and Chamalaun, F.H., 1969: Isotopic dating and geomorphic polararity studies on volcanic rocks from Mauritius, Indian Ocean, *Geological Society of America Bulletin*, 80, 1419-1442.

McMurtry, G.M., Snidvongs, A. and Glenn, C.R., 1995: Modelling sediment accumulation and soil erosion with ^{137}Cs and ^{210}Pb in the Ala Wai Canal and Central Honolulu watershed, Hawaii, *Pacific Science*, 49, 412-451.

Menéndez-Duarte, R., Marquínez, J., Fernández-Menéndez, S. and Santos, R., 2007: Incised channels and gully erosion in Northern Iberian Peninsula: Controls and geomorphic setting, *Catena*, 71, 267-278.

Merton, D.V., Atkinson, I.A., Strahm, W., Jones, C.J., Empson, R.A., Mungroo, Y., Dulloo, E. and Lewis, R., 1989: A management plan for the restoration of Round Island, Mauritius, Jersey Wildlife Preservation Trust.

Merritt, E., 1984: The identification of four stages during micro-rill development, *Earth Surface Processes and Landforms*, 9, 493-496.

Mihara, Y., 1951: Raindrops and soil erosion, *Bulletin of the National Institute of Agricultural Sciences*, A-1, 1-59.

Mongwa, T., 2011: Rainfall intensity, kinetic energy and erosivity of individual rainfall events on the island of Mauritius, Unpublished MSc Dissertation, University of Fort Hare, Alice, South Africa.

Morgan, W.J., 1981: Hotspot tracks and the opening of the Atlantic and Indian Oceans. In: Emilliani, C. (ed.), *The Sea*, Vol.7. John Wiley, New York, pp. 443-487.

Morgan, R.P.C., Quinton, J.N., Smith, R.E., Govers, G., Poesen, J.W.A., Auerswald, K., Chisci, G., Torri, D. and Styczen, M.E., 1998: The European Soil Erosion Model (EUROSEM): a dynamic approach for predicting sediment transport from fields and small catchments, *Earth Surface Processes and Landforms*, 23, 527-544.

Morgan, R.P.C., 2005: *Soil erosion and conservation*, 3rd Edition, Blackwell Publishing, Oxford, United Kingdom.

Mulholland, B. and Fullen, M.A., 1991: Cattle trampling and soil compaction on loamy sands, *Soil Use Management*, 4, 189-192.

Nearing, M.A., 2001: Potential changes in rainfall erosivity in the U.S. with climate change during the 21st Century, *Journal of Soil and Water Conservation*, 56, 229-232.

Nel, W. and Sumner, P.D., 2007: Intensity, energy and erosivity attributes of rainstorms in the KwaZulu-Natal Drakensburg, South Africa, *South African Journal of Science*, 103, 398-402.

Nel, W., Reynhardt, D.A. and Sumner, P.D., 2010: Effect of altitude on erosive characteristics of concurrent rainfall events in the northern KwaZulu-Natal Drakensberg, *WaterSA*, 36, 509-512.

Nel, W., Mongwa, T., Sumner, P.D., Anderson, R., Dhurmea, K., Boodhoo, Y., Boojhawon, R. and Rughooputh, S., 2012: The nature of erosive rainfall on a tropical volcanic island with an elevated interior, *Physical Geography*, 33, 269–284.

Nel, W., Anderson, R.L., Sumner, P.D., Boojhawon, R., Rughooputh, S.D.D.V. and Dunputh, B.H.J., 2013: Temporal sensitivity analysis of erosivity estimations in a high rainfall tropical island environment, *Geografiska Annaler: Series A, Physical Geography,* 95, 337-343.

Nel, W., Hauptfleisch, A., Sumner, P.D., Boojhawon, R., Rughooputh, S.D.D.V., and Dhurmea, K.R., 2016: Intra-event characteristics of extreme erosive rainfall on Mauritius, *Physical Geography*, 37, 264-275.

Németh, K. and Cronin, S., 2007: Syn-and post-eruptive erosion, gully formation, and morphological evolution of a tephra in a tropical climate erupted in 1913 in West Ambrym, Vanuatu, *Geomorphology*, 86, 115-130.

Nigel, R., and Rughooputh, S.D.D.V., 2010: Mapping of monthly soil erosion risk of mainland Mauritius and its aggregation with delineated basins, *Geomorphology*, 114, 110-114.

Nigel, R., and Rughooputh, S.D.D.V., 2012: Application of a RUSLE-based soil erosion modelling on Mauritius Island, *Soil Research*, 50, 645-651.

North, S.G. and Bullock, D.J., 1986: Changes in the vegetation and populations of introduced mammals on Round Island and Gunner's Quoin, Mauritius, *Biological Conservation*, 37, 99-118.

Nyssen, J., Vandenreyken, H., Poesen, J., Moeyersons, J., Deckers, J., Haile, M., Salles, C. and Govers, G., 2005: Rainfall erosivity and variability in the Northern Ethiopian Highlands, *Journal of Hydrology*, 311, 172-187.

Padya, B.M., 1984: *The climate of Mauritius*, 2nd Edition, Meteorological Services, Vacoas, Mauritius.

Panagos, P., Borrelli, P., Meusburger, K., Yu, B., Klik, A., Lim, K.J., Yang, J.E., Ni, J., Miao, C., Chattopadhyay, N., Sadeghi, S.H., Hazbavi, Z., Zabihi, M., Larionov, G.A., Krasnov, S.F., Gorobets, A.V., Levi, Y., Erpul, G., Birkel, C., Hoyos, N., Naipal, V., Oliveira, P.T.S., Bonilla, C.A., Meddi, M., Nel, W., Dashti, H.A., Boni1, M., Diodato, N., Van Oost, K., Nearing, M. and Ballabio, C., 2017: Global rainfall erosivity assessment based on high-temporal resolution rainfall records, *Scientific Reports*, 7, 4175.

Paul, D., Kamenetsky, V.S, Hofmann, A.W. and Stracke, A., 2007: Compositional diversity among primitive lavas of Mauritius, Indian Ocean: implication for mantle sources, *Journal of Volcanology and Geothermal Research*, 164, 76-94.

Pimental, D. and Kuonang, N., 1998: Ecology of soil erosion in ecosystems, *Ecosystems*, 1, 416-426.

Poesen, J., 1993: Gully typology and gully control measures in the European loess belt. In: Wicherek, E. (ed.), *Farm Land Erosion in Temperate Plains Environment and Hills*, Elsevier Science Publishers, Amsterdam, pp. 221-239.

Poesen, J., Vandaele, K. and Van Wesemael, B., 1996: Contribution of gully erosion to sediment production on cultivated lands and rangelands. In: Walling, D.E. & Webb, B.W. (eds), Erosion and Sediment Yield: Global and Regional Perspectives, IAHS Publications No. 236, Wallingford, pp. 251-266.

Poesen, J., Vandekerckhove, L., Nachtergaele, J., Oostwoud Wijdenes, D.J., Verstraeten, G. and van Wesemael, B., 2002: Gully erosion in dryland environments. In: Bull, L.J. & Kirkby, M.J. (eds), Dryland Rivers: *Hydrology and Geomorphology of Semi-Arid Channels*, Wiley, Chichester, pp. 229–262.

Poesen, J., Nachtergaele, J., Verstraeten, G. and Valentin, C., 2003: Gully erosion and environmental change: Importance and research needs, *Catena*, 50, 91-133.

Proag, V., 1995. *The geology and water resources of Mauritius*, Mahatma Gandhi Institute, Mauritius.

Renard, K.G. and Friemund J.R., 1994: Using monthly precipitation data to estimate the R-factor in the revised USLE, *Journal of Hydrology*, 157, 287-306.

Renard, K.G., Foster, G.R., Yoder, D.C. and McCool, D.K., 1994: RUSLE revisited: status, questions, answers and the future, *Journal of Soil and Water Conservation*, 49, 213-220.

Renard, K.G., Foster, G.R., Weesies, G.A., McCool, D.K. and Yoder, D.C., 1997: Prediction of soil erosion by water: a guide to conservation planning with the revised universal soil loss equation (RUSLE), Agricultural Handbook 703, USDA, Washington, DC.

Rey, F., 2003: Influence of vegetation distribution on sediment yield in forested marly gullies, *Catena*, 50, 549-562.

Rughooputh, S.D.D.V., 1997: Climate Change and Agriculture: Microclimatic Considerations. In: Lalouette, J.A., Bachraz, D.Y., Sukurdeep, N. & Seebaluck, B.D. (eds), *Second Annual Meeting of Agricultural Sciences,* Food and Agricultural Research Council, Mauritius, 73-82.

Rydgren, B., 1996: Soil erosion: Its measurement, effects and prediction. Case study from the southern Lesotho lowlands, *Zeitschrift fur Geomorphologie*, 40, 429-445.

Saddul, P. (ed.), 2002: *Mauritius – a geomorphological analysis*, Mahatma Ghandi Institute Press, Mauritius.

Salles, C., Poesen, J. and Sampere-Torres, D., 2002: Kinetic energy of rain and its functional relationship with intensity, *Journal of Hydrology*, 256-270.

Salako, F.K., Ghuman, B.S. and Lal, R., 1995: Rainfall erosivity in south-central Nigeria, *Soil Technology*, 2, 279-290.

Santosa, P.B., Mitani, Y. and Ikemi, H., 2010: Estimation of RUSLE EI30 based on 10 min interval rainfall data and GIS-based development of rainfall erosivity maps for Hitotsuse basin in Kyushu, Paper presented at the 18th International Conference of Geoinformatics, 18-20 June 2010, Beijing, China.

Schwab, G.O., Fangmeier, D.D. and Elliot, W.J., 1996: *Soil and water management systems*, 4th Edition, John Wiley and Sons.

Schwab, E.B., Reeves, D.W., Burmester, C.H. and Raper, R.L., 2002: Conservation tillage systems for cotton in the Tennessee Valley, *Soil Science Society of America Journal*, 66, 569-577.

Selby, M.J., 1994: Hillslope sediment transport and deposition. In: Pye, K. (ed.), *Sediment transport and depositional processes*, Blackwell Scientific Publications, UK, pp. 61-87.

Shamshad, A., Azhari, M.N., Isa, M.H., Wan Hussin, W.M.A. and Parida, B.P., 2008: Development of an appropriate procedure for estimation of RUSLE EI30 index and preparation of erosivity maps for Palau Penang in Peninsular Malaysia, *Catena*, 72, 423-432.

Singer, M.J. and Warkentin, B.P., 1996: Soils in an environmental context: an American perspective, *Catena*, 27, 179-189.

Stocking, M.A. and Elwell, H.A., 1976: Rainfall erosivity over Rhodesia, *Transactions of the British Institute of Geographers*, 1, 231-245.

Summerfield, M.A., 1991: *Global geomorphology*, Longman, Harlow.

Tatayah, R.V.V., 2010: The breeding biology of the Round Island petrel (*Pterodroma arminjoniana*) and the factors determining breeding success, Unpublished PhD Thesis, University of Mauritius, Moka, Mauritius.

Toy, T.J., Foster, G.R. and Renard, K.G., 2002: *Soil erosion: processes, prediction, measurement, and control*. John Wiley & Sons, New York.

Trustrum, N.A., Gomez, B., Page, M.J., Reid, L.M. and Hicks, D.M., 1999: Sediment production and output: the relative role of large magnitude events in steepland catchments, *Zeitschrift für Geomorphologie Supplement Band*, 115, 71-86.

Ugolini, F.C. and Dahlgren, R.A. 2002: Soil development in volcanic ash, *Global Environmental Research*, 6, 69-81.

United Kingdom Meteorological Office, 2017: South West Indian Ocean Tropical Cyclone Tracks. (https://www.metoffice.gov.uk/weather/tropicalcyclone/tracks/composites/swi)

Van Dijk, A.I.J.M., Bruijnzeel, L.A. and Roswell, C.J., 2002: Rainfall intensity-kinetic energy relationships: a critical literature appraisal, *Journal of Hydrology*, 261, 1-23.

Vinson, J. and Vinson, J.M., 1969: The saurian fauna of the Mascarene Islands, *Bulletin (Mauritius Institute)*, 64, 203-320.

Vrieling, A., Sterk, G. and de Jong, S.M., 2010: Satellite-based estimation of rainfall erosivity for Africa, *Journal of Hydrology*, 395, 235-241.

Wang, G., Gertner, G., Singh, V., Shinkareva, S., Parysow, P. and Anderson, A., 2002: Spatial and temporal prediction and the uncertainty of soil loss using the revised soil loss equation: a case study of the rainfall-runoff erosivity R factor, *Ecological Modelling*, 153, 143-155.

Waugh, D., 2014: *Geography: an integrated approach*, Oxford University Press, Oxford, UK.

Wei, W., Chen, L.D., Fu, B.J., Huang, Z.L., Wu, D.P. and Gui, L.D., 2007: The effect of land uses and rainfall regimes on runoff and soil erosion in the semi-arid loess hilly area, China, *Journal of Hydrology*, 335, 247-258.

Wischmeier, W.H. and Smith, D.D., 1958: Rainfall energy and its relationship to soil loss, *Transactions of the American Geophysical Union*, 39, 285-291.

Wischmeier, W.H. and Smith, D.D., 1978: Predicting rainfall erosion losses – a guide to conservation planning, USDA, Sciences and Education Administration, Agricultural Research, Agriculture Handbook No. 537, pp. 58.

Wohl, E.E., 1993: Bedrock channel incision along Piccaninny Creek, Australia, *The Journal of Geology*, 101, 749-761.

Wohletz, K.H. and Heiken, G., 1992: *Volcanology and geothermal energy*, University of California Press, Berkeley, USA.

WRU (Water Resources Unit), 2007: *Hydrology Data Book for the Period 1999-2005*. Water Resources Unit, Rose-hill, Mauritius.

Yang, D., Kanae, S., Oki, T., Koike, T. and Musiake, K., 2003: Global potential soil erosion with reference to land use and climate changes, *Hydrological Processes*, 17, 2913-2928.

Yin, S., Xie, Y., Nearing, M.A. and Wang, C., 2007: Estimation of rainfall erosivity using 5-60 – minute fixed interval rainfall data from China, *Catena*, 70, 306-312.

Zachar, D., 1982: Soil erosion: developments in soil erosion, 10, Elsevier Scientific Publishing Company, Netherlands.

Zhang, Y.G., Nearing, M.A., Zhang, X.C., Xie, Y. and Wei, H., 2010: Projected rainfall erosivity changes under climate change from multimodel and multiscenario projections in Northeast China, *Journal of Hydrology*, 384, 97-106.

Appendix 1

SAMPLE STATISTICS

		Site A	Site B
	ANALYST AND DATE:	.	.
	SIEVING ERROR:		
	SAMPLE TYPE:	Polymodal, Poorly Sorted	Polymodal, Poorly Sorted
	TEXTURAL GROUP:	Sandy Gravel	Sandy Gravel
	SEDIMENT NAME:	Sandy Very Fine Gravel	Sandy Very Fine Gravel
METHOD OF MOMENTS Arithmetic (μm)	MEAN ($\overline{x}_a$):	1351.5	1473.8
	SORTING (σ_a):	904.9	884.5
	SKEWNESS (Sk_a):	0.016	-0.205
	KURTOSIS (K_a):	1.342	1.426
METHOD OF MOMENTS Geometric (μm)	MEAN ($\overline{x}_g$):	917.9	1045.9
	SORTING (σ_g):	2.720	2.639
	SKEWNESS (Sk_g):	-0.755	-1.074
	KURTOSIS (K_g):	2.387	3.071
METHOD OF MOMENTS Logarithmic (ϕ)	MEAN ($\overline{x}_\phi$):	0.124	-0.065
	SORTING (σ_ϕ):	1.444	1.400
	SKEWNESS (Sk_ϕ):	0.755	1.074
	KURTOSIS (K_ϕ):	2.387	3.071
FOLK AND WARD METHOD (μm)	MEAN (M_G):	942.5	1046.4
	SORTING (σ_G):	2.673	2.623
	SKEWNESS (Sk_G):	-0.415	-0.563
	KURTOSIS (K_G):	0.652	0.967
FOLK AND WARD METHOD (ϕ)	MEAN (M_ϕ):	0.085	-0.065
	SORTING (σ_ϕ):	1.418	1.391
	SKEWNESS (Sk_ϕ):	0.415	0.563
	KURTOSIS (K_G):	0.652	0.967
FOLK AND WARD METHOD (Description)	MEAN:	Coarse Sand	Very Coarse Sand
	SORTING:	Poorly Sorted	Poorly Sorted
	SKEWNESS:	Very Fine Skewed	Very Fine Skewed
	KURTOSIS:	Very Platykurtic	Mesokurtic
	MODE 1 (μm):	2400.0	2400.0
	MODE 2 (μm):	302.5	855.0
	MODE 3 (μm):	1200.0	302.5
	MODE 1 (ϕ):	-1.243	-1.243
	MODE 2 (ϕ):	1.747	0.247
	MODE 3 (ϕ):	-0.243	1.747
	D_{10} (μm):	175.5	177.8
	D_{50} (μm):	1220.4	1499.2
	D_{90} (μm):	2556.1	2582.8
	(D_{90} / D_{10}) (μm):	14.56	14.53
	(D_{90} - D_{10}) (μm):	2380.6	2405.0
	(D_{75} / D_{25}) (μm):	6.390	3.493
	(D_{75} - D_{25}) (μm):	1880.6	1633.2
	D_{10} (ϕ):	-1.354	-1.369
	D_{50} (ϕ):	-0.287	-0.584
	D_{90} (ϕ):	2.510	2.492
	(D_{90} / D_{10}) (ϕ):	-1.854	-1.820
	(D_{90} - D_{10}) (ϕ):	3.864	3.861
	(D_{75} / D_{25}) (ϕ):	-1.313	-0.511
	(D_{75} - D_{25}) (ϕ):	2.676	1.805
	% GRAVEL:	36.9%	41.7%
	% SAND:	63.1%	58.3%
	% MUD:	0.0%	0.0%
	% V COARSE GRAVEL:	0.0%	0.0%
	% COARSE GRAVEL:	0.0%	0.0%
	% MEDIUM GRAVEL:	0.0%	0.0%
	% FINE GRAVEL:	0.0%	0.0%
	% V FINE GRAVEL:	36.9%	41.7%
	% V COARSE SAND:	18.8%	19.2%
	% COARSE SAND:	18.5%	19.6%
	% MEDIUM SAND:	15.2%	9.3%
	% FINE SAND:	8.1%	7.8%
	% V FINE SAND:	2.5%	2.5%
	% V COARSE SILT:	0.0%	0.0%
	% COARSE SILT:	0.0%	0.0%
	% MEDIUM SILT:	0.0%	0.0%
	% FINE SILT:	0.0%	0.0%
	% V FINE SILT:	0.0%	0.0%
	% CLAY:	0.0%	0.0%

SAMPLE STATISTICS

SAMPLE IDENTITY: **Site A**

ANALYST & DATE: D.R. Calvert, 09/07/2017

SAMPLE TYPE: Polymodal, Poorly Sorted

TEXTURAL GROUP: Sandy Gravel

SEDIMENT NAME: Sandy Very Fine Gravel

	µm	ϕ
MODE 1:	2400.0	-1.243
MODE 2:	302.5	1.747
MODE 3:	1200.0	-0.243
D_{10}:	175.5	-1.354
MEDIAN or D_{50}:	1220.4	-0.287
D_{90}:	2556.1	2.510
(D_{90} / D_{10}):	14.56	-1.854
(D_{90} - D_{10}):	2380.6	3.864
(D_{75} / D_{25}):	6.390	-1.313
(D_{75} - D_{25}):	1880.6	2.676

GRAIN SIZE DISTRIBUTION

GRAVEL: 36.9%	COARSE SAND: 18.5%
SAND: 63.1%	MEDIUM SAND: 15.2%
MUD: 0.0%	FINE SAND: 8.1%
	V FINE SAND: 2.5%
V COARSE GRAVEL: 0.0%	V COARSE SILT: 0.0%
COARSE GRAVEL: 0.0%	COARSE SILT: 0.0%
MEDIUM GRAVEL: 0.0%	MEDIUM SILT: 0.0%
FINE GRAVEL: 0.0%	FINE SILT: 0.0%
V FINE GRAVEL: 36.9%	V FINE SILT: 0.0%
V COARSE SAND: 18.8%	CLAY: 0.0%

	METHOD OF MOMENTS			FOLK & WARD METHOD		
	Arithmetic µm	Geometric µm	Logarithmic ϕ	Geometric µm	Logarithmic ϕ	Description
MEAN ($\bar{x}$):	1351.5	917.9	0.124	942.5	0.085	Coarse Sand
SORTING (σ):	904.9	2.720	1.444	2.673	1.418	Poorly Sorted
SKEWNESS (Sk):	0.016	-0.755	0.755	-0.415	0.415	Very Fine Skewed
KURTOSIS (K):	1.342	2.387	2.387	0.652	0.652	Very Platykurtic

GRAIN SIZE DISTRIBUTION

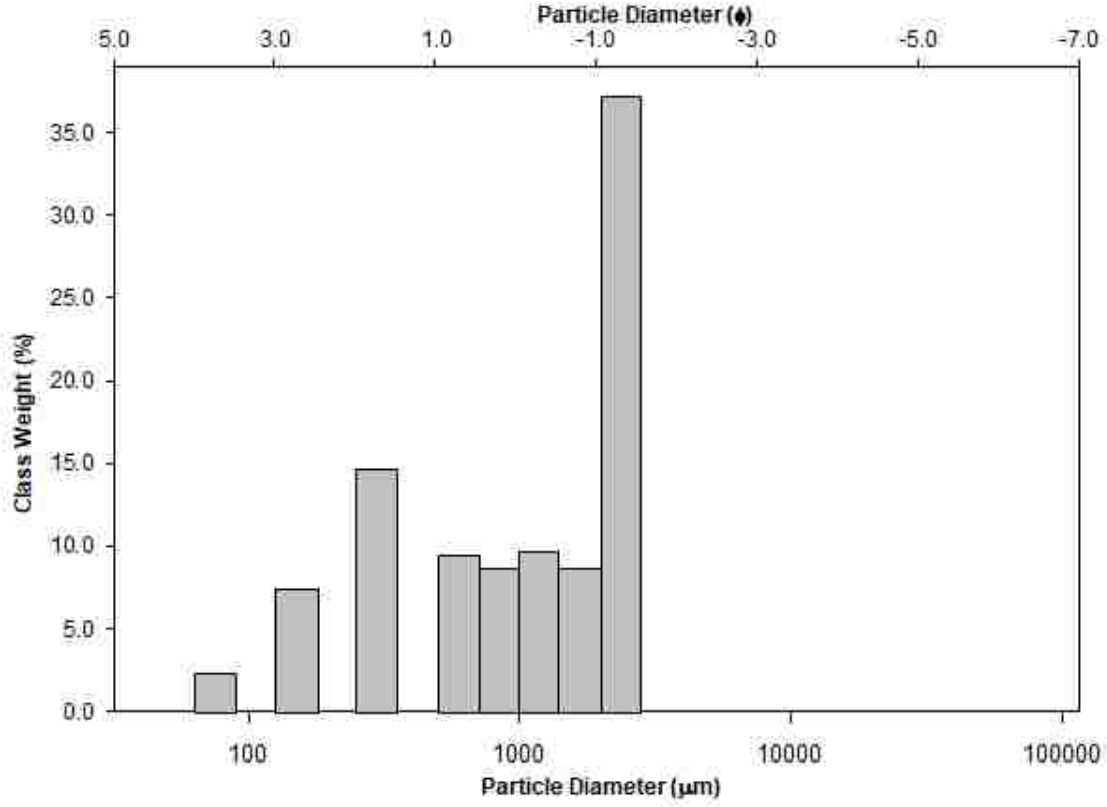

SAMPLE IDENTITY: **Site A**
TEXTURAL GROUP: Sandy Gravel
SEDIMENT NAME: Sandy Very Fine Gravel

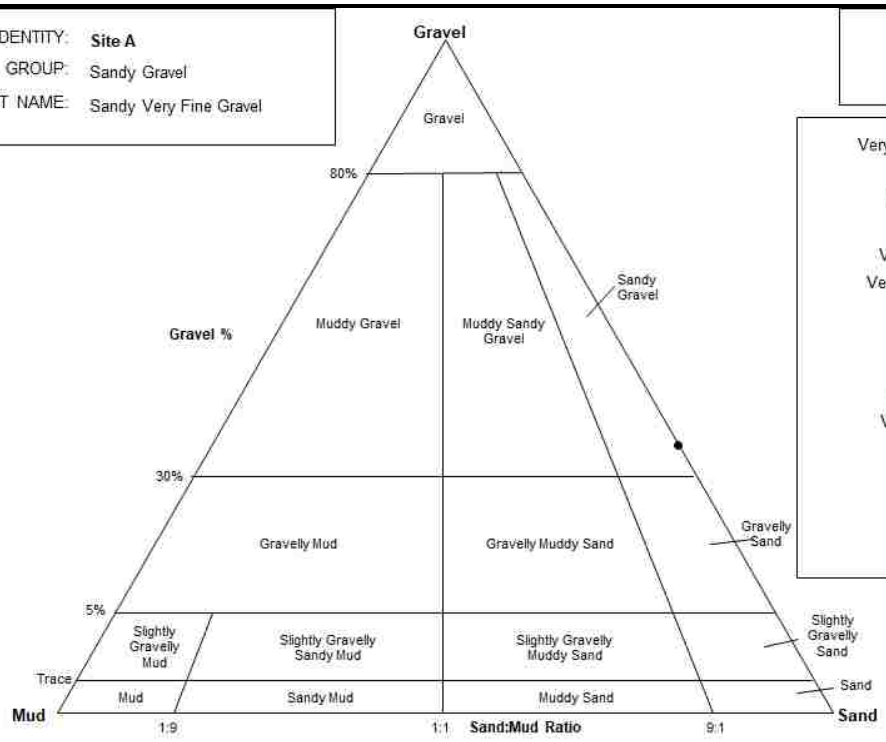

Gravel:	36.9%
Sand:	63.1%
Mud:	0.0%

Very Coarse Gravel:	0.0%
Coarse Gravel:	0.0%
Medium Gravel:	0.0%
Fine Gravel:	0.0%
Very Fine Gravel:	36.9%
Very Coarse Sand:	18.8%
Coarse Sand:	18.5%
Medium Sand:	15.2%
Fine Sand:	8.1%
Very Fine Sand:	2.5%
Very Coarse Silt:	0.0%
Coarse Silt:	0.0%
Medium Silt:	0.0%
Fine Silt:	0.0%
Very Fine Silt:	0.0%
Clay:	0.0%

SAMPLE IDENTITY: **Site A**
TEXTURAL GROUP IGNORING GRAVEL FRACTION: Sand

NOTE
Gravel is also present in this sample

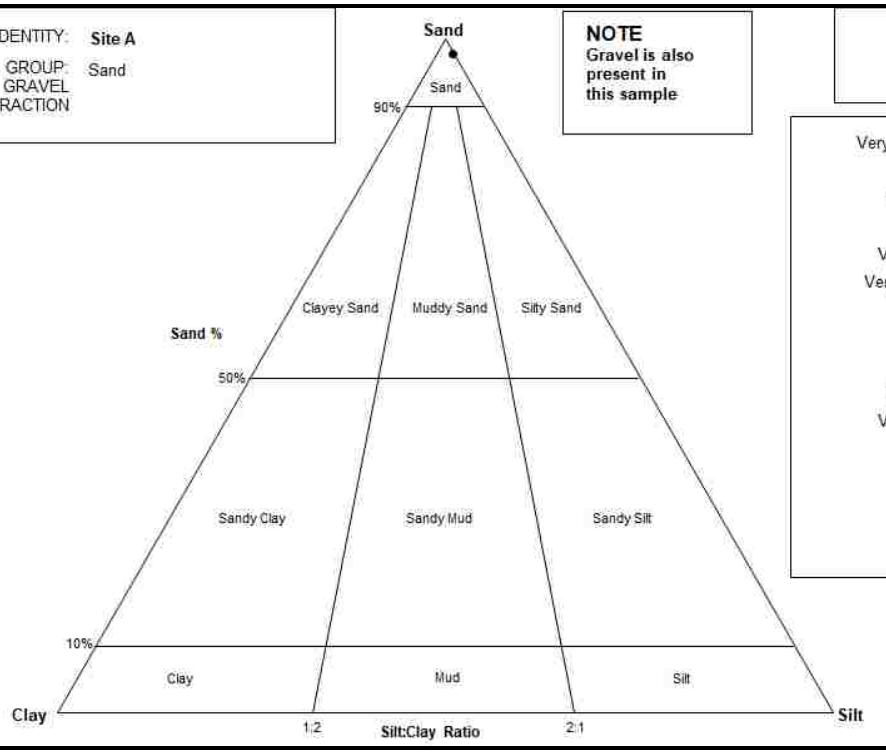

Gravel:	36.9%
Sand:	63.1%
Mud:	0.0%

Very Coarse Gravel:	0.0%
Coarse Gravel:	0.0%
Medium Gravel:	0.0%
Fine Gravel:	0.0%
Very Fine Gravel:	36.9%
Very Coarse Sand:	18.8%
Coarse Sand:	18.5%
Medium Sand:	15.2%
Fine Sand:	8.1%
Very Fine Sand:	2.5%
Very Coarse Silt:	0.0%
Coarse Silt:	0.0%
Medium Silt:	0.0%
Fine Silt:	0.0%
Very Fine Silt:	0.0%
Clay:	0.0%

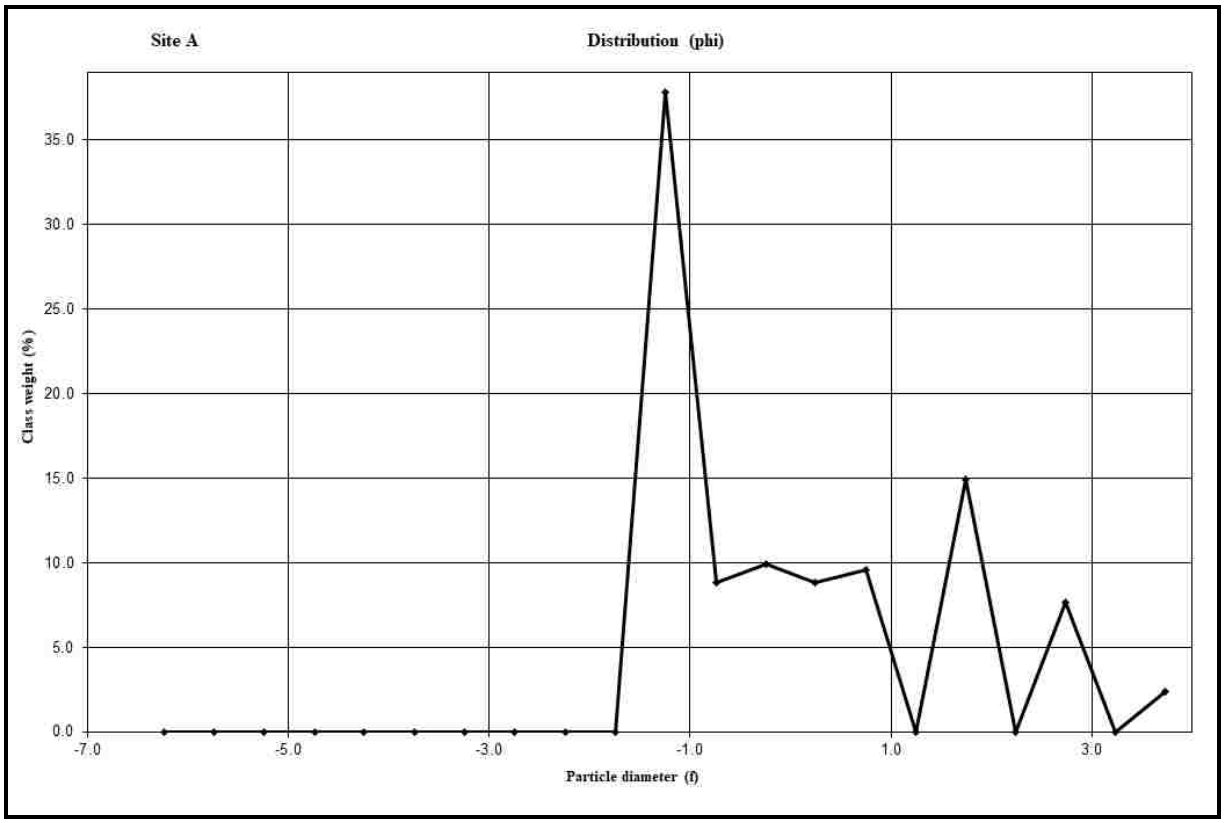
Site A
Distribution (phi)
Class weight (%)
35.0
30.0
25.0
20.0
15.0
10.0
5.0
0.0
-7.0
-5.0
-3.0
-1.0
1.0
3.0
Particle diameter (f)

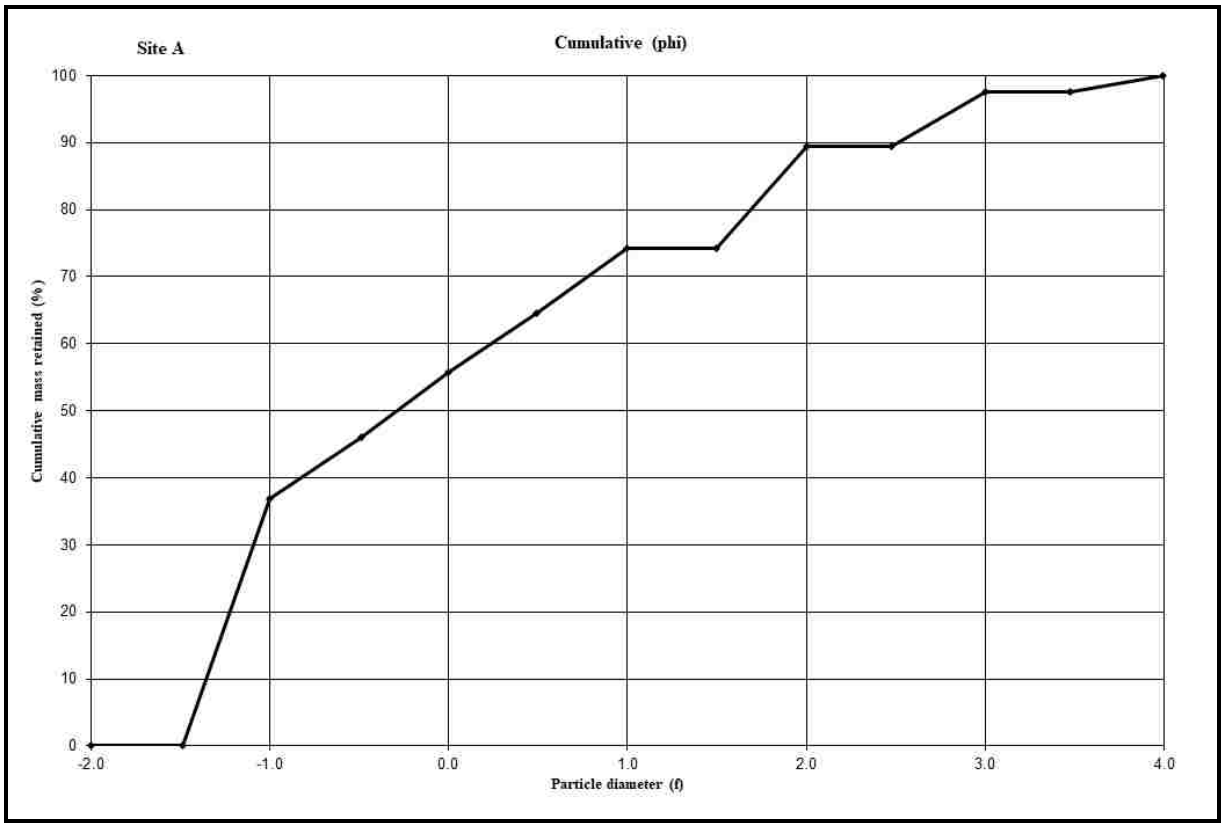
Site A
Cumulative (phi)
Cumulative mass retained (%)
100
90
80
70
60
50
40
30
20
10
0
-2.0
-1.0
0.0
1.0
2.0
3.0
4.0
Particle diameter (f)

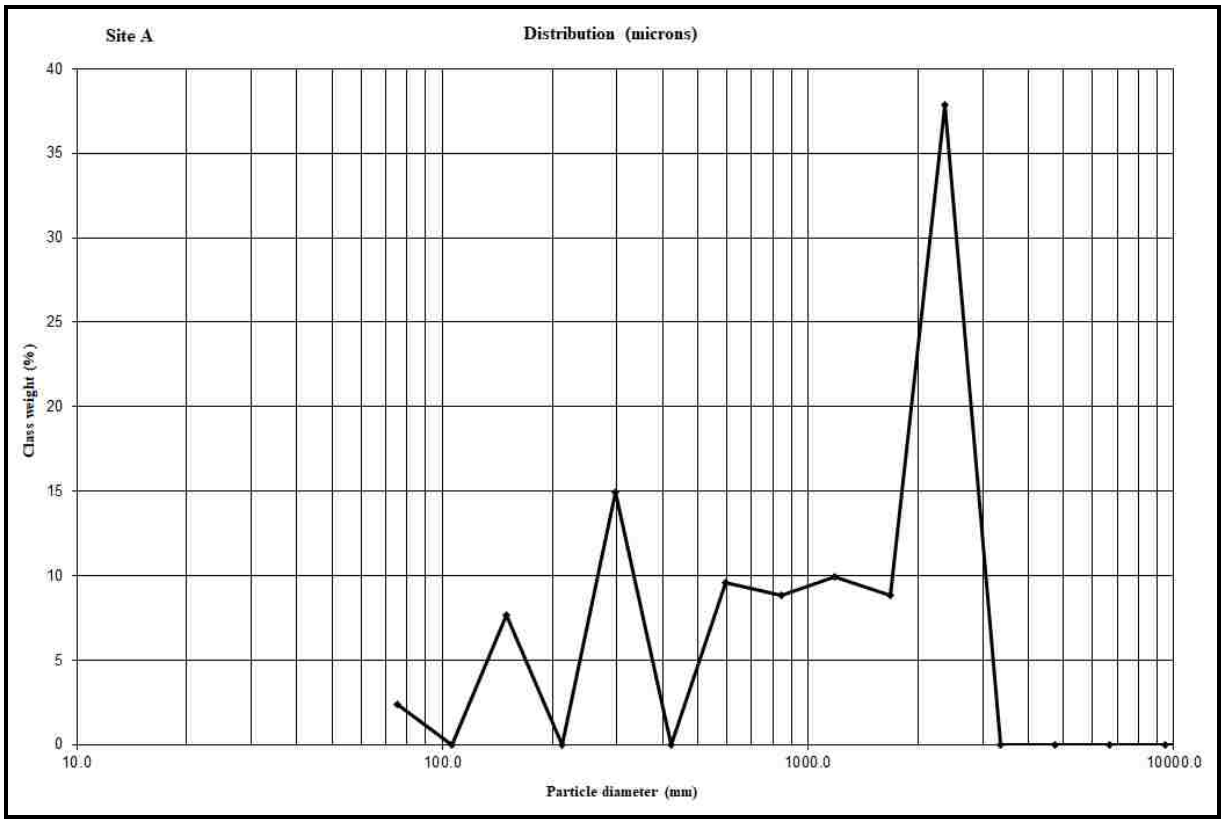
Site A
Distribution (microns)
Class weight (%)
40
35
30
25
20
15
10
5
0
10.0
100.0
1000.0
10000.0
Particle diameter (mm)


Site A
Cumulative (microns)
Cumulative mass retained (%)
100
90
80
70
60
50
40
30
20
10
0
10.0
100.0
1000.0
10000.0
Particle diameter (mm)

SAMPLE STATISTICS

SAMPLE IDENTITY: **Site B**

ANALYST & DATE: D.R. Calvert, 09/07/2017

SAMPLE TYPE: Polymodal, Poorly Sorted

TEXTURAL GROUP: Sandy Gravel

SEDIMENT NAME: Sandy Very Fine Gravel

	µm	ϕ
MODE 1:	2400.0	-1.243
MODE 2:	855.0	0.247
MODE 3:	302.5	1.747
D_{10}:	177.8	-1.369
MEDIAN or D_{50}:	1499.2	-0.584
D_{90}:	2582.8	2.492
(D_{90} / D_{10}):	14.53	-1.820
(D_{90} - D_{10}):	2405.0	3.861
(D_{75} / D_{25}):	3.493	-0.511
(D_{75} - D_{25}):	1633.2	1.805

GRAIN SIZE DISTRIBUTION

GRAVEL: 41.7%	COARSE SAND: 19.6%
SAND: 58.3%	MEDIUM SAND: 9.3%
MUD: 0.0%	FINE SAND: 7.8%
	V FINE SAND: 2.5%
V COARSE GRAVEL: 0.0%	V COARSE SILT: 0.0%
COARSE GRAVEL: 0.0%	COARSE SILT: 0.0%
MEDIUM GRAVEL: 0.0%	MEDIUM SILT: 0.0%
FINE GRAVEL: 0.0%	FINE SILT: 0.0%
V FINE GRAVEL: 41.7%	V FINE SILT: 0.0%
V COARSE SAND: 19.2%	CLAY: 0.0%

	METHOD OF MOMENTS			FOLK & WARD METHOD		
	Arithmetic	Geometric	Logarithmic	Geometric	Logarithmic	Description
	µm	µm	ϕ	µm	ϕ	
MEAN ($\bar{x}$):	1473.8	1045.9	-0.065	1046.4	-0.065	Very Coarse Sand
SORTING (σ):	884.5	2.639	1.400	2.623	1.391	Poorly Sorted
SKEWNESS (Sk):	-0.205	-1.074	1.074	-0.563	0.563	Very Fine Skewed
KURTOSIS (K):	1.426	3.071	3.071	0.967	0.967	Mesokurtic

GRAIN SIZE DISTRIBUTION

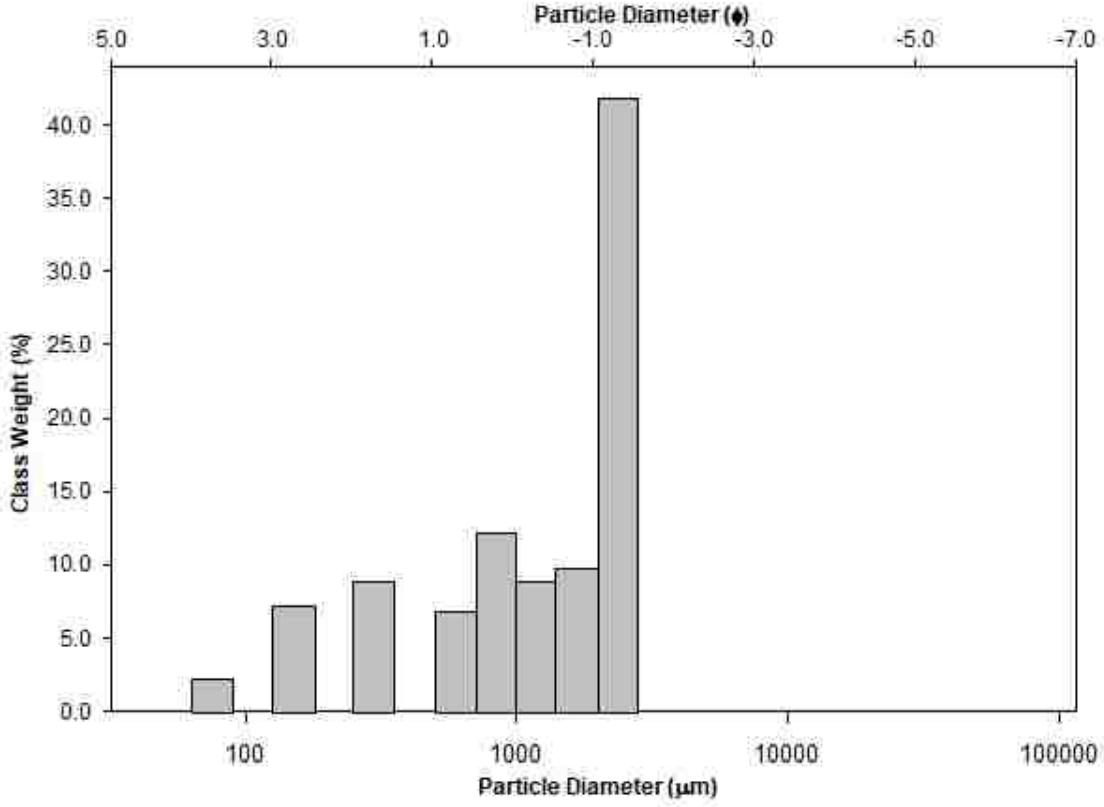

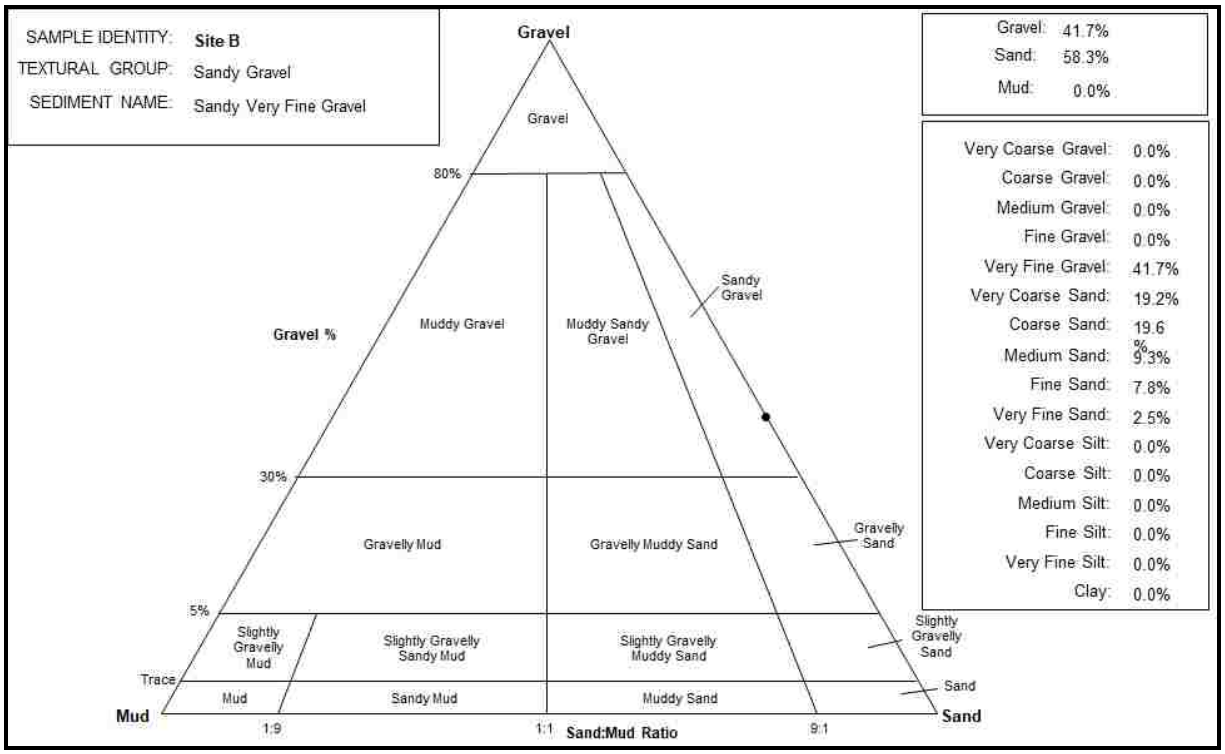
SAMPLE IDENTITY: Site B
TEXTURAL GROUP: Sandy Gravel
SEDIMENT NAME: Sandy Very Fine Gravel
Gravel
Gravel
80%
30%
5%
Trace
Gravel %
Muddy Gravel
Muddy Sandy Gravel
Sandy Gravel
Gravelly Mud
Gravelly Muddy Sand
Gravelly Sand
Slightly Gravelly Mud
Slightly Gravelly Sandy Mud
Slightly Gravelly Muddy Sand
Slightly Gravelly Sand
Mud
Sandy Mud
Muddy Sand
Sand
Mud
Sand
1:9
1:1
9:1
Sand:Mud Ratio
Gravel: 41.7%
Sand: 58.3%
Mud: 0.0%
Very Coarse Gravel: 0.0%
Coarse Gravel: 0.0%
Medium Gravel: 0.0%
Fine Gravel: 0.0%
Very Fine Gravel: 41.7%
Very Coarse Sand: 19.2%
Coarse Sand: 19.6 %
Medium Sand: 9.3%
Fine Sand: 7.8%
Very Fine Sand: 2.5%
Very Coarse Silt: 0.0%
Coarse Silt: 0.0%
Medium Silt: 0.0%
Fine Silt: 0.0%
Very Fine Silt: 0.0%
Clay: 0.0%

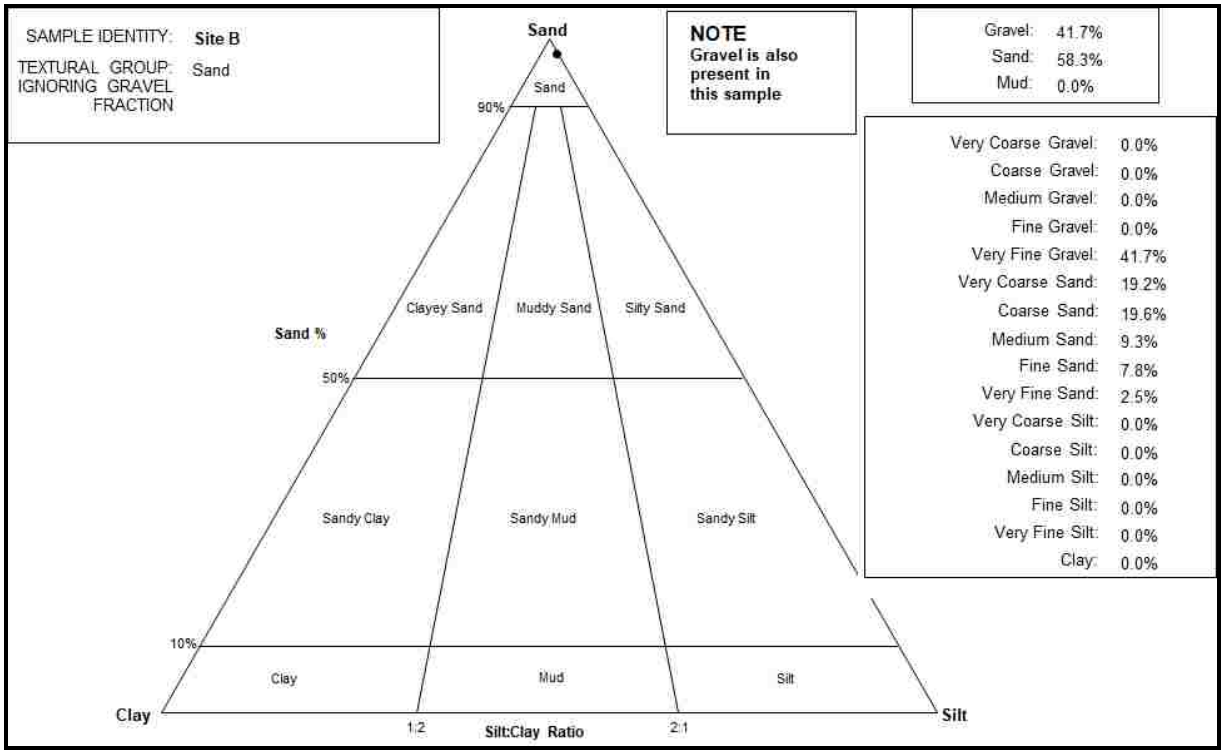
SAMPLE IDENTITY: Site B
TEXTURAL GROUP: IGNORING GRAVEL FRACTION Sand
NOTE
Gravel is also present in this sample
Sand
Sand
90%
50%
10%
Sand %
Clayey Sand
Muddy Sand
Silty Sand
Sandy Clay
Sandy Mud
Sandy Silt
Clay
Mud
Silt
Clay
Silt
1:2
2:1
Silt:Clay Ratio
Gravel: 41.7%
Sand: 58.3%
Mud: 0.0%
Very Coarse Gravel: 0.0%
Coarse Gravel: 0.0%
Medium Gravel: 0.0%
Fine Gravel: 0.0%
Very Fine Gravel: 41.7%
Very Coarse Sand: 19.2%
Coarse Sand: 19.6%
Medium Sand: 9.3%
Fine Sand: 7.8%
Very Fine Sand: 2.5%
Very Coarse Silt: 0.0%
Coarse Silt: 0.0%
Medium Silt: 0.0%
Fine Silt: 0.0%
Very Fine Silt: 0.0%
Clay: 0.0%

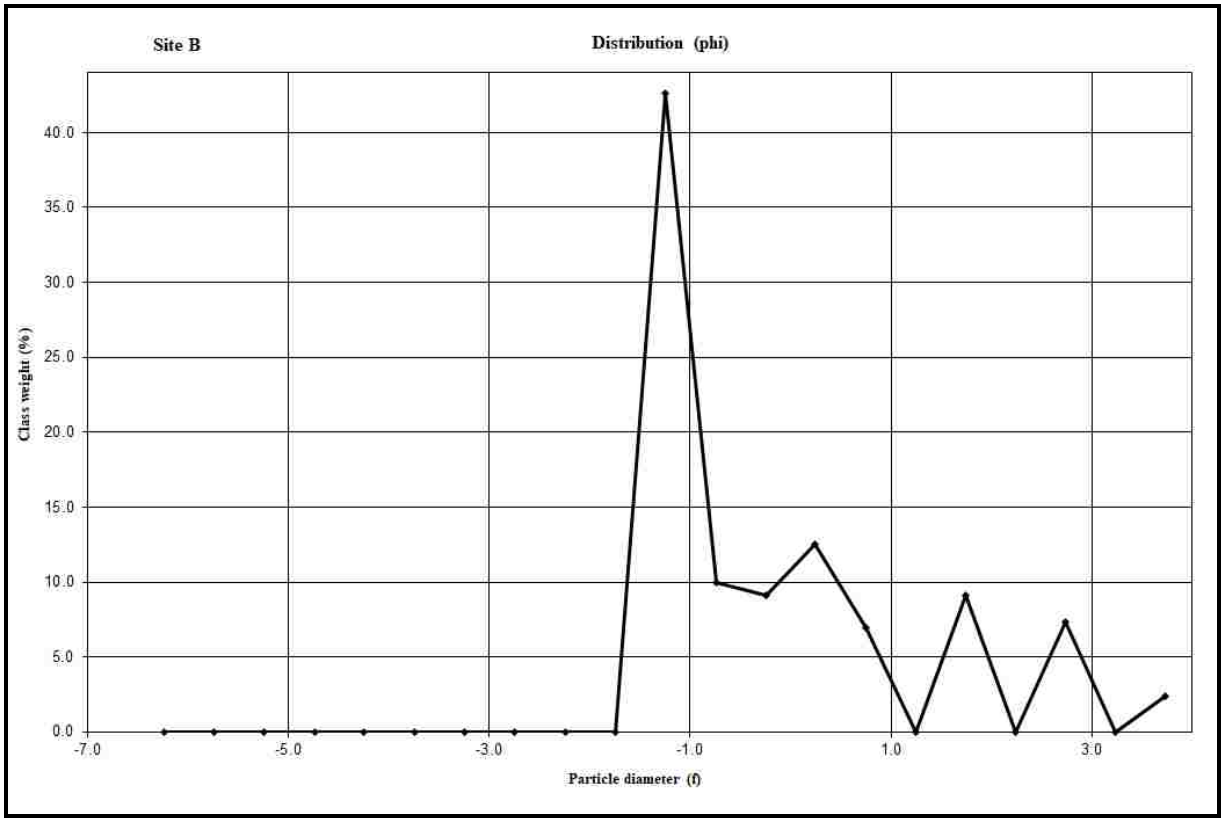
Site B
Distribution (phi)
Class weight (%)
40.0
35.0
30.0
25.0
20.0
15.0
10.0
5.0
0.0
-7.0
-5.0
-3.0
-1.0
1.0
3.0
Particle diameter (f)

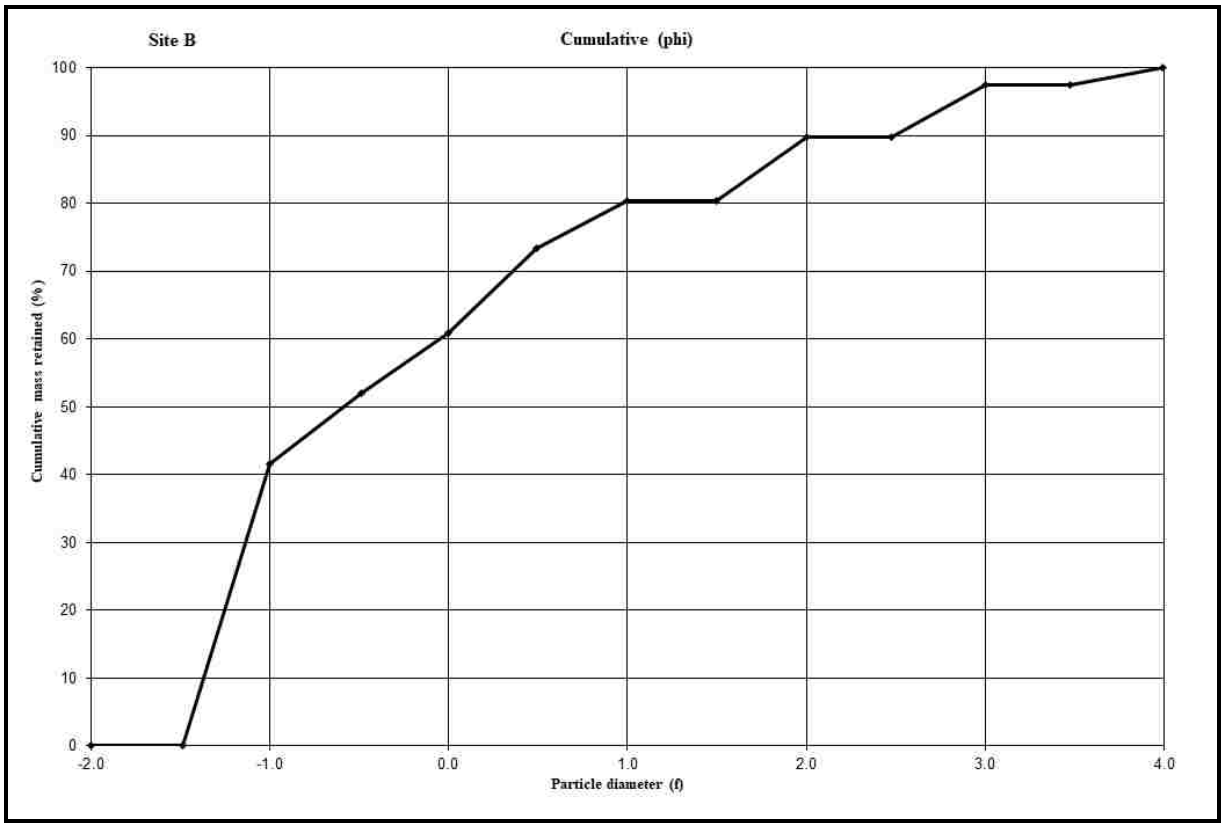
Site B
Cumulative (phi)
Cumulative mass retained (%)
100
90
80
70
60
50
40
30
20
10
0
-2.0
-1.0
0.0
1.0
2.0
3.0
4.0
Particle diameter (f)

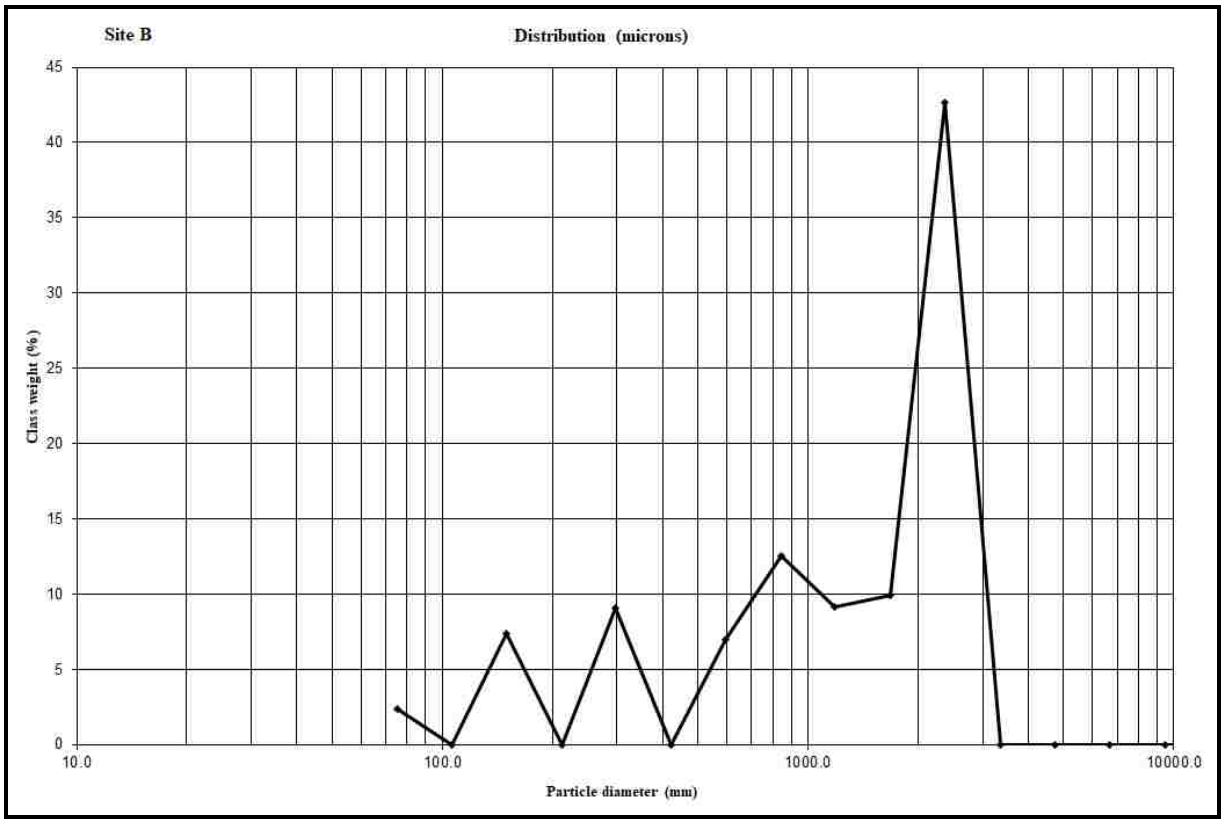
Site B
Distribution (microns)
Class weight (%)
45
40
35
30
25
20
15
10
5
0
10.0
100.0
1000.0
10000.0
Particle diameter (mm)

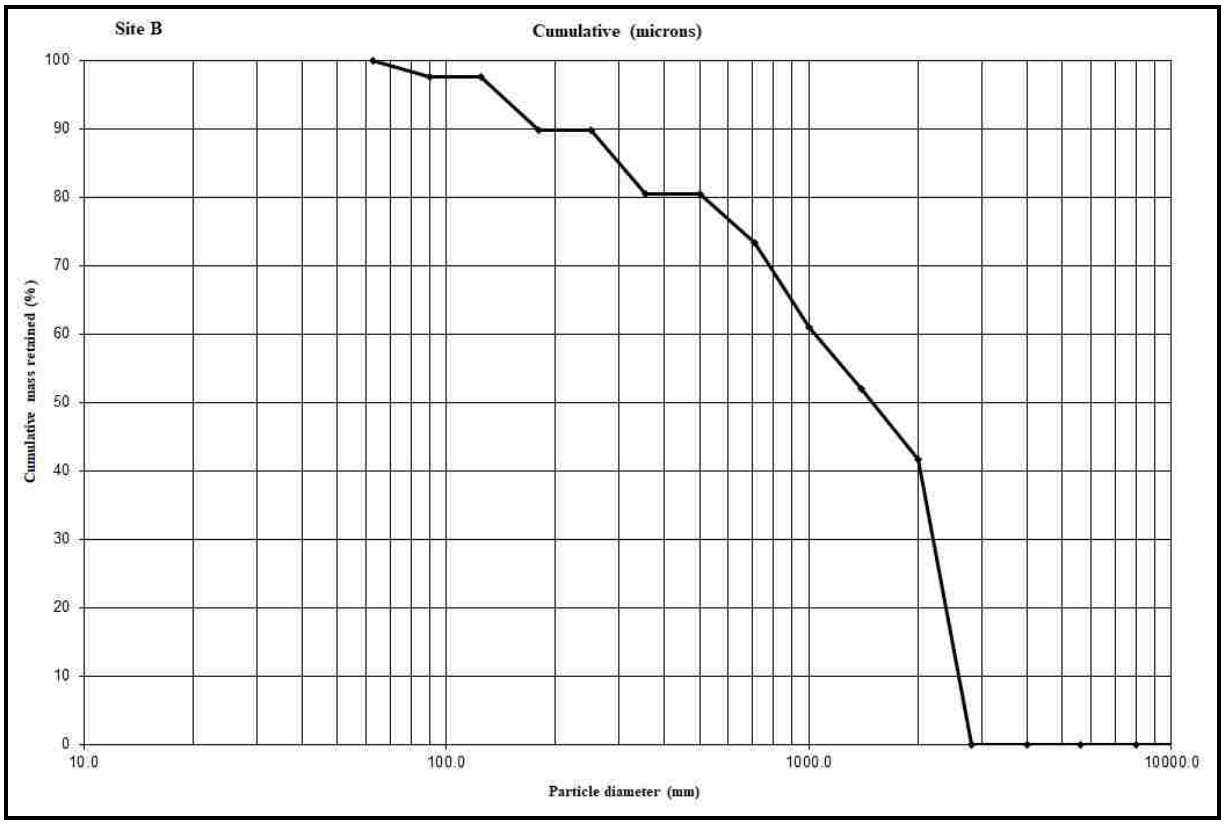
Site B
Cumulative (microns)
Cumulative mass retained (%)
100
90
80
70
60
50
40
30
20
10
0
10.0
100.0
1000.0
10000.0
Particle diameter (mm)